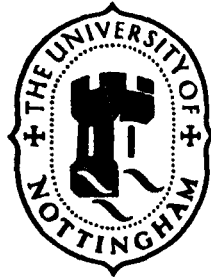University of Nottingham

Department of Mining Engineering

AN APPLICATION OF NUMERICAL METHODS TO THE

PREDICTION OF STRATA METHANE FLOW

IN LONGWALL MINING

BY

I. G. EDIZ, B.Sc., M.Sc.

Thesis submitted to the University of Nottingham for the degree of

Doctor of Philosophy

October 1991

CONTENTS

i

LIST OF FIGURES

vi

LIST OF TABLES

ABSTRACT

This research describes an application of numerical methods for the prediction of strata methane flow into mine workings around a longwall coal face employing methane drainage. This method of methane prediction was developed by solving the time-dependent gas flow equation using the finite element analysis. Having obtained the gas pressure distribution throughout the finite element mesh, a mass flow equation was derived to calculate methane flow rate for a given mining boundary. A computer program for the prediction of methane flow was then developed by devising appropriate modifications and additions to a finite element package originally written for heat flow by PAFEC limited. Stress analysis was also carried out in order to provide an understanding of stress fields around a longwall face to evaluate the induced permeabilities under these stress fields.

Three main routines of the original package required modifications to accommodate the solution of a different equation. These were element routines, solution routines and flux calculation routines. These routines, after modification, were used to simulate advance and retreat longwall mining, with and without drainage. Several different sensitivity tests were carried out by changing parameters such as borehole pressure, length, and spacing in order to aid the planning of methane drainage systems for longwall mining.

INTRODUCTION

The release of methane from coal seams and surrounding strata into mine workings has been of great concern since the earliest days of underground mining. The advent of modern underground mining machinery and mining methods, coupled with improved environmental control techniques, has allowed higher levels of production to be achieved with faster rates of face advance. These factors, combined with increasing depth of working, have exacerbated the problems of methane emission in underground mining. Although the number of ignitions and explosions has decreased because of improved safety measures, the percentage of fatalities due to ignitions and explosions has increased.

Methane emission also adversely affects coal production. If the methane concentration at the face exceeds 1.25 % (a statutory limit which may vary according to country), coal production must stop until the air flow is sufficient to dilute the methane concentration to an acceptable level. With modern mining methods resulting in higher levels of coal production, this situation is not uncommon. As deeper and gassier coalbeds are mined, conventional ventilation methods may not be able to cope consistently with methane emission during the coal-production cycle. Traditional methods of methane control involving increased air quantities into mine workings cannot always deal with the rate of methane in-flow and may cause dust problems and increase ventilation costs unreasonably. In these circumstances, drainage becomes an important method of alleviating methane emission problems to improve both safety and productivity. The advantages of employing methane drainage techniques in underground coal mining can be given as follows:

i. Reduction of methane emission into the mine environment significantly improves the safety of the working environment.

ii. Coal production can increase since the restrictions of excessive methane emission become less obstructive.

iii. A decrease in methane emission allows a reduction in the quantity of air required for diluting the gas which in turn reduces the ventilation costs, and could enable the cross-sectional areas of future mine airways to be reduced for ventilation purposes.

iv. Reduction in the methane emission rate allows face lengths to be increased thereby reducing development costs of gate roads for a given area of coal.

v. Coal production efficiency and the face advance rate are increased because of the reduction of idle time due to excess of gas.

vi. Possibility of commercial exploitation of a large quantity of gas of high calorific value.

vii. Methane's contribution to global warming is reduced by the commercial utilisation of drained gas.

Methane is a fairly inert gas, the principal danger of methane lies in its explosible character when its concentration in the air is between 5 % and 15 %. At a methane level in about the middle of this range, the air/methane mixture is at its most explosive. However, mining law requires that the methane concentration in the general air body must be less than 2 % for men to work and

2

must not exceed 1.25 % where electrical power is in use [1]. Therefore, to keep the methane concentration below the specified limits the ventilation engineer must ensure adequate quantities of air supplied to the workings and if necessary make provision for methane drainage. A prediction of methane emission is therefore of great use during the design of underground ventilation to meet the statutory requirements for the dilution of methane in air.

The prediction of methane flow in and around working coal mines has been investigated by various researchers using 'empirical', and 'mathematical' methods. Empirical methods define the degree of gas emission as the percentage of the gas contained within the strata at a specific level which flows into the mine workings. A certain percentage of the coal seam content is usually taken to define the gas content for strata other than coal. Methane emission from a source seam is calculated by multiplying the degree of gas emission for the seam considered, by its gas content and the relative thickness, which is the ratio of the thickness of the source seam to that of the worked seam.

Since all empirical prediction methods are based on past experience and statistical data, the same approach is of limited use outside of the specific geographical area and mining situations which they were designed for. Therefore, the application of an empirical method in different circumstances may require extensive modification. Although empirical methods are relatively simple, requiring few input parameters, they lack the theoretical base required for accurate prediction.

Numerical methods of predicting methane flow are based on the principles of gas flow in porous permeable media, in other words the computer solutions of a gas flow equation mainly derived from Darcy's law. The required input to the computer programs include parameters to define the model size, initial and time-dependent boundary conditions, properties of the coal seams and strata such as directional permeabilities and porosities and the properties of the flowing gas such as viscosity. The programs terminate when the flow equation has been solved and the output gives the predicted gas pressure distribution and the methane flow rates on a time basis. Among the parameters stated above, permeability is considered to be the most crucial one affecting the reliability of the results. Therefore, recent studies on the simulation of methane flow using numerical methods have incorporated the essential components of stress analysis and stress-permeability analysis.

Although there has been a great deal of research carried out on the subject of gas flow simulation for coal strata by mathematical methods, very little of this work has dealt specifically with the prediction of methane for full-field scale underground mining especially in terms of longwall applications. Therefore, the objectives of this research have been to develop a reliable prediction method based on a mathematical approach to calculate strata methane flow into mine workings around a moving longwall face employing methane drainage. These objectives were influenced by previous work carried out in the Department of Mining Engineering, at the University of Nottingham which attempted to simulate methane flow towards a simple advancing longwall face without data validation. In general, US attention has been focused on increasing the accuracy of the flow equation describing the gas flow from coal strata. However, US research lacks application to underground longwall mining and is orientated mainly towards the development of coal seam degasification models.

Consideration of the effect of changing stress fields around a working longwall face on permeability of coal seams and strata is as important as the accuracy of the mathematical techniques employed. Therefore, in this research emphasis has been shifted from a more complex mathematical simulation attempt to developing a numerical model applicable to underground longwall mining with field data validation. The main reason for this approach is to show that the accuracy of such a prediction method is heavily dependent upon stress-permeability behaviour of coal and coal strata, the reliability of field data and applicability of the method rather than the mathematical perfection involved with making fewer assumptions in the solution process.

This research, aiming to help further understanding in this area by providing numerical evidence, will be treated in two stages:

i.   Simulation of stresses around a mine working and evaluation of induced permeabilities under these stress conditions.

ii.   Simulation of methane flow around a moving longwall coal face using a mathematical modelling technique for the purpose of methane prediction.

CHAPTER ONE

REVIEW OF CURRENT KNOWLEDGE ON METHANE FLOW AND MATHEMATICAL MODELS FOR METHANE PREDICTION

1.1 Introduction

Before attempting any simulation of a practical problem, one should have a knowledge of the physical principles relevant to that problem. Understanding the phenomenon of methane flow around a longwall coal face is essential for any mathematical prediction method. Therefore, a general review about methane, its retention in coal and flow through coal strata into mine workings is given prior to Darcy's fundamental Law governing the fluid flow through porous media.

This chapter also discusses a recent review on mathematical simulation models for the prediction of methane flow from coal strata.

1.2 The Properties of Methane

Methane is a colourless, odourless and tasteless gas, with a specific gravity of 0.554 relative to air. At 0 °C and 750 mm Hg pressure, 1 m³ of methane weighs 0.716 kg [2]. Because of its low density it accumulates in the high places of mine workings. Methane has the ability to easily pass through porous materials since it diffuses 1.6 times as fast as air. The principal danger of methane lies in its explosible character when its concentration in the air is between 5 % and 15 %. At a methane level in about the middle of this range, the air/methane mixture is at its most explosive. However, mining law requires that the methane concentration in the general air body must be less than 2 % for men to work and must not exceed 1.25 % where electrical power is in use [1]. Therefore, while planning mine environmental conditions, a ventilation engineer must ensure that methane concentrations must not exceed such statutory levels in mine workings. Traditional methods of methane control involve increasing air quantities into mine workings to dilute methane concentration to acceptable levels. However, this method cannot always deal with the rate of methane in-flow and methane drainage may become an essential method of alleviating methane emission problems to improve both safety and productivity.

The ignition or burning of methane depends on the composition of air [3]. Either a lowered oxygen or a high carbon dioxide content will make the ignition or burning more difficult. Investigations have shown that methane ceases to ignite at an oxygen content below 12 % (see figure 1.1). The explosibility limits of the air/methane are also affected by the existence of combustible gases and materials such as ethane, hydrogen and coal dust.
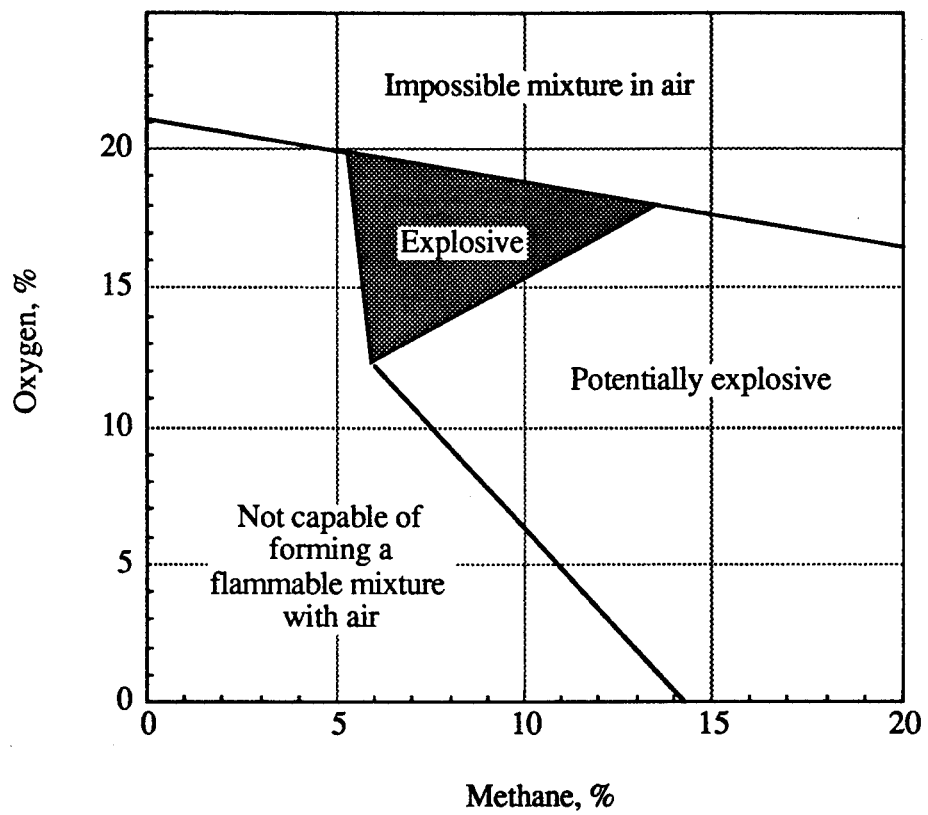
Figure 1.1 Explosibility Curve for Methane (after Coward and Jones [3]).

1.3 The Retention of Methane

Methane or firedamp, as it is called in many coalfields, is formed together with the coal material during a transformation process called coalification [4]. During the early stages of coal formation, there is only a thin and permeable covering over the deposits and most of the gases formed escaped. As a result little gas is found in most low-rank coal seams. However, most of the methane is retained in higher rank coals since they have been buried more deeply and enclosed by more compact rocks. The process of methane retention is called sorption and when the gas leaves the coal it is said to be desorbed [5,6]. Sorption is sub-classified into two basic categories:

i.   <u>Absorption</u>   describes the uniform penetration of one substance into the molecular structure of another and is not considered to play a significant role in the flow of methane from coal [7,8].

ii. <u>Adsorption</u>   explains a reversible surface effect whereby one substance is physically held onto the surface of another. The adsorption of methane gas onto the surface of coal is a good example.

Some methane is retained by coal as a free gas within the internal structure of coal, however at normal coal bed pressures most of the gas is adsorbed onto the surface of coal . At 20 atmospheres the adsorbed methane is ten times greater than methane as a free gas in some US coals [9]. The high methane adsorption capacity of coal is due to the very large internal surface area of coal which could be as high as ~200 m^2/g [8].

Most of the adsorbed gas on the internal surfaces of coal is present as a mono-molecular layer [8]. Many models have been proposed to describe the process of adsorption onto the coal surfaces. Langmuir [10] relates the quantity of gas adsorbed per unit mass of solid to the partial vapour pressure of the gas, and describes the mono-molecular layer adsorption of gases with the following equation:

$$V = \frac{V_m \, b' \, P}{1 + b'P} \qquad \ldots [1.1]$$

where

V   = volume of gas adsorbed,

P   = gas pressure,

V_m = maximum volume of gas adsorbable,

b'   = desorption coefficient.

Langmuir's theory gives the fraction of the adsorbent surface that is covered by the molecules of adsorbed gas. If the maximum sorption capacity of the surface is known, then the volume of gas that can be adsorbed may be determined.

Brunauer, Emmett and Teller [11] have given another equation, the (BET) equation, which is an extension of the Langmuir equation for multi-layer adsorption, whereas Langmuir considers only mono-layer adsorption. However, Keen [12] states that the secondary layer of adsorption is not apparent in coal under normal mining conditions (at pressures of less than 50

atmospheres) and therefore, Langmuir's equation is considered to be sufficiently accurate to apply to the adsorption process.

The adsorptive capacity of coal increases with coal rank [5]. Pressure is the critical parameter affecting the adsorptive capacity of coal. In general, the greater the pressure the greater the adsorptive capacity of coal. Increased temperatures reduce the adsorptive capacity of coal. The presence of water has a considerable effect on the adsorptive capacity of coal. Moisture content is mainly related to the oxygen content of coals. Strong interaction between the polar water molecules and the surfaces of oxygen complexes hold water in pore spaces in an adsorbed state. As the coalification proceeded towards higher ranks, oxygen was lost in the form of carbon dioxide or water resulting in decreased water adsorption capacity. Methane sorption capacity of coals, at a given pressure, decreases with increasing moisture content to a certain percentage of moisture which is a characteristic of each coal. Thereafter no further reduction of methane capacity occurs despite increasing moisture content.

Methods of determining the methane content of coal seams can be classified as 'direct' and 'indirect'. The direct method involves the direct sampling of coal underground followed by the measurement of gas in the laboratory [13]. The indirect, methods calculate the methane content from measurements of the in-situ gas pressure with a knowledge of the relevant 'adsorption isotherm' of the coal which is the plot of the volume of gas adsorbed against pressure at a constant temperature [14].

1.4 The Release and Flow of Methane

The methane, which is present in coal after the coalification process both in adsorbed or free gas state, eventually reaches a stable equilibrium. However, underground mining operations disturb the strata and upset this equilibrium of adsorbed gas in strata. These activities also cause relaxation of strata and the resultant fracturing provides flow paths for the gas to migrate into mine workings. In the original state gas in coal is at high pressure. Mine workings, containing air at near atmospheric pressure, provide a 'pressure sink' into which methane flows from the zone of gas emission surrounding the working [15,16]. The flow of methane is considered as a two-step process [8,17];

i.   <u>diffusion</u> through the micropore structure of the coal,

ii.   <u>flow</u> along interconnected fissures in the coal bed.

Methane moves by diffusion through solid coal from the desorption site until it intercepts a fracture in the coal. The diffusion process is governed by concentration gradients, and is given by 'Fick's Law' [5]. Methane flow, described by 'Darcy's Law' [18], along the fissures within coal is caused by the pressure differences between the in-situ gas pressure and atmospheric pressure of mine air. Although, both diffusion and laminar flow occur simultaneously during the gas emission process, the volume of methane entering mine workings by flow through fissures is generally far greater than that by diffusion alone [19].

Flow within the fissures is considered to be laminar in accordance with Darcy's flow equation [8]. Darcy's Law also requires fluid flow to be viscous where fluid flowing over a solid surface adheres to that surface. However, in the case of gases this does not happen and slip occurs along the fracture walls [20,21]. The occurrence of slip results in a higher flow rate than calculated using Darcy's equation, a consequence of the apparent dependence of permeability on gas pressure which is described by the 'Klinkenberg effect' which will be discussed later in this chapter. From the literature reviewed [12,22], it was decided to ignore the Klinkenberg effect to simplify the model developed in this thesis. The error due to ignoring the Klinkenberg effect would be very much less than that caused by the definition of strata permeabilities after stress redistribution.

The release of any strata gas from source beds and its subsequent migration towards the working areas is dependent upon geological, physical and mining factors, some of which are [23];

i.   the gas content and the thickness of the coal seam,

ii.   the pressure at which the gas is held,

iii.   the permeability of the virgin coal seam and the surrounding strata,

iv.   the modifications of coal seam and strata permeabilities by mining,

v.   the subsidence of the overlying rock,

vi.   the method of mining and roof control,

vii.   the method of ventilation,

viii.   depth of working,

ix.   presence of other source beds in the vicinity of the seam worked,

x.   barometric pressure,

xi.   rate of coal production.

Permeability is considered to be the principal factor controlling gas emission into mine workings. The release of methane from coal and its flow through strata towards the workings is controlled mainly by the permeability of the formations concerned. Stress disturbances created by mining operations affect the permeability of both the seam being worked and that of adjacent strata and therefore determine the pattern of methane emission [24].

1.4.1 The Source of Methane Flow

Methane entering coal mine workings may originate from the seam being worked or adjacent seams or strata. Methane from the seam being worked is called 'coal front gas' and can flow through the seam to the coal face or can migrate through adjacent strata to the relaxed zone behind the moving face. Methane from the source beds of carbonaceous material above and below mine workings migrates into the roadways from the roof and floor and is termed 'strata gas' [25,26]. Methane which is desorbed before coal reaches the face may be released when the coal is cut. The remaining gas will gradually desorb from the coal as it is transported from the mine but this desorption may not be complete when the coal leaves the mine [5,27]. It is generally accepted that there are three main sources from which methane is emitted;

i.   the actual seam being worked,

ii. the waste area behind the face,

iii. the source beds of carbonaceous materials above and below the mine workings.

It is clear that the emission of methane into mine workings is a complex combination of processes. However, in general mining practice it is suggested that the main part of methane emission is comprised by strata gas and therefore, the research topic was focused on the study of strata gas. The references in later chapters to gas emission will be taken to mean strata emission rather than emission from the worked coal seam. However, for a comprehensive simulation of methane flow around a working longwall coal face, account should be taken of both coal front gas emission and strata gas emission as well as emission from coal in conveyance.

1.4.2 Single-Phase Flow

The permeability of a coal seam to methane, and therefore the flow of methane, is also dependent on the presence of water. In some situations the pores and fissures in the coal and coal measure strata can be filled by water and methane can only exist in the adsorbed state which makes gas flow impossible [28]. With high strata pressure the permeability of coal to water is less than or equal to the gas permeability. However, at low strata pressure the permeability to water can be greater than the gas permeability since the coal tends to fracture internally under the shear stress of the flowing water [29].

In strata with a large amount of water, the assumption of single-phase flow may lead to inaccurate results. However, for normal mining conditions it is reasonable enough to assume that the gas flow is single-phase in order to simplify the simulation.

1.4.3 Temperature and Compressibility Effects on Gas Flow

In the course of gas flow, temperature differences can change the density and viscosity of a gas, which in turn affect the flow rate. However, for mining purposes, the flow rates of gases are relatively low and the change in gas temperature may be up to 15 °C. This change would correspond to variations in both density and viscosity of about 5 % [22].

It has been shown in the USSR that there is a drop in temperature of between 10 °C and 30 °C at the coal surface, when methane is desorbed, due to the heat requirements of the desorption process. This temperature change is not considered to have a significant effect on the flow mechanism of methane through coal [29,30]. It was therefore decided to assume isothermal flow conditions, in order to simplify the differential equations in the model.

Another assumption made, was that methane obeys the perfect gas law. This requires that the gas should not exhibit high compressibility. Keen [12] discussed the problem of the compressibility factor, and concluded that any compressibility effect can be ignored.

1.5 The Theories of Fluid Flow in Porous Permeable Media

The fundamental theory of laminar flow through homogeneous porous media is based on experiments originally performed by Darcy in 1856 [18,31]. He conducted a series of experiments on the flow of water through filter sands by varying the different quantities involved and finally arrived at the relationship:

$$Q = -K' \frac{A}{L} (h_2 - h_1) \qquad \ldots [1.2]$$

where

Q = total volume of fluid flowing through the filter sand in unit time,

A = cross-sectional area of the filter sand,

$h_2 - h_1$ = difference in the head of the fluid across the filter sand with length L,

K' = a constant depending on the properties of the fluid and of the porous medium.

The negative sign indicates that flow is in the opposite direction to increasing L. This relationship is known as Darcy's Law and literature is available for more detailed discussion of Darcy's work [32]. For the case of one dimensional, non-compressible fluid flow equation 1.2 takes the forms [31]:

$$Q = -K' A \frac{dP}{dx} \qquad \ldots [1.3]$$

where

$\dfrac{dP}{dx}$ = pressure gradient.

$$Q = -K' \, A \, \dfrac{dP}{L} \qquad\qquad \ldots [1.4]$$

In order to increase the applicability of Darcy's Law, Nutting [33] proposed the following relationship:

$$K' = \dfrac{k}{\mu}$$

where

μ = fluid viscosity,

k = permeability of the material.

Substituting k/μ for K', Darcy's equation for steady-state non-compressible fluid flow through porous media can be written as [31]:

$$Q = \dfrac{k \, A}{\mu \, L} \, \Delta P \qquad\qquad \ldots [1.5]$$

for compressible fluids,

$$Q_2 = \dfrac{k \, A \, \Delta P \, \bar{P}}{\mu \, L \, P_2} \qquad\qquad \ldots [1.6]$$

where

Q_2 = volume flow measured at pressure P_2,

$\bar{P}$ = mean pressure,

ΔP = pressure difference.

1.5.1 Slip Flow in Porous Media

Flow experiments using Darcy's equations have shown that air permeabilities are higher than liquid permeabilities when using the same porous medium. In the case of compressible fluids, the fluid velocity at the capillary walls does not reach zero, this eventually gives an increase in the flow rate. The phenomenon is called 'slip' and it is considered that Darcy's Law gives results of limited accuracy under this condition. For slip to occur, the necessary condition is that the pore diameters become comparable with, or less than, the molecular mean free path of the flowing gas [31].

Adzumi [20] and Klinkenberg [21] studied the anomalies observed in gas flow through porous media using molecular slip theory. Adzumi's approach to the problem was mainly theoretical. However, Klinkenberg based his theory mainly on experiments.

1.5.1.1 Semi-Empirical Adzumi Theory

Adzumi [20] used the theory of molecular slip in order to explain anomalies observed in gas flow measurements through porous media. His theoretical model was represented by a bundle of parallel capillaries with different lengths and diameters. He eventually derived an equation for gas flow through a porous medium using Knudsen's Law of slip [34] flow through a single capillary on his theoretical model. This equation is given as follows:

$$Q_2 = \frac{\pi \Delta P}{8\mu} \varepsilon \frac{\bar{P}}{P_2} + v \frac{4}{3} \sqrt{\frac{2\pi RT}{M} \kappa \frac{\Delta P}{P_2}} \qquad \dots [1.7]$$

where

v = Adzumi constant and is suggested to have a value of about 0.90 for single gases and 0.66 for a gaseous mixture,

n = number of pores in the cross-section of the porous medium,

$\bar{R}$ = average radius of the pores,

L = thickness of the porous medium,

ε, κ = constants, as given below:

$$\varepsilon = [\frac{n\bar{R}^4}{L}]$$

and

$$\kappa = [\frac{n\bar{R}^3}{L}]$$

1.5.1.2 Semi-Empirical Klinkenberg Theory

Klinkenberg [21] found that the permeability of a porous medium remained fairly constant for any type of liquid used. However, when gases were employed, the permeability changed with the applied pressure and the type of gas. In order to explain these discrepancies, he used slip theory and suggested a correction to Darcy's equation as follows:

$$Q_2 = k_d \frac{A}{\mu} \frac{\Delta P}{L} \frac{\bar{P}}{P_2} \qquad \dots [1.8]$$

where k_d gives apparent permeability for each different type of gas and applied pressure. This value can be defined by the following equations:

$$k_d = k_L \left(1 + \frac{b}{\bar{P}} \right) \qquad \dots [1.9]$$

$$k_d = k_L + k_L b \frac{1}{\bar{P}} \qquad \dots [1.10]$$

where

k_L = liquid permeability,

b = Klinkenberg constant which is different for each material depending on the structure of the pore system.

21

As seen from figure 1.2, when k_d is plotted against the reciprocal mean pressure, $1/\bar{P}$, it should yield a straight line with intercept equal to k_L and gradient $k_L b$ from which the Klinkenberg constant, b, can be obtained.
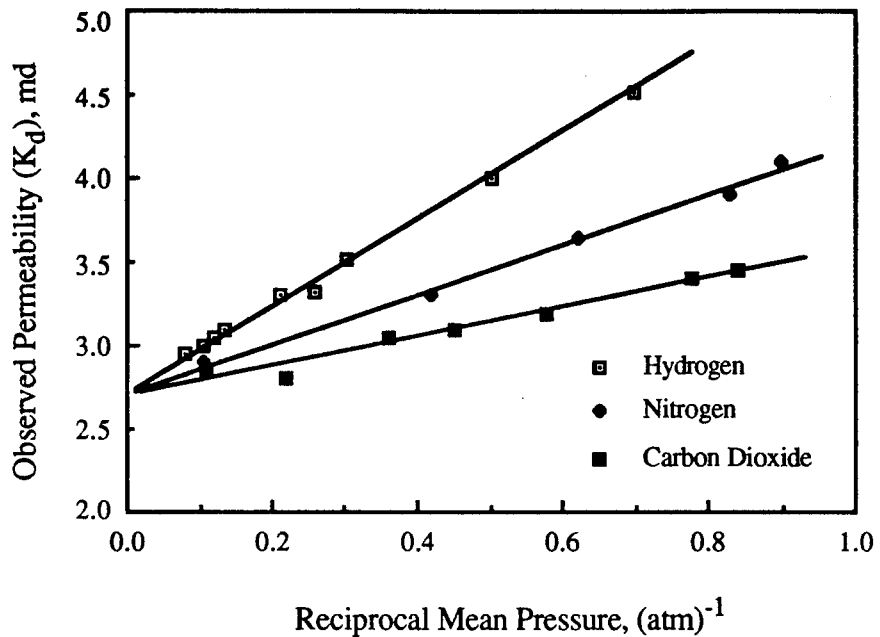
Figure 1.2 Permeability Constant of Core Sample 'L' to Hydrogen, Nitrogen, and Carbon Dioxide at Different Pressures (after Klinkenberg [21]).

Sowier [35] re-examined Klinkenberg's findings on the flow of different gases through porous media and concluded that liquid permeability was changed for different types of gas. He finally suggested the following equation for the apparent permeability of a medium:

$$K_d = K_I \left(1 + \frac{S}{\bar{P}} \right) \qquad \ldots [1.11]$$

where

K_I = coefficient of gas conveyance which changes for different gases,

S = a constant that varies with temperature.

1.6 Summary of the Assumptions

The main objectives of this research are to develop a reliable prediction method based on a mathematical approach to calculate strata methane flow into mine workings around a moving longwall face. Therefore, emphasis has been placed on the development and applicability of a prediction model to underground longwall mining rather than a more complex mathematical approach. The main reason for this is to show that the accuracy of such a prediction method is very much dependent upon the reliability of field data and applicability of the method rather than the degree of mathematical perfection. The gas flow simulation model to predict strata methane flow around a moving longwall face discussed in later chapters was based on the following assumptions:

i. Gas emission is mainly comprised by the strata gas.

ii. The effect of adsorption is ignored.

iii. Flow is laminar.

iv. Darcy's Law is valid.

v. Klinkenberg and Sowier effects (slip effect) are ignored.

vi. Flow is single-phased.

vii. Isothermal conditions exist.

viii. Methane obeys the perfect gas law (shows no abnormal compressibility).

1.7 Review of Mathematical Models for Methane Prediction

Since 1958 over thirty five distinct mathematical models for predicting methane flow from coal seams have been developed [36]. Most of these models were designed for vertical and horizontal degasification wells to predict methane flow from coal strata. Only a few of them allow full scale mining application. These models differ by the assumptions used in the formulations, the degrees of rigour used in the solutions, and finally, the capabilities considered by the models. The models are formulated either empirically or analytically and were solved by both analytical and numerical techniques. The numerical techniques include traditional finite difference, as well as method of lines and finite element methods. However, all these models can be classified by the treatment of the gas sorption (desorption/adsorption) process such as empirically based models, equilibrium (pressure-dependent) sorption models, and non-equilibrium (pressure and time-dependent) sorption models.

The most simple models are the empirically based models. These models are based on simple mathematical descriptions of observable physical phenomenon. Examples of empirically based models include Airy's first model, decline curves, Lindine's model, and the model of McFall et al. [36]. Although the empirical based models models are relatively simple, requiring few input parameters, they are limited by the assumptions and observations used in their development.

1.7.1 Equilibrium Sorption Models

Equilibrium (pressure-dependent) sorption models are theoretically derived models which account for the physics of the adsorption/desorption process. In this approach, it is assumed that gas desorption from coal surfaces and diffusion through the micropore system is sufficiently rapid, so that equilibrium with the gas phase pressure is continuously maintained. Consequently, these models are single porosity reservoir models. An approach of this type does not account for the time lag (time-dependence) incurred during transport through the micropore system. Non-equilibrium sorption models (pressure and time-dependent) take this transport into consideration. Examples of equilibrium sorption based models are given in figure 1.3 and a full discussion on these models can be found in King and Ertekin's comprehensive survey of mathematical models related to methane production from coal seams [36].

Of the models given in figure 1.3, Owili-Eger's model, from the Pennsylvania State University, was the first which use numerical techniques for the prediction of methane to full scale mining activities [14]. The model they developed assumed steady-state, single-phase, isothermal, and Darcian type of flow. Keen [12] and O'Shaughnessy [22], from Nottingham University, sought to apply numerical techniques to longwall mining by developing transient solutions for methane flow. Their research made use of equilibrium sorption models which are based on the assumption that adsorbed gas is in a continuous state of equilibrium with the free gas pressure. Keen used the finite difference method while O'Shaughnessy prefered the finite element method due to the inflexible nature of the finite difference method, particularly in the vicinity of boreholes.
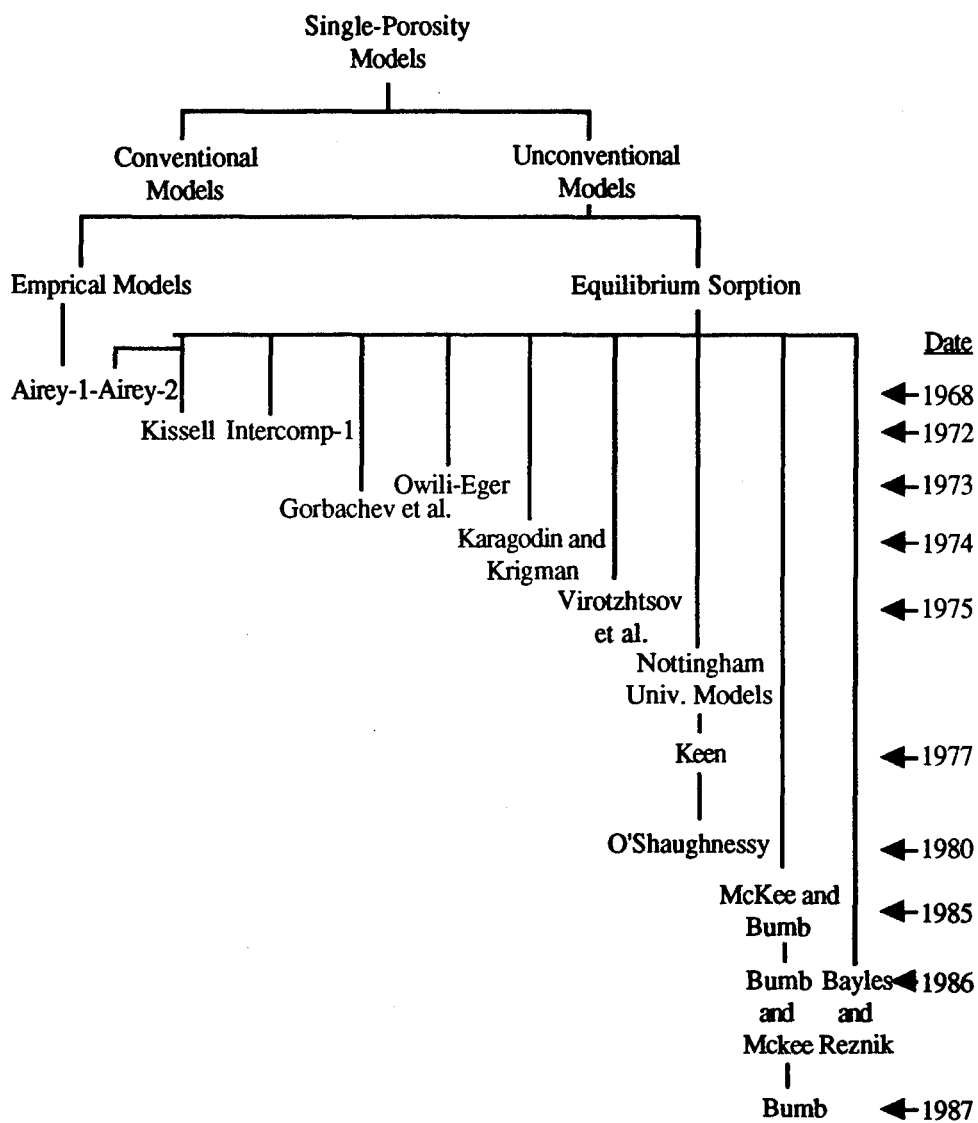
Figure 1.3 Relationships of Equilibrium Sorption Models (after King and Ertekin [36]).

1.7.2 Non-Equilibrium Sorption Models

Non-equilibrium sorption formulations are essentially modified forms of conventional dual porosity models [37]. These modifications to the conventional dual porosity models arise because;

i.   in coal seams methane is considered to be compressible,

ii. methane in the micropore structure of coal is in adsorbed state,

iii. gas transport through the micropore system is a diffusion process.

As with conventional dual porosity models, two approaches have been used to formulate coal seam models. Pseudo steady-state formulations use a discretized form of Fick's First Law to describe gas transport through the micropore system, while unsteady-state formulations use Fick's Second Law. The assumptions which are common to all non-equilibrium sorption models are given below:

i.   Coal has a dual porosity (micro and macro porosity) system.

ii. Water is regarded as a slightly compressible fluid and water flow in macro pores obeys Darcy's Law while gas transport through macro pores can obey Darcy's Law, Fick's Law or a combined form of these laws.

iii. Flow is isothermal and free gas behaves as a real gas.

iv. Gas transport through micropore system is a diffusional process. Pseudo steady-state transport is governed by Fick's First Law, while unsteady-state transport is governed by Fick's Second Law.

Examples of non-equilibrium sorption based models are given in figure 1.4 and figure 1.5, whose formulations and discussions also appear in the literature [37].

Among the models given in figure 1.4 and figure 1.5, those of Federov et al. and Kovaley and Kuznetsov include application to longwall mining. Federov used a single-phase pseudo steady-state flow model for simulating gas emission into a stationary mine face [38]. Kovaley and Kuznetsov's unsteady-state model calculated the rate of methane emission into an advancing longwall face [39] while the others were mainly designed for the prediction of methane flow from either single or full-field scale degasification wells.

Although non-equilibrium sorption models provide a better description of methane flow from coal, the equilibrium sorption approach was chosen due to its simplicity. It was thought that this would adequately serve the purpose to develop an applicable prediction model to underground longwall mining.
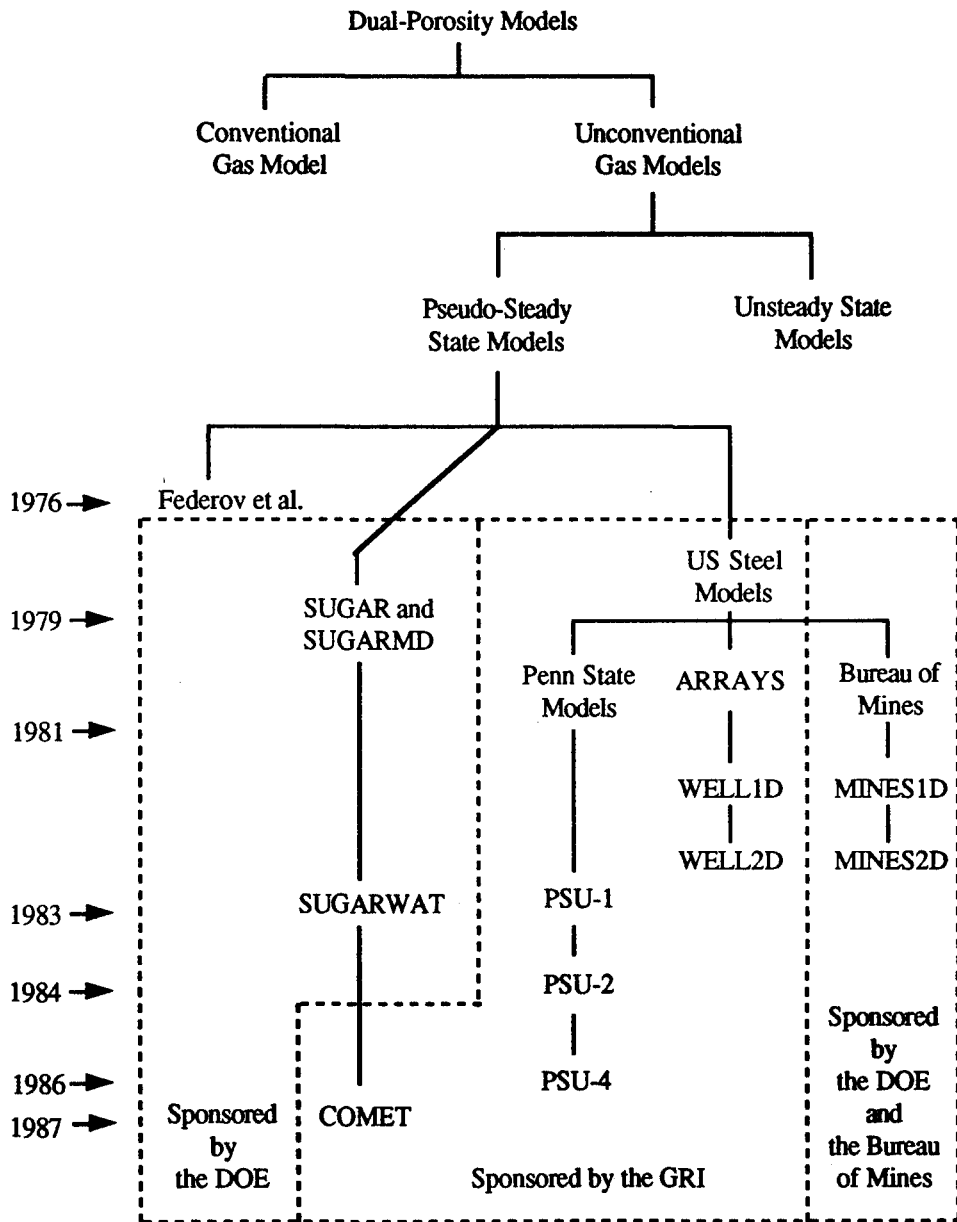
Figure 1.4 Relationships of Pseudo Steady-State, Non-Equilibrium Sorption
Models (after King and Ertekin [36]).
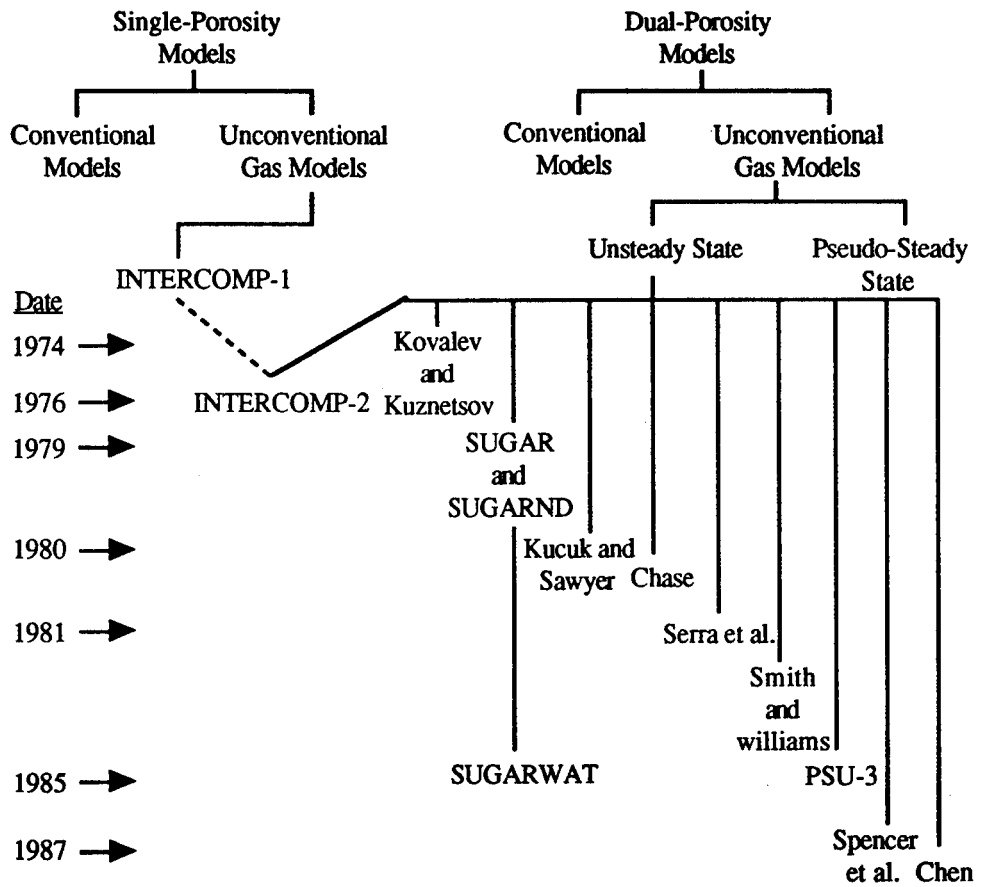
Figure 1.5 Relationships of Unsteady-State, Non-Equilbrium Sorption Models (after King and Ertekin [36]).

CHAPTER TWO

DERIVATION OF THE TIME-DEPENDENT GAS FLOW EQUATION

2.1 Introduction

Darcy's flow equation for compressible fluids as derived in chapter one is as follows:

$$Q_2 = \frac{k}{\mu} \frac{A}{L} \frac{\Delta P}{P_2} \bar{P}$$

This equation can be applied to a bed with constant thickness L and permeability k being percolated vertically by a compressible fluid with viscosity μ. However, this form of definitions has very restricted use because it allows only constant parameters. For more general applications it is necessary to write it in differential form.

This chapter deals with the differential definition of Darcy' flow equation given above.

2.2 Derivation of the Time-Dependent Gas Flow Equation

Consider an element of rock with anisotropic permeabilities k_x, k_y, k_z with respect to the x, y and z coordinate axes, as seen in figure 2.1. Darcy's Law states that:

$$\dot{m}_x = -\frac{kAP}{\mu RT}\frac{dP}{dx} \qquad \ldots [2.1]$$

where

$\dot{m}_x$ = mass flux in x-direction through an area A,

k   = permeability of the surface of area A,

A   = area,

μ = viscosity of fluid,

R   = gas constant,

P   = gas pressure.

Applied to the element shown in figure 2.1, in the x-direction this gives:

$$\dot{m}_x = -\frac{k_x \delta y \delta z}{\mu RT} P_x \frac{\partial P_x}{\partial x} \qquad \ldots [2.2]$$

$$\dot{m}_x + \delta\dot{m}_x = -\frac{(k_x + \delta k_x)\delta y \delta z}{\mu RT}(P_x + \delta P_x)\left(\frac{\partial P_x}{\partial x} + \delta\frac{\partial Px}{\partial x}\right) \quad \ldots [2.3]$$

32
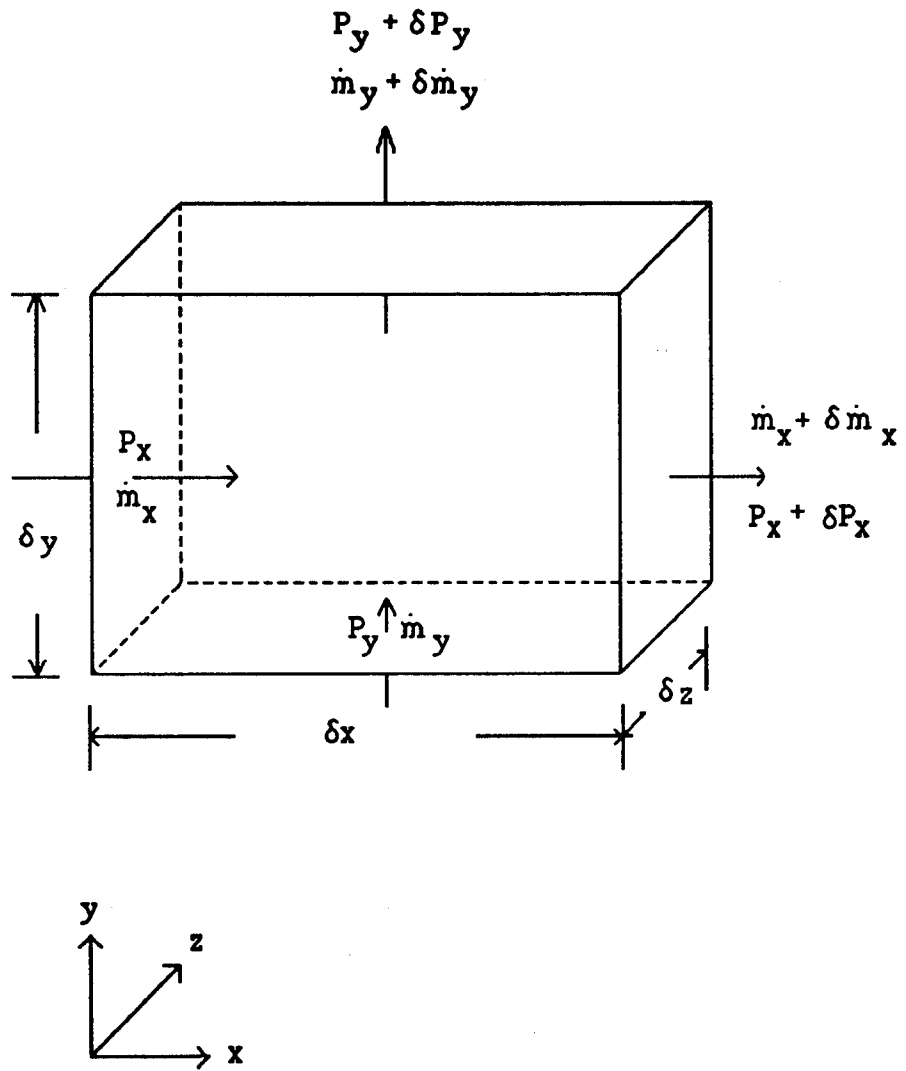
Figure 2.1 Element of Rock with Variable Anisotropic Permeability (after Keen [12]).

Therefore, by subtraction of equation 2.2 from 2.3

$$\delta \dot{m}_x = - \frac{\delta y \delta z}{\mu RT} \{ k_x \{ \delta P_x (\frac{\partial P_x}{\partial x}) + P_x \delta (\frac{\partial P_x}{\partial x}) + \delta P_x \delta (\frac{\partial P_x}{\partial x}) \}$$

$$+ \delta k_x \{ P_x (\frac{\partial P_x}{\partial x}) + \delta P_x (\frac{\partial P_x}{\partial x}) + P_x \delta (\frac{\partial P_x}{\partial x})$$

$$+ \delta P_x \delta (\frac{\partial P_x}{\partial x}) \} \} \qquad \ldots [2.4]$$

hence

$$\delta \dot{m}_x = - \frac{\delta y \delta z}{\mu RT} \{ k_x \delta P_x (\frac{\partial P_x}{\partial x}) + k_x P_x \delta (\frac{\partial P_x}{\partial x})$$

$$+ \delta k_x P_x (\frac{\partial P_x}{\partial x}) + O (\delta^2) \} \qquad \ldots [2.5]$$

A similar result may be derived in the y- and z- directions giving:

$$\delta \dot{m} = \delta \dot{m}_x + \delta \dot{m}_y + \delta \dot{m}_z$$

and

34

$$\delta\dot{m} = -\frac{1}{\mu RT} \{ \; \delta y \delta z \, [\, k_x \delta P_x \, (\frac{\partial P_x}{\partial x}) + k_x P_x \delta \, (\frac{\partial P_x}{\partial x}) + \delta k_x P_x \, (\frac{\partial P_x}{\partial x}) \,]$$

$$+ \delta x \delta z \, [\, k_y \delta P_y \, (\frac{\partial P_y}{\partial y}) + k_y P_y \delta \, (\frac{\partial P_y}{\partial y}) + \delta k_y P_y \, (\frac{\partial P_y}{\partial y}) \,]$$

$$+ \delta x \delta y \, [\, k_z \delta P_z \, (\frac{\partial P_z}{\partial z}) + k_z P_z \delta \, (\frac{\partial P_z}{\partial z}) + \delta k_z P_z \, (\frac{\partial P_z}{\partial z}) \,]$$

$$+ O\,(\delta^4) \; \} \qquad \qquad \dots [2.6]$$

From the continuity equation, a small increase in the mass is given by the product of the porosity, density and a small increase in volume, i.e.

$$\delta m = \phi \, \rho \; \delta x \delta y \delta z$$

so,

$$\delta\dot{m} = \phi \, \dot{\rho} \; \delta x \delta y \delta z$$

where

$\dot{m}$ = rate of change in mass,

$\dot{\rho}$ = density,

ϕ = porosity, which is assumed to be constant.

and the element has volume $\delta x \delta y \delta z$. Dividing equation 2.6 by $\delta x \delta y \delta z$ and ϕ gives:

$$\dot{\rho} = -\frac{1}{\phi\mu RT}\{[k_x\frac{\delta P_x}{\delta x}(\frac{\partial P_x}{\partial x}) + k_x P_x\frac{\delta(\frac{\partial P_x}{\partial x})}{\delta x} + \frac{\delta k_x}{\delta x}P_x(\frac{\partial P_x}{\partial x})]$$

$$+[k_y\frac{\delta P_y}{\delta y}(\frac{\partial P_y}{\partial y}) + k_y P_y\frac{\delta(\frac{\partial P_y}{\partial y})}{\delta y} + \frac{\delta k_y}{\delta y}P_y(\frac{\partial P_y}{\partial y})]$$

$$+[k_z\frac{\delta P_z}{\delta z}(\frac{\partial P_z}{\partial z}) + k_z P_z\frac{\delta(\frac{\partial P_z}{\partial z})}{\delta z} + \frac{\delta k_z}{\delta z}P_z(\frac{\partial P_z}{\partial z})]$$

$$+ O(\delta)\} \qquad \qquad \dots [2.7]$$

In the limit where

$$\delta x, \delta y, \delta z \to 0$$

$$\delta P_x, \delta P_y, \delta P_z \to 0$$

$$P_x, P_y, P_z \to P$$

then

$$\frac{\partial \rho}{\partial t} = \frac{1}{2\mu\phi RT}\nabla \cdot (\bar{k}\nabla P^2) \qquad \qquad \dots [2.8]$$

where $\bar{k}$ is the permeability tensor and is given as follows:

36

$$\begin{bmatrix} k_x & 0 & 0 \\ 0 & k_y & 0 \\ 0 & 0 & k_z \end{bmatrix}$$

For a perfect gas,

$$\rho = \alpha \, P^{1/n}$$

where n is the polytropic index of the process (n=1 if the conditions are isothermal).

$$\alpha = \left(\frac{\rho^{n-1}}{RT} \right)^{1/n}$$

Therefore, for isothermal conditions the following equations can be obtained:

$$\rho = \alpha \, P$$

$$\rho = \frac{1}{RT} \, P$$

$$\frac{\partial \rho}{\partial t} = \frac{1}{RT} \frac{\partial P}{\partial t} \qquad \qquad \dots [2.9]$$

substituting equation 2.9 into equation 2.8 we have

$$\frac{1}{RT}\frac{\partial P}{\partial t} = \frac{1}{2\mu\phi RT}\nabla.(\bar{k}\nabla P^2) \qquad \ldots [2.10]$$

or

$$\frac{\partial P}{\partial t} = \frac{1}{2\mu\phi}\nabla.(\bar{k}\nabla P^2) \qquad \ldots [2.11]$$

Equation 2.11 is the general time-dependent equation for a perfect gas with viscosity μ, flowing through an anisotropic porous medium with variable permeability $\bar{k}$ and porosity ϕ, in the absence of gravity.

2.3 Simplifications of the Equations

Depending on the physical circumstances in which gas flow is believed to occur, equation 2.11 may be simplified. For the simulation of methane flow through underground strata the equation to be applied should be the one which considers transient gas flow (dp/dt $\neq$ 0) through an anisotropic media with variable permeability (k is not constant). If there are circumstances, where these assuptions do not apply, equation 2.11 can be simplified accordingly. For example:

i. The steady-state approximation with isotropic permeability

In this case, the gas pressure remains constant with time, i.e. $\dfrac{\partial P}{\partial t} = 0$, and strata permeability does not vary directionally in the flow area, i.e. $k_x = k_y = k_z = k$.

$$0 = \frac{k}{2\mu\phi} \nabla^2 (P^2)$$

where k is a constant scalar. Hence

$$\nabla^2 (P^2) = 0$$

ii. The steady-state approximation with variable permeability

The same conditions as above apply but the gas flow area has variable anisotropic permeabilities, k_x, k_y, k_z = functions of x, y and z.

$$0 = \frac{1}{2\mu\phi} \nabla \cdot (\bar{k} \nabla P^2)$$

or

$$\nabla \cdot (\bar{k} \nabla P^2) = 0$$

iii. The transient case with isotropic permeability

In this case boundary conditions are not constant and gas pressure varies with time whilst media permeability remains isotropic, $k_x=k_y=k_z = k$.

$$\frac{\partial P}{\partial t} = \frac{k}{2\mu\phi} \nabla^2 (P^2)$$

iv. The transient case with anisotropic variable permeability

In mining situations gas pressure boundaries are subject to continuous changes and permeabilities are also differing throughout the mining area. Therefore, equation 2.11 should be used without any simplifications as given below.

$$\frac{\partial P}{\partial t} = \frac{1}{2\mu\phi} \nabla \cdot (\bar{k} \nabla P^2)$$

CHAPTER THREE

NUMERICAL SOLUTION OF THE TIME-DEPENDENT METHANE FLOW EQUATION

3.1 Introduction

The time-dependent gas flow equation for variable anisotropic permeability which was derived in the previous chapter can also be expressed as:

$$\frac{\partial p}{\partial t} = \frac{1}{2\mu\phi} \left\{ \frac{\partial}{\partial x_1} \left[k_1 \frac{\partial p^2}{\partial x_1} \right] + \frac{\partial}{\partial x_2} \left[k_2 \frac{\partial p^2}{\partial x_2} \right] + \frac{\partial}{\partial x_3} \left[k_3 \frac{\partial p^2}{\partial x_3} \right] \right\} \quad \ldots \text{[3.1]}$$

The solution of equation 3.1 is the key to a greater understanding of strata gas flow around mine workings since it was derived from Darcy's law, which is considered to be valid in the type of flow concerned under the assumptions made in chapter 1.

Equation 3.1 will therefore be taken to describe the transient methane pressures around the longwall in the model. The solution of time-dependent gas pressures will be used for the calculation of methane flow through strata into a roadway or borehole system.

3.2 Possible Solution Methods for the Gas Flow Equation

In the solution process for equation 3.1 two approximation techniques are available to model the differential equations, namely 'finite difference' and 'finite element' methods. Fundamental to both methods is the concept of discretization wherein a mesh of points, termed nodes, is specified, enabling a continuous domain to be represented as a number of contiguous sub-regions. The finite difference method defines approximations to a continuous solution at isolated nodes, whereas the finite element method is used to provide an approximate solution over the entire domain [40]. Consequently, when using the finite element method, it is not necessary to apply additional interpolation schemes to obtain a solution at an arbitrary point in the domain. Keen [12] used the finite difference method to solve the gas flow equation, but several problems, due to the inflexible nature of the finite difference method, particularly in the definition of the borehole boundaries, were encountered. In addition, there are a number of other difficulties pertaining to the computational techniques required in the solution process and Keen concluded that the method was completely inadequate as a solution technique for the gas flow equation.

The next solution technique to be considered is the finite element method which is widely used in the solution of a large number of engineering problems [41,42]. Keen and O'Shaughnessy [22] were successful in using the finite element method to solve the gas flow equation and therefore, it was decided to use finite element techniques for the prediction of gas flow around a longwall working.

3.3 Solution of the Time-Dependent Gas Flow Equation

Equation 3.1 can be reduced to a linear form for problems of practical interest, employing ϕ (= P^2), which will later be called field variable, as given below:

$$\frac{\partial}{\partial x}[k_x \frac{\partial \phi}{\partial x}] + \frac{\partial}{\partial y}[k_y \frac{\partial \phi}{\partial y}] + \frac{\partial}{\partial z}[k_z \frac{\partial \phi}{\partial z}] - c\frac{\partial \phi}{\partial t} = 0 \qquad \ldots [3.2]$$

where

$$c \quad = \quad \mu\phi \quad \text{(see equation 2.11)},$$

k_x, k_y, k_z = directional permeabilities.

The general solution of this type of differential equation is found by using a variational principle valid over the whole region [43]. The correct solution minimizes a functional which is defined by the integration of a function of the unknown quantities over the whole domain. The general functional for equation 3.2 which will be minimized, is given as:

$$\chi = \iiint\limits_R [\ \frac{1}{2}\ [k_x[\frac{\partial \phi}{\partial x}]^2 + k_y[\frac{\partial \phi}{\partial y}]^2 + k_z[\frac{\partial \phi}{\partial z}]^2] + c\frac{\partial \phi}{\partial t}\phi\ ]\ dxdydz . [3.3]$$

The true minimization of χ would require that

43

$$\frac{\partial \chi}{\partial \phi} = 0$$

If the field variable ϕ is defined element by element as given below:

$$\phi = \{ N \}^T \{ \phi \}^e \qquad \dots [3.4]$$

where

$\{N\}^T$ = shape function,

$\{\phi\}^e$ = listing of the nodal field values.

Then, differentiating equation 3.3 and employing equation 3.4, the following set of minimizing equations for the whole region is obtained [22]:

$$\frac{\partial \chi}{\partial \phi} = [S] \{ \phi \} + [M] \{ \frac{\partial \phi}{\partial t} \} = \{ 0 \} \qquad \dots [3.5]$$

where

$\{S\}$ = matrix representing spatially-dependent terms,

$\{M\}$ = matrix representing field variables.

3.4 The PAFEC'75 Program Package

Finite element programs have been written by many researchers and it is common practice to use existing generalized routines for the solution of equations. This, of course, reduces the amount of work required of users. The PAFEC program package contains thermal routines for the solution of the time-dependent equation for a temperature distribution [44,45].

$$\frac{\partial}{\partial x}[k\frac{\partial T}{\partial x}] + \frac{\partial}{\partial y}[k\frac{\partial T}{\partial y}] + \frac{\partial}{\partial z}[k\frac{\partial T}{\partial z}] - c\frac{\partial T}{\partial t} = 0 \quad \ldots [3.6]$$

This equation has certain similarities with the time-dependent gas flow equation, equation 3.1, if ϕ, the field variable, is set to T, the temperature, and $k_x = k_y = k_z$ to a constant k, the thermal conductivity. When the appropriate region has been discretized there will be only one parameter to be determined, namely the temperature, which is the equivalent of the square of the gas pressure from the gas flow equation.

After minimizing equation 3.6, the following system of equations can be obtained:

$$[S]\{T\} + [M]\{\dot{T}\} = \{Q\} \quad \ldots [3.7]$$

where

{T}   = vector of temperatures for each node,

[S]   = square symmetric matrix containing spatially-dependent terms,

[M]   = square symmetric thermal mass matrix,

$\{\dot{T}\}$ = vector of temperature derivatives with respect to time,

{Q}   = vector of heat fluxes which enter the structure at the nodes.

If {T} is partitioned to give,

$$\{T\} = \left\{ \begin{array}{c} T_a \\ T_b \end{array} \right\}$$

in which $\{T_a\}$ are the unknown temperatures and $\{T_b\}$ are the known temperatures, and since the time-dependent temperature derivatives, $\{\dot{T}\}$, are constrained to zero in the steady-state case, equation 3.7 becomes:

$$[S]\{T\} = \{Q\}$$

If [S] and {Q} are partitioned appropriately then the resultant system of equations becomes:

$$\left\{ \begin{array}{cc} S_a & S_b \\ S_b^T & S_b \end{array} \right\} = \left\{ \begin{array}{cc} T_a & Q_a \\ T_b & Q_b \end{array} \right\}$$

From the uppermost partition:

$$\{ T_a \} = [S_a]^{-1} [\{ Q_a \} - [S_b] \{ T_b \}] \qquad \dots [3.8]$$

To obtain the unknown temperatures, $\{T_a\}$, it is required to know the components of $\{Q_a\}$ which are specified by the package program itself. Having obtained $\{T\}$, the time-dependent temperature gradients, $\{\dot{T}\}$ can be calculated. If equation 3.8 is partitioned one has the uppermost partition as given below:

$$[M_a] \{ \dot{T}_a \} = \{ Q_a \} - [S_a] \{ T_a \} - [S_b] \{ T_b \} - [M_b] \{ \dot{T}_b \} \quad . [3.9]$$

Now, at time t=0 the initial temperature distribution $\{T_a\}_{t=0}$ and $\{\dot{T}_a\}_{t=0}$ can be found from equations 3.7 and 3.8. In the PAFEC'75 package the subsequent temperature distributions are found using the 'Crank-Nicholson' finite difference scheme which makes the approximations:

$$\{ T \} = [\frac{\{ T \}_t + \{ T \}_{t+\Delta t}}{2}]$$

$$\{ \dot{T} \} = [\frac{\{ T \}_{t+\Delta t} - \{ T \}_t}{\Delta t}]$$

where

Δt = the time step.

As noted previously, the gas pressure ($\phi=p^2$) obeys the same equation as the temperature, T, and therefore the same scheme can be used for a gas pressure distribution with appropriate mapping as given below:

$$p = +\sqrt{T}$$

$$\frac{\partial T}{\partial t} = \frac{\partial p^2}{\partial t}$$

$$\frac{\partial T}{\partial t} = 2p\frac{\partial p}{\partial t}$$

Substituting the above relationships into equation 3.2 and minimizing the appropriate functional gives a system equation:

$$[S]\{P^2\} + [M]\{\dot{P}\} = \{0\} \qquad \ldots [3.10]$$

Pressure derivatives with respect to time other than t=0 can be obtained by employing the 'Crank-Nicholson' method which makes the approximation:

$$\{P^2\} = [\frac{\{P^2\}_t + \{P^2\}_{t+\Delta t}}{2}]$$

$$\{\dot{P}\} = [\frac{\{P\}_{t+\Delta t} - \{P\}_t}{\Delta t}]$$

If the above approximations are substituted into the equation 3.10 then,

$$[M] \left[\frac{\{P\}_{t+\Delta t} - \{P\}_t}{\Delta t}\right] + [S][\{P^2\}_t + \{P^2\}_{t+\Delta t}] = \{0\} \quad .[3.11]$$

Solution of this set of non-linear equations can be computationally time consuming, therefore a simple alternative approach suggested by O'Shaughnessy [22], can be used by employing the following:

$$\{P\} = \{P\}_t$$

and

$$\{\dot{P}\} = \frac{1}{2} \left[\frac{\{P^2\}_{t+\Delta t} - \{P^2\}_t}{\{P\}_t \Delta t}\right]$$

Incorporating the above equations into equation 3.10 and re-arranging:

$$[M] \left[\frac{\{P^2\}_{t+\Delta t} - \{P^2\}_t}{2\Delta t}\right] + \{P^T\}_t [S]\{P^2\}_t = \{0\} \quad .[3.12]$$

hence

$$\frac{[M]}{2\Delta t}\{P^2\}_{t+\Delta t} = \frac{[M]}{2\Delta t}\{P^2\}_t - \{P^T\}_t [S]\{P^2\}_t \quad \ldots [3.13]$$

From equation 3.13 $\{P^2\}_{t+\Delta t}$ can be evaluated to give the time-dependent pressure distribution, after modification of the relevant routines of the PAFEC'75 package program. From now on, all references to the PAFEC'75 thermal solutions or routines will be taken as analogous to gas flow solutions, and the analogy of temperature for this will be gas pressure.

The modifications required for the solution of the time-dependent gas pressure distribution when using the thermal routines will be explained in chapter 6.

CHAPTER FOUR

STRESS-PERMEABILITY RELATIONSHIPS OF STRATA AND STRATA MECHANICS

4.1 Introduction

Permeability may be defined as the fluid conductivity of the strata under consideration, and can be subdivided into micro and macro permeability [28]. Micro permeability may be considered as the permeability of pores, whilst macro permeability can be defined as the permeability of the fissures in coal. Permeability should not be confused with porosity which governs the free methane storage capacity of coal [5].

The measurement of the permeability of coal or coal measure strata to methane flow is a difficult task. Ideally laboratory tests will give the original matrix permeability of the rock. However, to predict methane flow the in-situ strata permeability is required. This may be orders of magnitude greater than the matrix permeability [46]. Therefore, greater importance should be attached to the determination of strata permeability.

There is no doubt that the permeability of coal seams and adjacent strata has a considerable effect on the flow of methane. Research [47,48,49,50,51,52] has emphasized the significance of the effect of stress on permeability and gas

release from coal. Therefore, any attempt at simulation of methane emission through strata adjacent to a working coal face, should consider the question of permeability, since this is of the greatest importance to the ultimate reliability and accuracy of such a simulation.

4.2 Review of Stress-Permeability Relationship of Strata

The earliest inquiry into the effects of stress on the permeability of rocks was made by Fatt and Davis [48] in 1952. They studied the effect of overburden pressure on the permeabilities of eight different sandstones upon which hydraulic pressure was applied. Measurements showed that the specific permeability of sandstone decreased with increases in hydraulic pressure. At a hydraulic pressure of 20.70 MN/m^2 the permeability of the sandstone cores ranged from 59 % to 89 % of their permeability at normal pressure.

Patching [49] studied the effects of confining pressure on coal, and found that the permeability of the coal specimens was reduced by more than three orders of magnitude as the confining pressure was increased to 20.70 MN/m^2. He also examined the hysterisis of permeability as a specimen was loaded and unloaded and concluded that the permeability of coal was dependent upon its stress history.

Mordecai [50] carried out some laboratory tests to investigate the changes in the permeability of samples of coal measure strata which were triaxially stressed. He concluded that, on first applying a hydrostatic state of stress, permeability

markedly decreased (figure 4.1). Further stressing by means of increasing vertical load led to a further reduction of permeability until a minimum value was reached. Permeability then rose until the specimen failed.

He suggested that the application of stress first closes up permeable channels, then fractures begin to propagate leading to a rise in permeability. He also remarked that the magnitude of the confining pressure has a great effect on the stress-dependence of permeability. That is to say, the higher the confining pressure the greater the resulting decrease in permeability will be from the first application of a hydrostatic state of stress. It was a general observation from all the tests conducted on the various rocks, that the more impermeable the rock, the greater was the sensitivity of its permeability to stress.

In 1975, Sommerton et al. [51] studied the effect of stress on the permeability of coal by passing nitrogen through it axially, under various conditions of applied axial and radial stress. They also investigated the effect of flow direction on the permeability. Permeabilities were found to be strongly stress-dependent, decreasing by more than two orders of magnitude in the stress range of 9 to 70 MN/m^2. They concluded that the permeability of fractured coal was highly dependent on its stress history, decreasing in magnitude with each loading cycle except in cases where the applied stress caused further fracturing.

Recent research into the effects of triaxial stress on coal permeability was carried out by Gawuga [52], in 1979 , and Durucan [47], in 1980. Gawuga studied the effects of applied stress and gas pressure on the permeability of coal. Durucan investigated the stress-permeability relationship of coals and the

flow of methane around working longwall faces. He suggested that the axial permeability of coal, after failure at face stress conditions, would increase by a factor of 100-500.

It was recognized by Durucan that the permeability of coal was a controlling factor in the flow of methane around working longwall faces. It is therefore, necessary to determine the permeability changes under stresses which simulate the actual conditions created underground by mining operations (figure 4.2). In order to achieve this, an understanding of the stress disturbances in the strata around a working longwall face is required.

The latest study into the changes of stress and release of methane from longwall coal faces was carried out by Riley [28], in 1986. He attempted to explain the behaviour of a coal seam affected by mining-induced stresses, using a borehole monitoring system within the pillars, both on advancing and retreating faces. He concluded that the advancing face investigations were more closely related to the general behaviour of coal seams under stress. The nature of in-situ gas emission from coal and changes in stress were found to be more complex than had been indicated by previous laboratory measurements. In the field, the measured changes in the parameters of stress, gas pressure and gas flow were found to be rapid and dramatic, indicating a more dynamic process than previously considered.
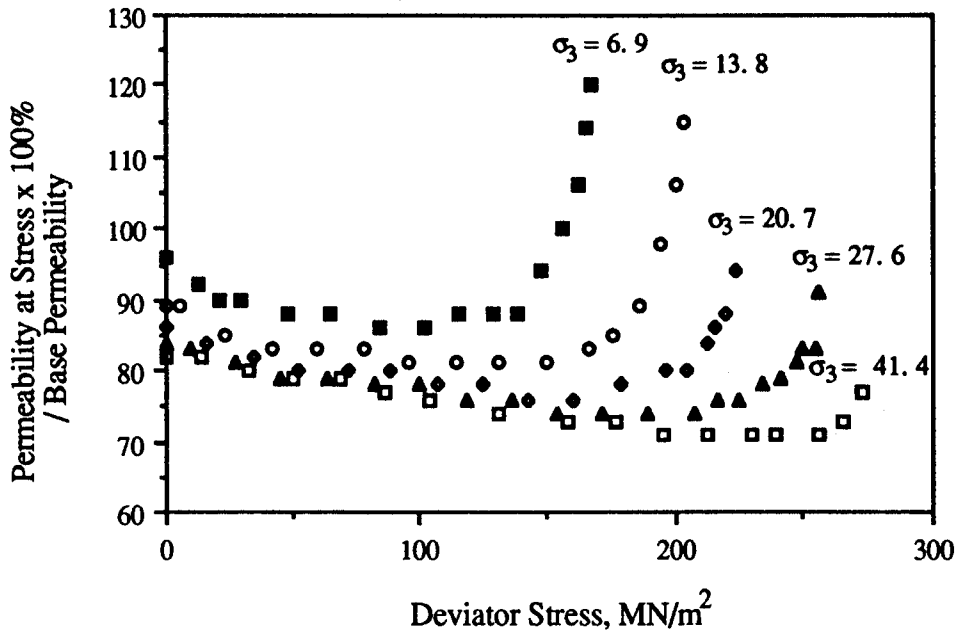
Figure 4.1 Stress-Permeability Curves for Darley Dale Specimens at Various Confining Pressures (after Mordecai [50]).
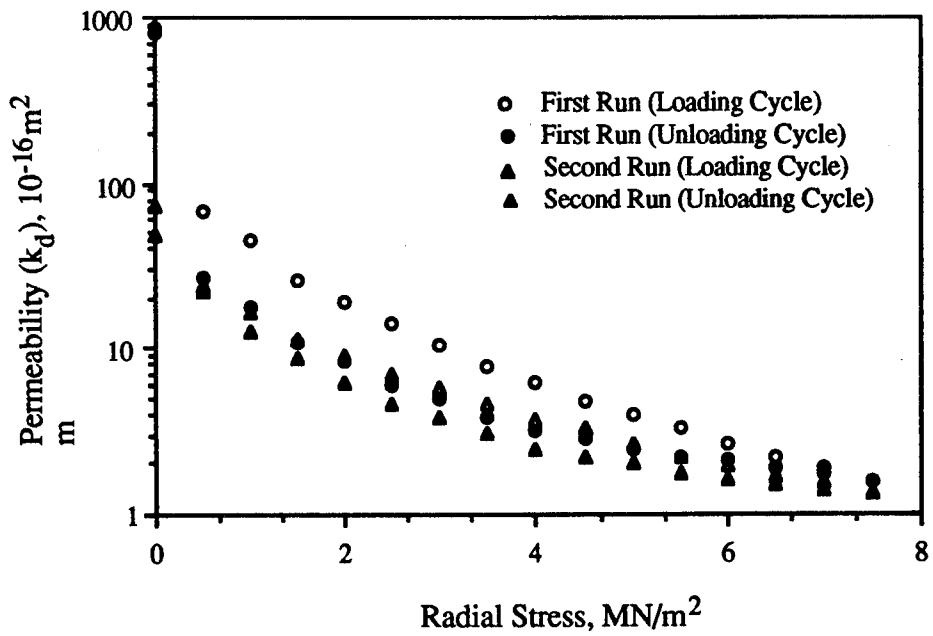
Figure 4.2 Effect of Stress-History on Permeability of Dunsil Coal (after Durucan [47]).

55

4.3 Post-Failure Stress-Permeability Relationships of Strata

As explained, previous research into the stress-permeability behaviour of coal seams has shown that the permeability of coal is mainly dependent on the state of stresses acting on the coal mass. It has also found that the extent of changes in the permeability of coal due to increasing or decreasing stresses varies from one coal seam to another depending on their inherent properties such as mechanical strength, elastic behaviour, rank etc [53]. It is therefore, important that the stress-permeability behaviour of strata should be studied in depth (in both in-situ and laboratory investigations) to achieve an understanding of methane flow through them.

This simulation model of methane flow considers the strata gas as the main source of gas entering the mine atmosphere other than the coal seam being worked. It is obvious that many parts of the mining area, especially the roof of the working level, are subject to some degree of failure, and most of the gas flow occurs through this failed area. The permeability of the strata to this gas flow is of course, quite different from its virgin or pre-failure values. There is the likelihood that fracture permeabilities are more dominant than strata permeabilities in this area. In any geological cross-section, the thickness of coal measure strata through which gases pass is much larger than the total thickness of coal seams. The above points indicate the need for further knowledge on the post-failure stress-permeability behaviour of coal strata (and coal) for such a simulation model. In fact, there has been some research showing pre and post-failure stress-permeability behaviour of different coal seams [53,54], and some for coal measures up to failure [48,49,50]. However, hardly any reliable data has been found for post-failure permeability behaviour of coal measure rocks [55].

4.4 Strata Mechanics Around a Longwall Coal Face

The concept of permeability, which is highly stress-dependent, is considered to be the most important factor in predicting the methane flow from strata. Permeability is also the main variable of the gas flow equation, equation 3.11, which was derived in the previous chapter. In order to obtain better results from the solution of the gas flow equation the main variable, the permeability of the strata, must be given as close to real in-situ values as possible.   It is therefore, necessary to achieve an understanding of stress fields around working longwall faces and to evaluate the induced-permeability values under these stress conditions. The results obtained from the solution of equation 3.1 can then be more representative and a comprehensive simulation of methane flow may be achieved.

Before mining commences, underground formations are loaded by the weight of the overlying strata, and the stresses are thus uniformly distributed. As coal is extracted, stress conditions on the longwall panel are readjusted and, at some stage, a new equilibrium is reached in the form of 'high' and 'low' pressure zones around a longwall face [56]. The high pressure zones are called 'pressure abutment zones' and are shown in figure 4.3. Although the exact location, width and magnitude of the stresses in the abutment zones are not known, a detailed knowledge about these factors is essential in determining the crucial changes induced in the permeability of the strata by the forward movement of the face. Whittaker [56] suggested that, in general, the magnitude of the peak abutment pressure would be 4-5 times the cover load. As seen from figure 4.3, in the vicinity of the face, where the roof is totally destressed, the vertical pressure would be reduced to much less than the cover load. Towards the waste
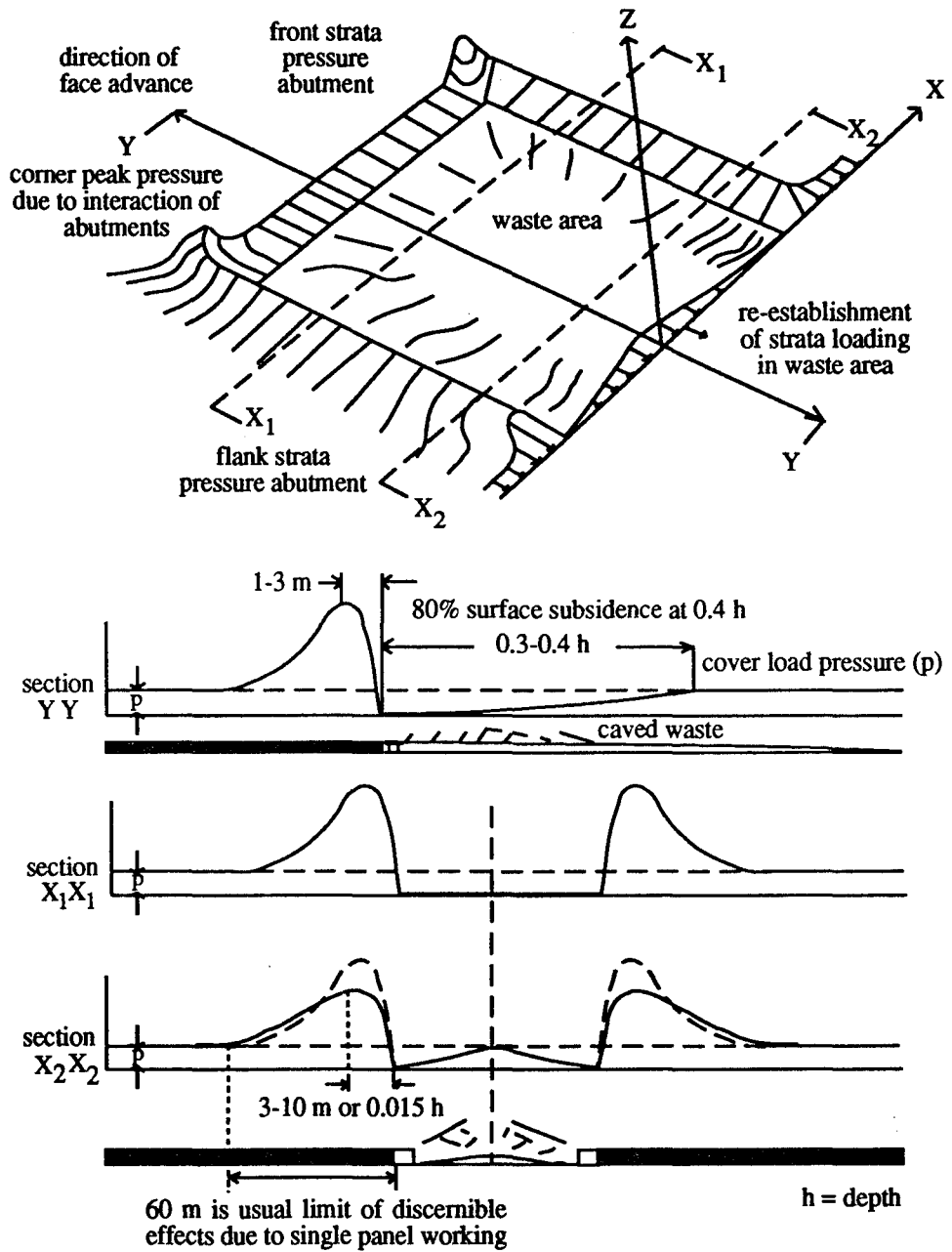
Figure 4.3 Strata Pressure Redistribution in the Plane of the Seam
Around a Longwall Face (after Whittaker [56]).

pressure gradually builds up on the cover load at a distance between 3/10 and 4/10 of the overburden thickness behind the faceline.

4.5 Principal Stresses Around a Longwall Face

The stresses on an element of material situated underground may be resolved into three principal stresses [57]. These stresses are at right angles to each other so that each of the principal stresses may be visualized as being on two opposite sides of a cube as shown in figure 4.4. When the three principal stresses are unequal then shear stresses are induced. These are given by a function of the difference of two principal stresses on the same plane.
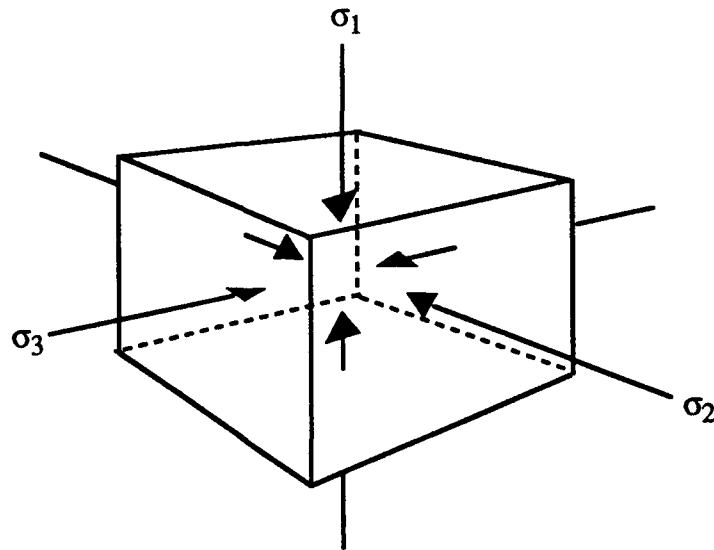
Figure 4.4 Principal Stresses on an Elementary Volume (after Hoek and Brown [57].

Stress systems likely to be experienced around a working face can be summarized as follows [47,58]:

i. <u>Triaxial compression in the coal seam</u>

$$[\sigma_1] > [\sigma_2] = [\sigma_3]$$

where

σ_1 = maximum principal stress,

σ_3 = minimum principal stress, $(\sigma_2 = \sigma_3)$.

ii. <u>A complex stress system at the face in which two of the stresses are compressive and the third is tensile</u>

$$\sigma_3 > 0 > \sigma_1 > \sigma_2$$

Coal seams will behave differently under the above stress conditions, and the structural changes occurring during these stages will dictate their permeability to gas. Generally, two types of fracturing and failure of coal can occur under these stress systems:

i. Triaxial compression or induced shear failure.

ii. Uniaxial compression or induced tensile failure.

60

4.5.1 Triaxial Compression or Induced Shear Failure

This type of failure occurs when the maximum principal stress becomes excessively high [58]. The maximum principal stress at failure, σ_1, can be given as:

$$\sigma_1 = \sigma_{ult} + \frac{1 + \sin\phi}{1 - \sin\phi}\, \sigma_3 \qquad \ldots [4.1]$$

where

σ_1 = maximum principal stress at failure,

σ_3 = compressive stress,

σ_{ult} = uniaxial compressive strength of the material,

ϕ = the internal friction angle of the material.

4.5.2 Uniaxial Compression or Induced Tensile Failure

Griffiths [59] was the first to show that the presence of cracks in a medium would serve to generate tensile stresses, even if a uniform compressive stress was exerted at the boundaries of a sample, as experienced in the crushing zone. Coal has three prominent crack systems, along the bedding planes, and the two cleat planes perpendicular to the beddings. When subjected to a uniaxial compressive stress, it is likely that one of these systems, parallel to the applied stress, will be affected by induced tensile stresses, and failure can

occur with the propagation of these cracks. When the coal seam is mined the high induced vertical stresses will cause tensile stresses in the horizontal plane of the newly exposed coal face. Therefore, coal is expected to fail in the area between the face and the front abutment zone.

The tensile stress induced on a disc specimen subjected to compressive stress is given as [58]:

$$\sigma_t = \frac{2\ P}{\pi\ D} \qquad \dots [4.2]$$

where

P   = load per unit length at right angles to the plane of the disc,

D   = diameter of the disc.

As a conclusion, studies on the maximum and minimum principal stress distributions around working longwall faces, have shown that the most important structural changes in coal seams are expected to occur in the front abutment zone due to triaxial compression, and in the crushing zone due to induced tensile fracturing.

4.6 Stress-Permeability Profiles for Strata Around Working Longwall Faces

McPherson [46] combined the theories of rock mechanics with the results of Mordecai's work [50] to produce a permeability profile of a longwall coal face as shown in figure 4.5. He suggested that the permeability of a coal seam would decrease in the stressed zone ahead of the face despite the fact that microfracturing would occur in this zone. The effect of macrofracturing would be to cause partial sealing of the interconnected pores within the coal. This would cause a further decrease in the already low permeability. Behind the face, where the rock is relaxed, there would be an increase in permeability by a few orders of magnitude due to the opening of microfractures, relaxation of normal cleavage, and planes of weakness between beds. This induced permeability provides the paths along which gas can flow. As the cover load is re-established, the permeability decreases, but to a level greater than its original value.

Durucan [47] produced a stress/permeability profile for a working longwall face, illustrated in figure 4.6. Referring to the figure, in the 'front abutment zone' both principal stresses are assumed to be compressive in nature and increasing towards the face. At 3 to 5 metres ahead of the face σ_1 is considered to reach its maximum value, whilst σ_3 decreases to become highly tensile causing fracturing of the coal seam. This zone,where permeability increases dramatically, is known as the 'crushing zone'. As seen in the figure, the state of the stresses in the 'stress relief zone', from the face into the waste, is very complex, and the maximum value of permeability is reached here. As the cover load is re-established the principal stresses are believed to take the form of
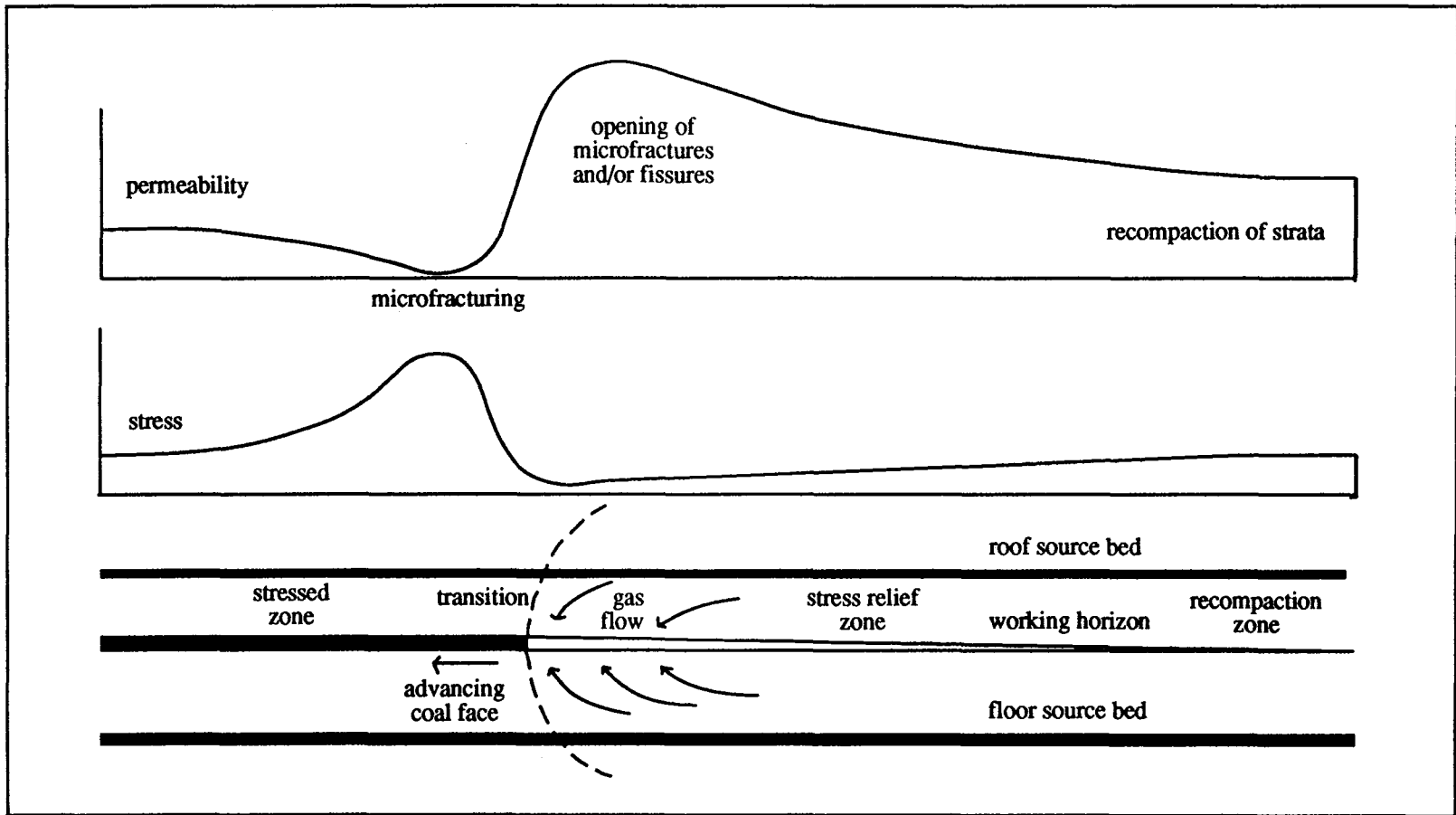
Figure 4.5 The Variation of Stress and Permeability in Strata Above and Below an Advancing Longwall Coal Face (after McPherson [46]).
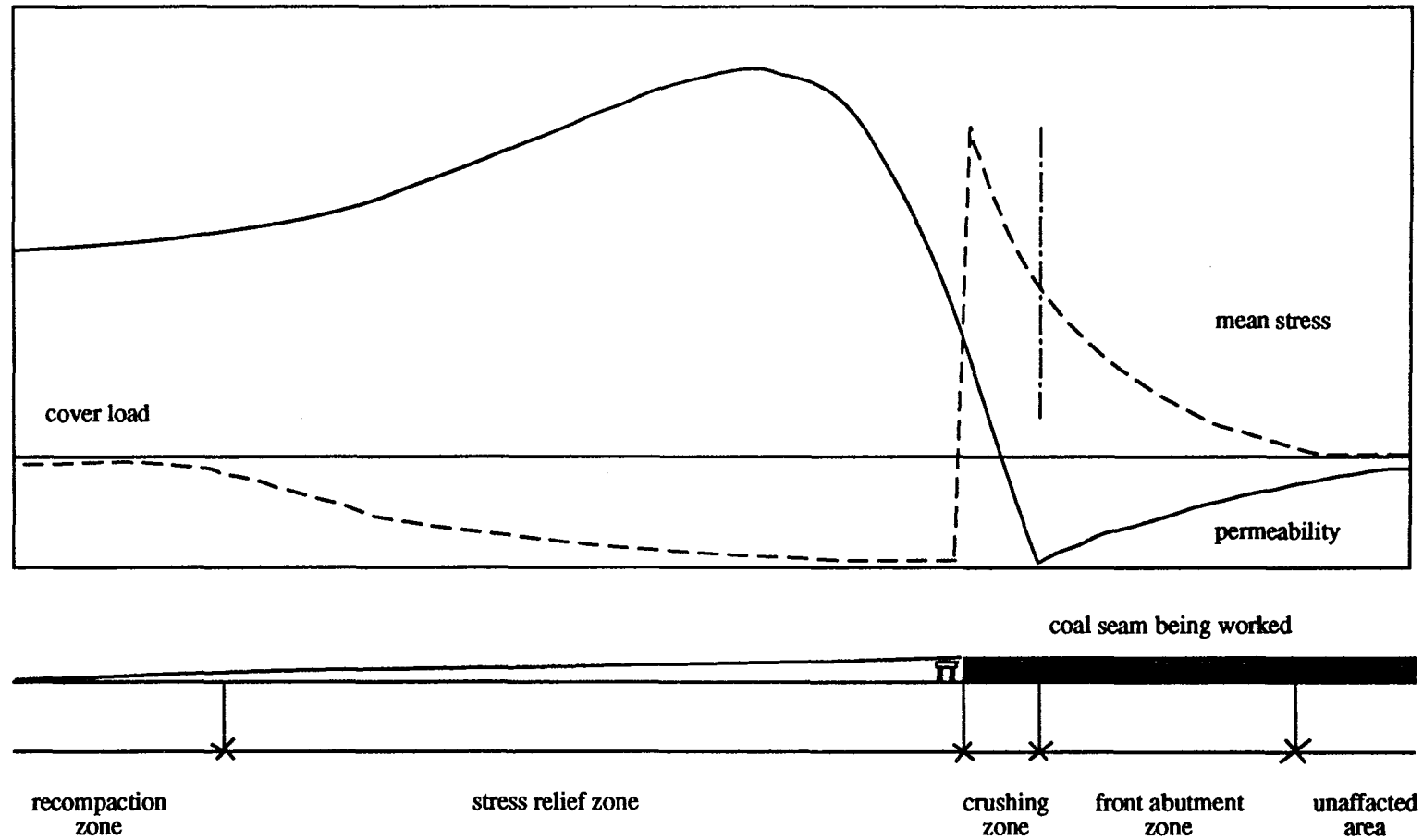
Figure 4.6 General Stress-Permeability Profile at the Roof Level of a Working Longwall Face (Not to Scale), (after Durucan [47]).

triaxial compression and permeability decreases. This area is known as the 'recompaction zone'.

Figure 4.7 shows the different permeability zones and the suggested flow paths of methane around a working longwall face which is assumed to be a new mining area [47]. Ahead of the face, the permeability values of coal seams are very low due to high abutment pressures. The outer boundaries of this low permeability zone are defined by the parabola on the right hand side of the figure. Permeability of coal seams will start to increase in the crushing zone which lies between the inner parabola and the maximum permeability line. Behind the face, points of maximum permeability will lie at angles of 60 and 45 degrees above and below the working horizon respectively. The majority of the gas, flowing into the working would be expected from areas behind these points, in which permeability remains very high. Coal seams at distances more than 100 m above, and 50 m below the working face are not expected to be highly affected by stress disturbances. The permeabilities of these areas will generally remain constant and very little gas flow takes place towards the workings.
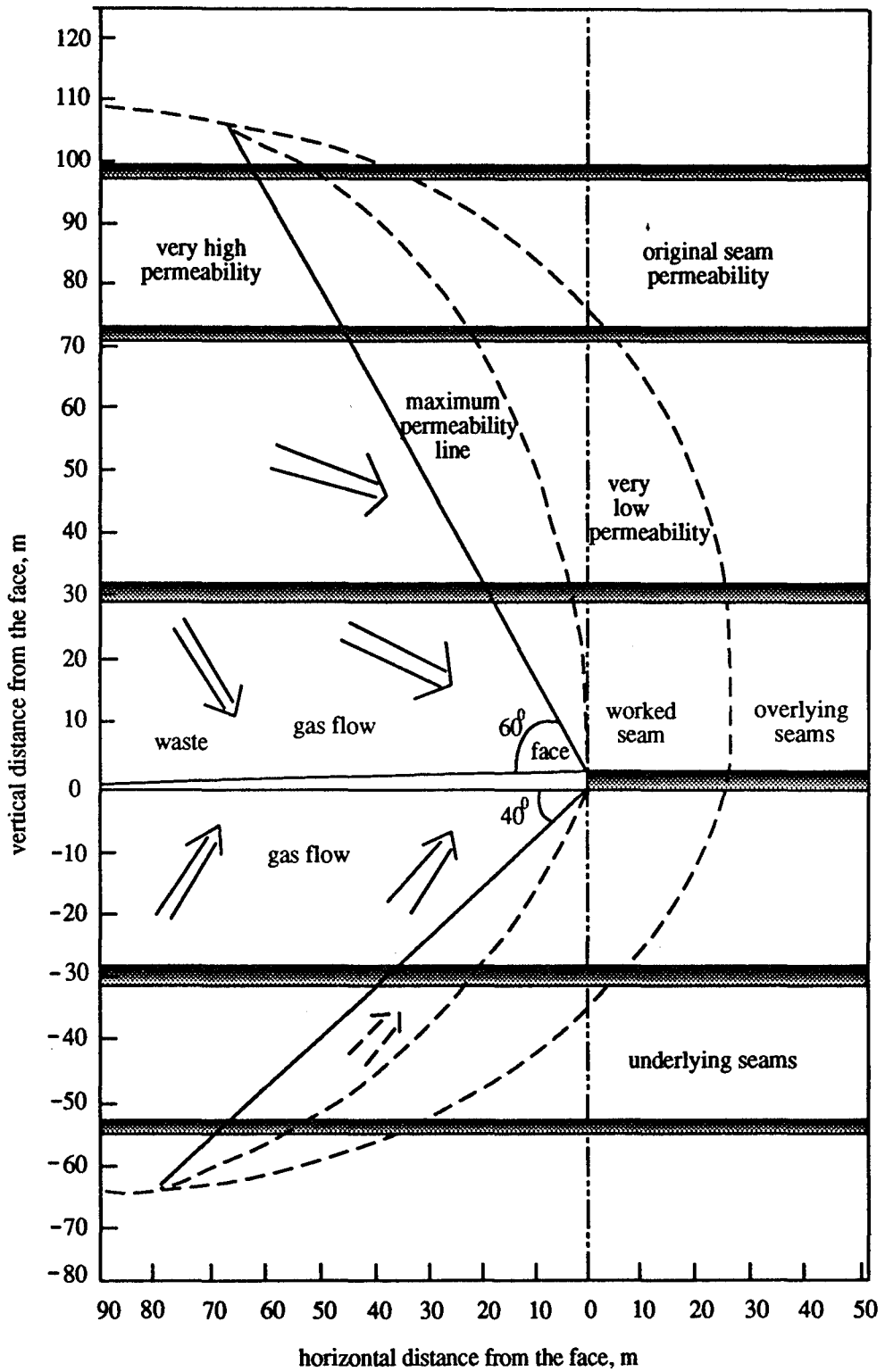
Figure 4.7 Different Permeability Zones and Suggested Flow Paths of Methane Around a Working Longwall Face (after Durucan [47]).

CHAPTER FIVE

STRESS ANALYSIS USING FINITE ELEMENT METHOD

5.1 Introduction

There is no doubt that the permeability of strata is a controlling factor in methane flow and it is also the main variable of the gas flow equation, equation 2.11, which will be used as a basis for the gas flow simulation. In order to obtain better results from solution of the gas flow equation, the main input, permeability of the strata, must be given as close to real, in-situ values as possible. Therefore, any attempt at simulation of methane emission should consider the question of permeability, since this is of the greatest importance to the ultimate reliability and accuracy of such a simulation.

Permeability is considered to be highly stress-dependent. Recent research has emphasized the significance of the effect of stress upon permeability, and upon gas release from coal. It is therefore, necessary to achieve an understanding of stress fields around working longwall faces and to evaluate the induced permeability values created by underground mining operations, under these stress conditions. The results from such a mathematical prediction model are then made more representative, allowing a comprehensive simulation of methane flow.

5.2 Stress Simulation Using Finite Element Techniques

The failure of the strata above large excavations results in a complex redistribution of stress around that excavation. The nature of these changes is important in terms of their effect on surface structures, hydrology, methane emission, and further mining. Many different techniques have been applied to assess the significance of mining parameters in terms of this stress redistribution. For example, physical modelling and direct measurement have shown distinctive failure patterns associated with longwall excavations. The finite element technique provides a powerful additional tool to assist in a fuller understanding of the nature of large scale ground movements. The finite element technique is well known for predicting elastic material behaviour, however, it is also possible to model non-linear material behaviour [60,61].

A structural problem can be systematically broken down into simpler parts called elements, the independent behavioural qualities of these parts being defined in terms of load, stiffness and displacement. These elements each satisfy a relatively simple relational equation. All element equations in a particular problem can be combined into a system of simultaneous equations which allows the solution of any load displacement relationships for the whole structure. The stress-strain relationship for the whole structure consists of many simultaneous equations each relating stress to strain for an element. The relationship between stress and strain can be either elastic or non-linear depending on the engineering material chosen [61]. The finite element method has been used successfully to analyse stress distributions around mining openings and to predict roadway closures and ground movements [61,62,63,64].

5.3 Stress Analysis Using PAFEC'75 Package Program

In order to analyse stress distributions around mining openings and evaluate induced permeabilities under these stress conditions, a finite element package program, PAFEC'75, has been used. This package was chosen because it was freely available on the University of Nottingham's main computing system. This package can be used to solve various structural engineering problems such as stress distribution for given loads, steady-state or transient temperature variations, creep behaviour, plasticity etc. The use of the package is very well documented and these documents are readily available at the University [44,45].

In order to define the physical structure of the model there are several element type options. In the analysis 8-noded rectangular, and 6-noded triangular element types have been used for the ease of definition (figure 5.1 and 5.2). In areas where stresses are likely to vary rapidly small elements are used, whereas large element sizes are used where stresses either do not vary much or where high precision is not needed.
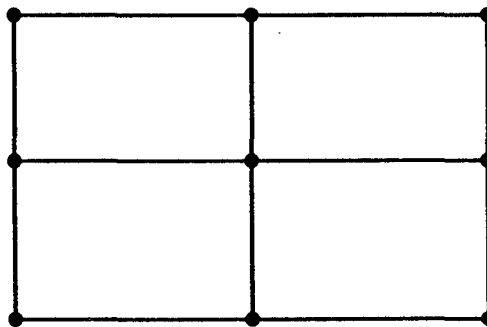
Figure 5.1 8-Noded Rectangular Stress Calculation Element Type.
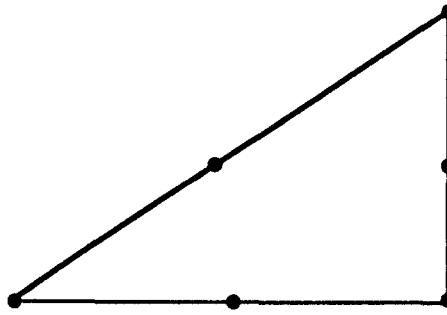
Figure 5.2 6-Noded Triangular Stress Calculation Element Type.

Vertical and horizontal stresses are generated using the GRAVITY module, which calculates stress as a function of depth and material type (defined by Poisson's ratio and density). Known pressures can also be given manually to the structure using the PRESSURE module. Goaf material properties have a profound effect on stress calculation. It was not possible to define the goaf material as weak as was required, using the material properties in the PAFEC package, since unrealistic stress concentrations were produced. The best results were obtained by assuming the goaf area to be an open space, thus unable to generate anomalous stress distributions.

As a practical example of the use of these numerical techniques the geology of the Great Row seam at Silverdale Colliery was modelled (figure 5.3). The geological section of Silverdale is given in appendix 1. The depth of mining and the seam thickness were taken as 773 m, and 3 m respectively. The typical width of faces in the Great Row seam is 220 m and coal production averages 20,000 tonnes/week with retreats rates of up to 35 m a week. The nearest seams to the Great Row are the unworked Spencroft seam lying approximately 30 m above and the unworked Cannel Row seam lying 14 m below.

737 m
739 m — spencroft seam
770 m
773 m — great row seam
785 m
788 m — cannel row seam

other strata
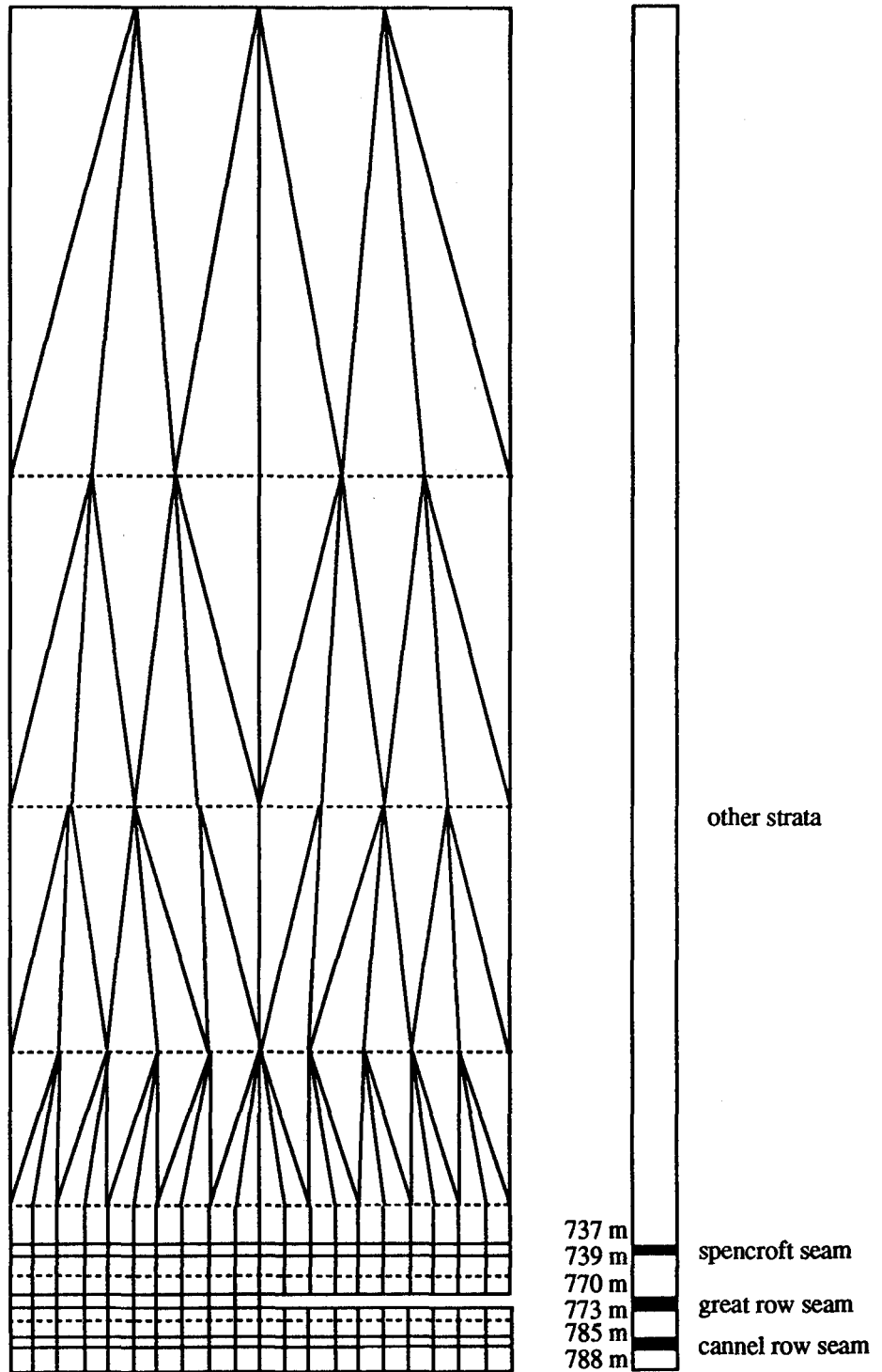
Figure 5.3 Finite Element Mesh Used.

72

As this analysis was carried out under the assumption of elastic conditions, greater vertical stresses were obtained than can occur in practice, especially in the front abutment zone where failure is expected. In fact, if the stress concentration is higher than the strength of the material, the rock will fail in that area, forming a yield zone [62]. In an attempt to obtain more realistic stresses, the analysis was done employing plastic conditions for critical areas. When used only for the front abutment zone the small advantage given by plastic analysis was still outweighed by the complexity involved and the greatly increased computing time required.

A sample set of data, prepared for the stress analysis, is given in appendix 2. The results obtained from the stress analysis were shown graphically and were used to assess the permeability values of strata for the gas flow simulation.

In the assessment of the induced permeability values for underground strata, three dimensional stress-permeability patterns around longwall coal faces are considered with respect to the face/strata position (see chapter 4) together with available laboratory data describing the relationships between stress and permeability for coal seams and coal measure strata. In order to make better use of the stress analysis results, considerable time has been spent in finding reliable data, especially for coal measure strata, on the stress-permeability relationship, including the post-failure relationship. In fact, there has been some research for coal, and coal measure rocks up to failure, but none for coal measures after failure [24,47,50,53,54]. All gas emissions in the model are considered to be from strata other than the coal seam being worked, and the changes in permeability after failure are more significant than pre-failure changes. The above indicates the need for research into the post-failure stress-

permeability relationship for coal measure rocks. This would not only improve understanding of gas flow mechanisms through strata affected by underground mining, but would also improve the reliability of the current model.

5.4 Results of Stress Analysis

Stress analysis has been performed several times using the finite element method, with conditions as given above, figure 5.3. From these analyses maximum and minimum stress distributions around a mining area were obtained graphically, figures 5.4 to 5.7. Moreover, stress distributions at different levels above and below the mining area were given to show the areas in which critical stresses occur, figures 5.8 to 5.19.

The stress analysis results were eventually used to evaluate induced permeability values of the strata for the gas flow analysis. This was done by comparing the stress results to laboratory work, describing the relationship between stress and permeability. The assessed permeability distributions for several strata levels are shown in figures 5.20 to 5.25.

Max Stress
/10^8
A 0.59
B 0.53
C 0.47
D 0.41
E 0.35
F 0.28
G 0.22
H 0.16
I 0.10
J 0.03
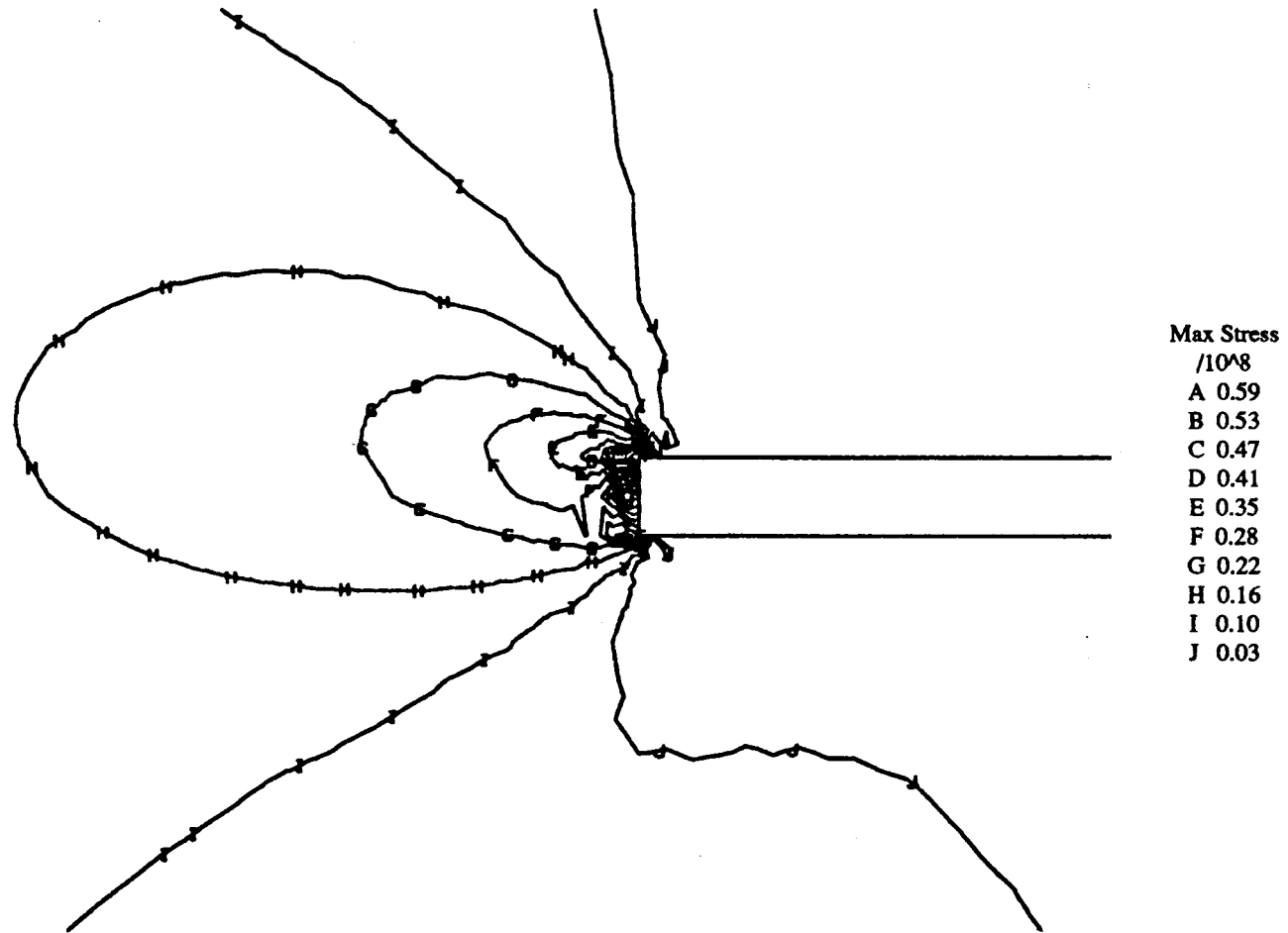
Figure 5.4 Maximum Stress Distribution Around a Mine Opening.

Min Stress	
/10^8	
A	1.90
B	1.73
C	1.57
D	1.40
E	1.24
F	1.07
G	0.90
H	0.76
I	0.57
J	0.40
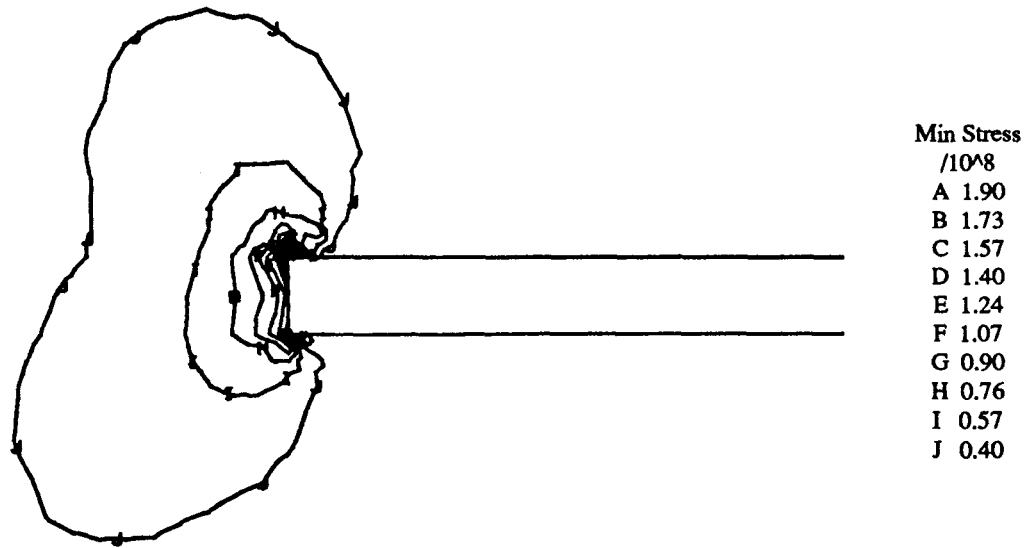
Figure 5.5 Minimum Stress Distribution Around a Mine Opening.
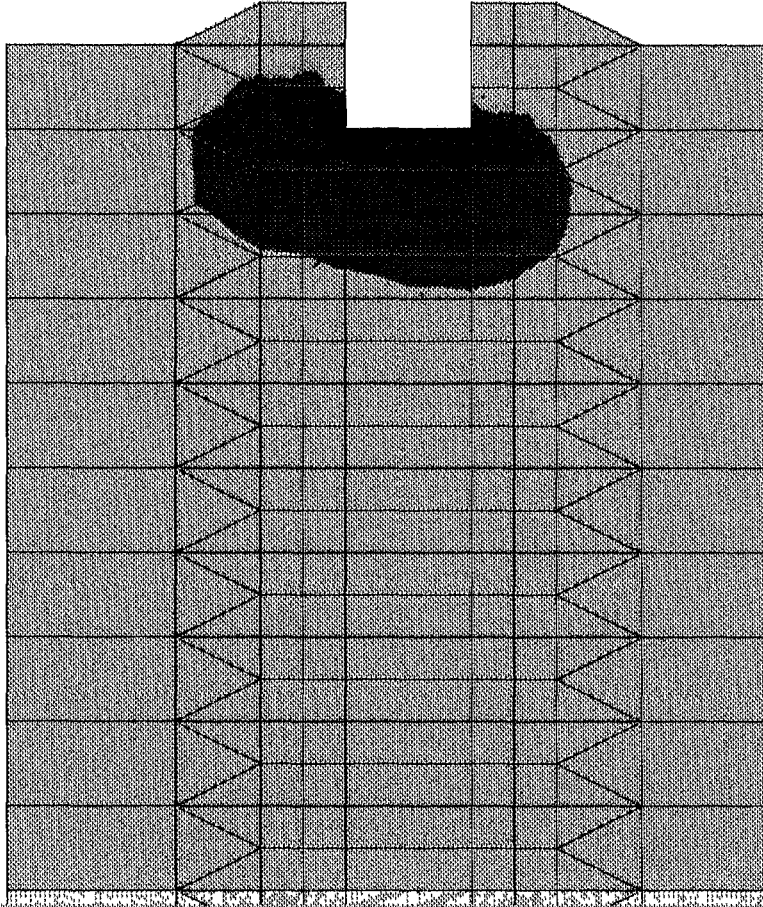
MIN STRESS DIVIDED BY 10 TO THE POWER =7
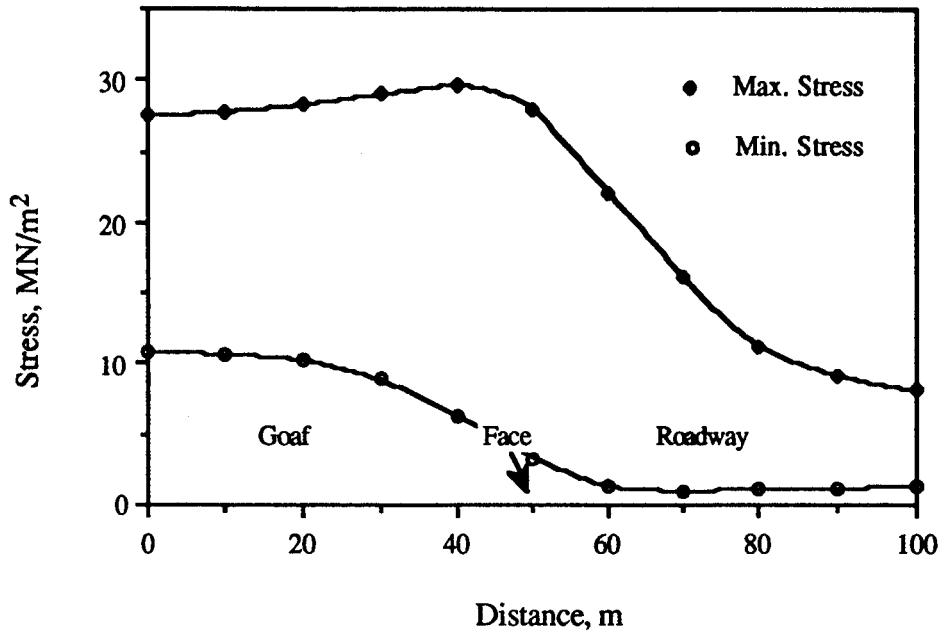
Figure 5.8 Maximum and Minimum Stress Distribution at a Level of 24 m
Above the Roof of the Mine Opening.
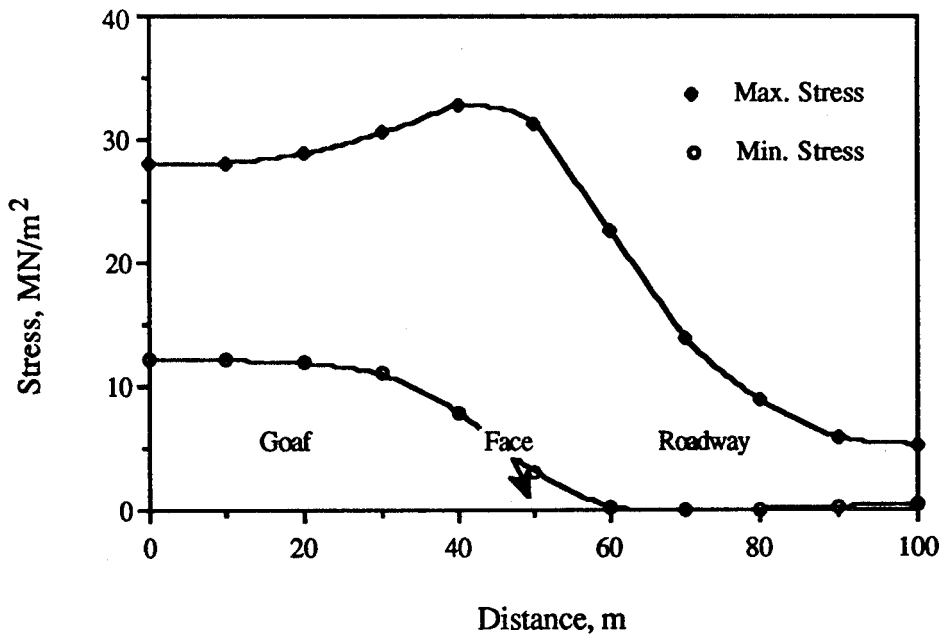
Figure 5.9 Maximum and Minimum Stress Distribution at a Level of 17 m
Above the Roof of the Mine Opening.

79
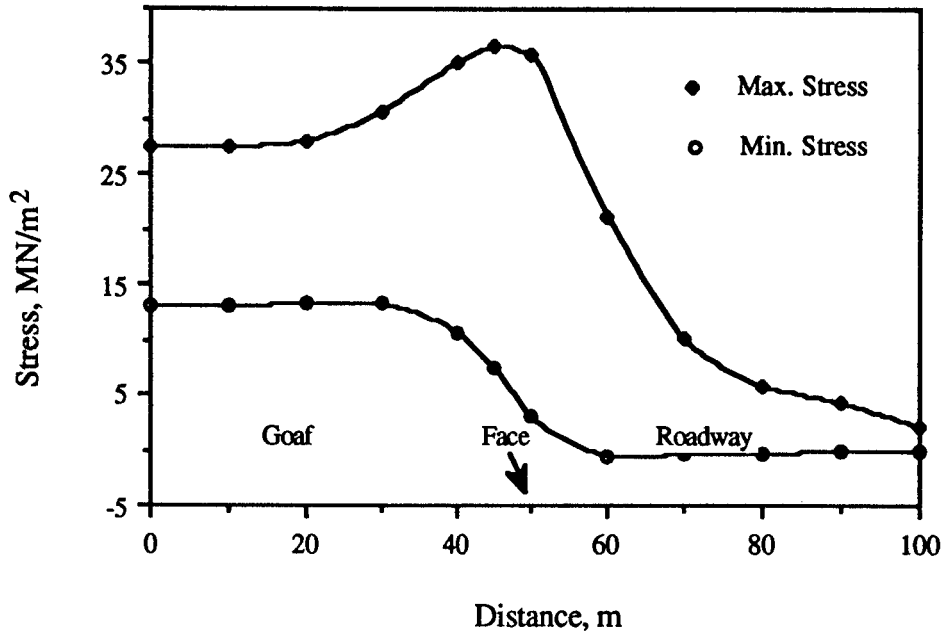
Figure 5.10 Maximum and Minimum Stress Distribution at a Level of 12 m
Above the Roof of the Mine Opening.
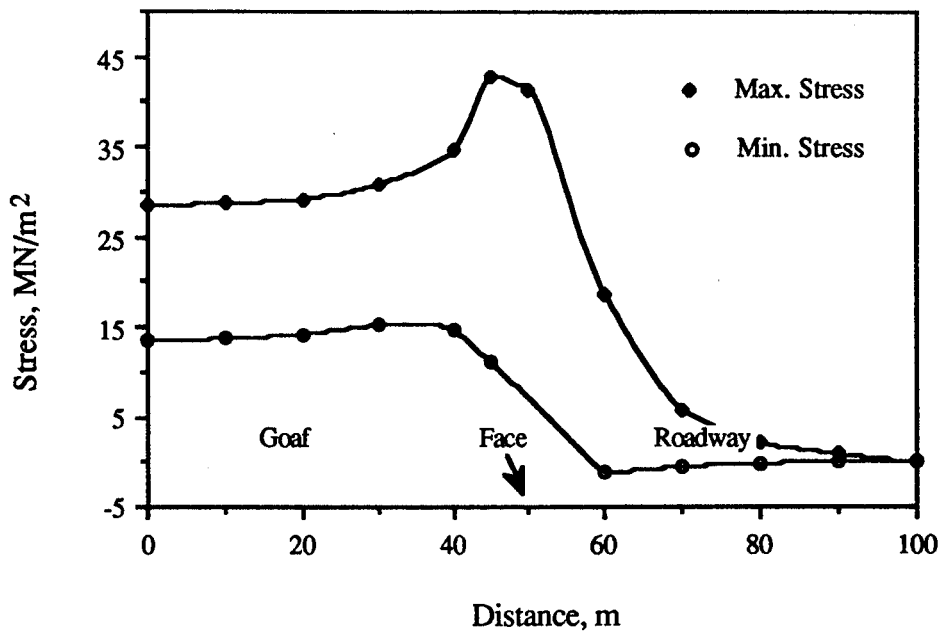
Figure 5.11 Maximum and Minimum Stress Distribution at a Level of 8 m
Above the Roof of the Mine Opening.

80
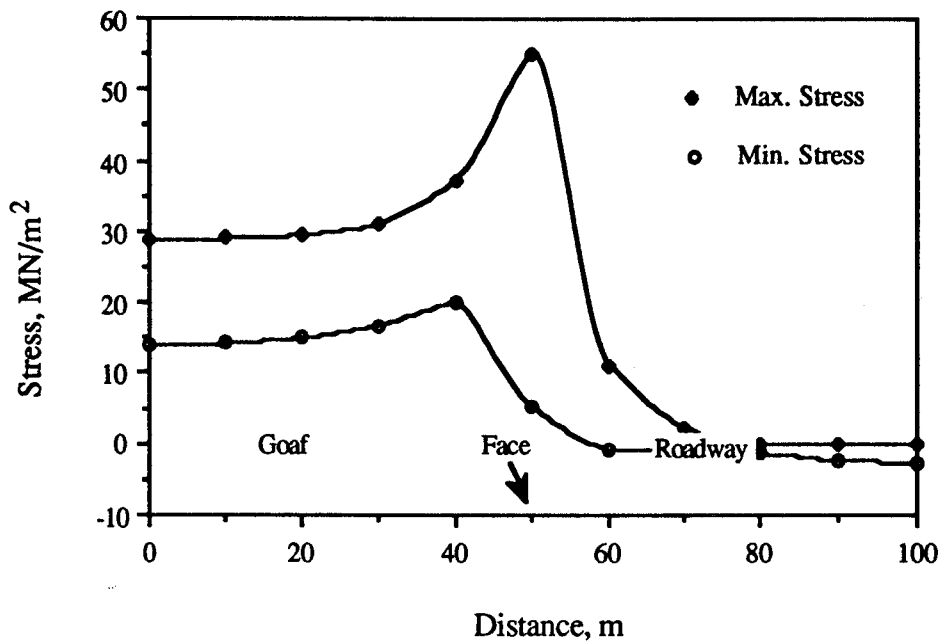
Figure 5.12 Maximum and Minimum Stress Distribution at a Level of 4 m
Above the Roof of the Mine Opening.
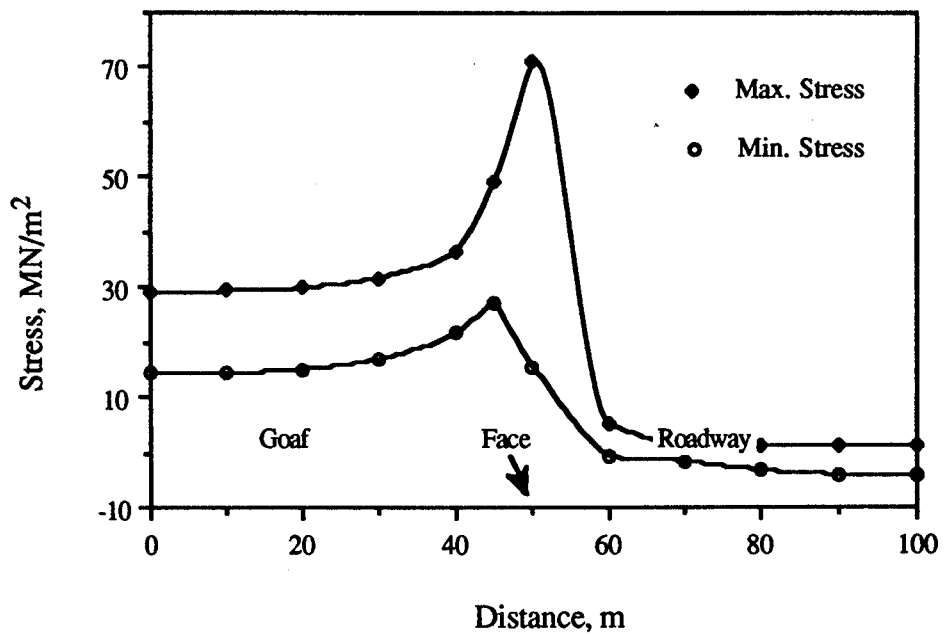
Figure 5.13 Maximum and Minimum Stress Distribution at a Level of 2 m
Above the Roof of the Mine Opening.
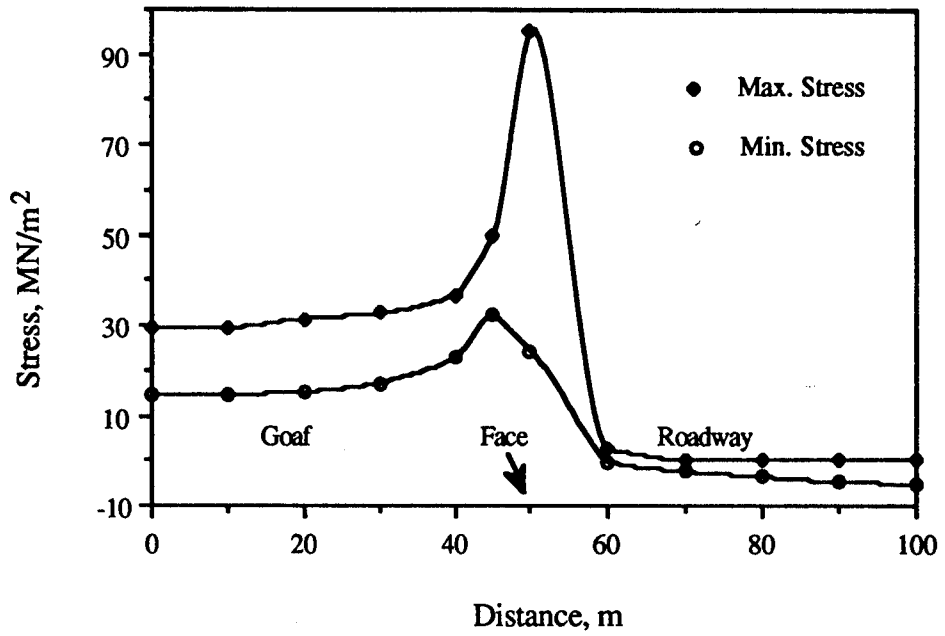
Figure 5.14 Maximum and Minimum Stress Distribution at a Level of 1 m
Above the Roof of the Mine Opening.
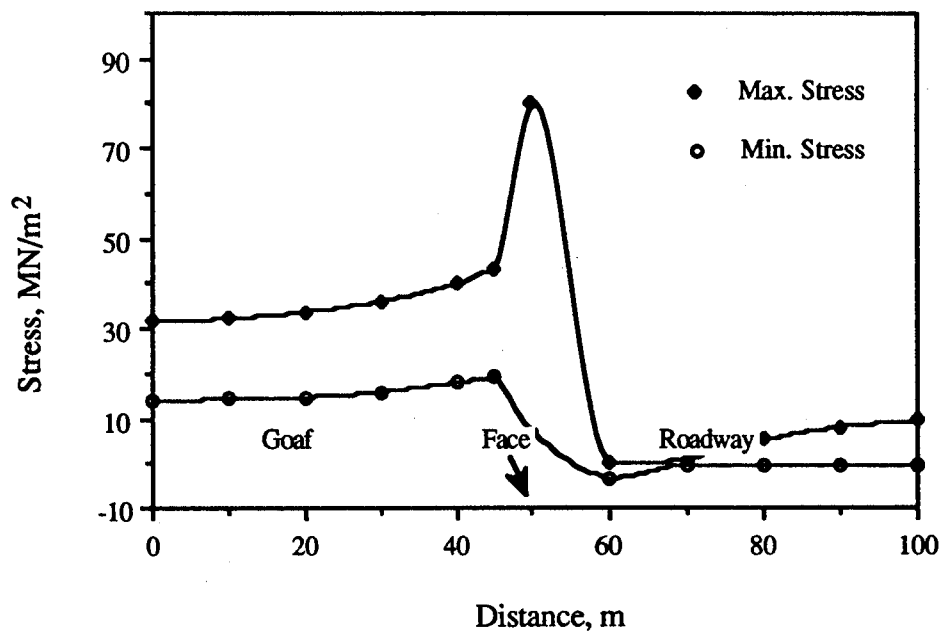
Figure 5.15 Maximum and Minimum Stress Distribution at a Level of 1 m
Below the Floor of the Mine Opening.

82
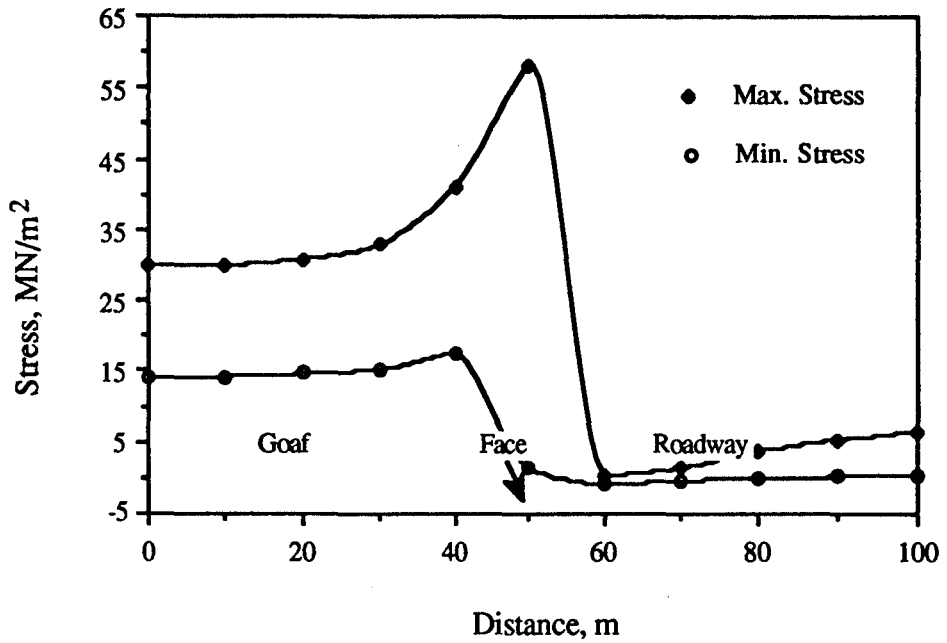
Figure 5.16 Maximum and Minimum Stress Distribution at a Level of 2 m
Below the Floor of the Mine Opening.
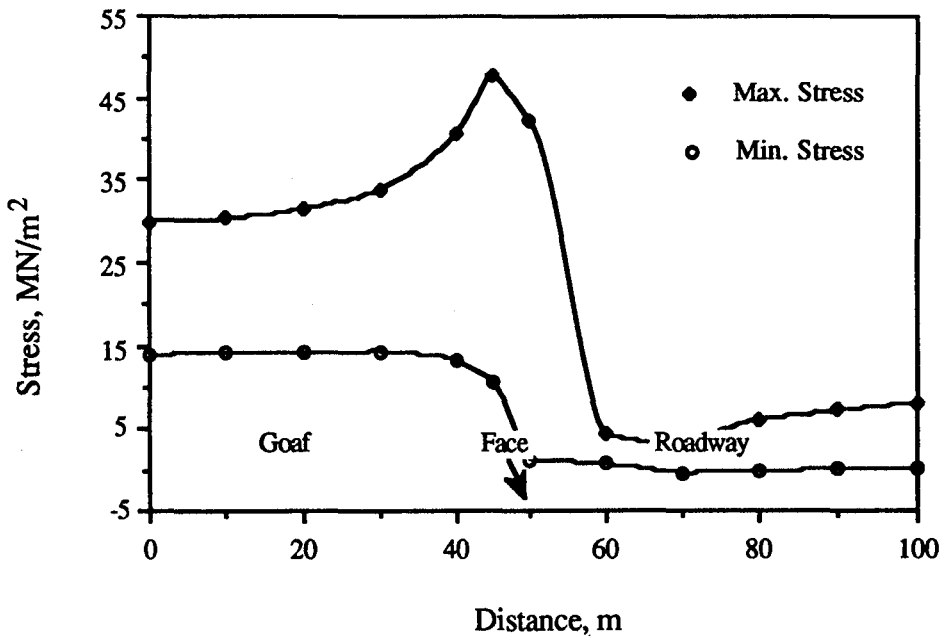
Figure 5.17 Maximum and Minimum Stress Distribution at a Level of 4 m
Below the Floor of the Mine Opening.
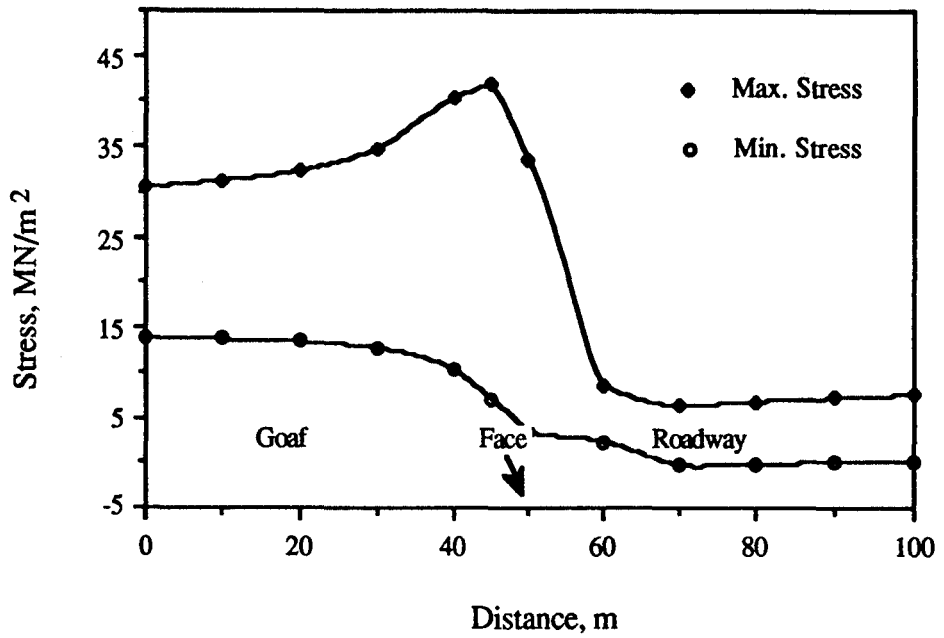
Figure 5.18 Maximum and Minimum Stress Distribution at a Level of 7 m
Below the Floor of the Mine Opening.
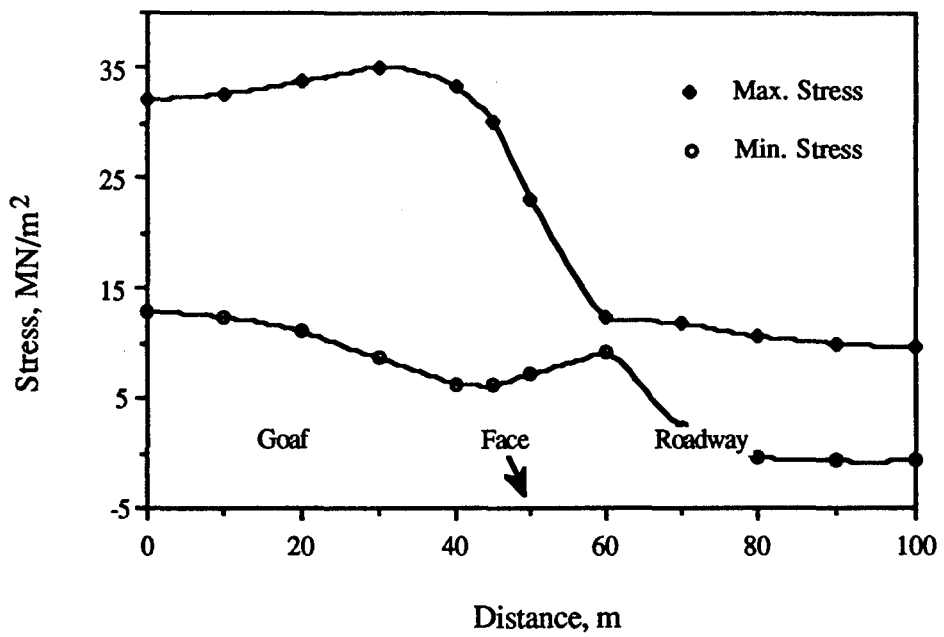
Figure 5.19 Maximum and Minimum Stress Distribution at a Level of 21 m
Below the Floor of the Mine Opening.

84
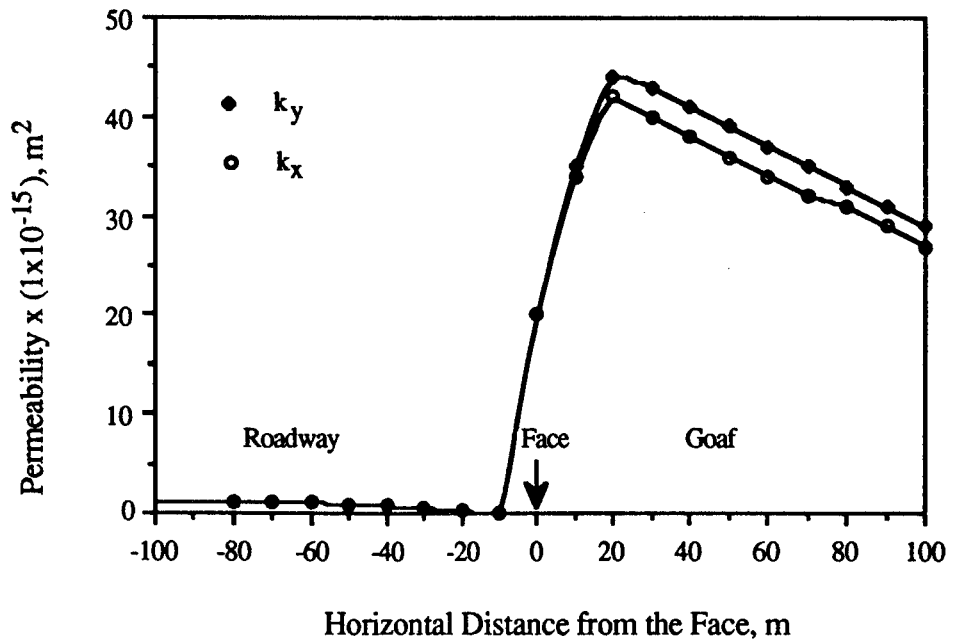
Figure 5.20 Permeability Variations at a Level of 0 - 7.5 m above the Working
Level (Sandstone).
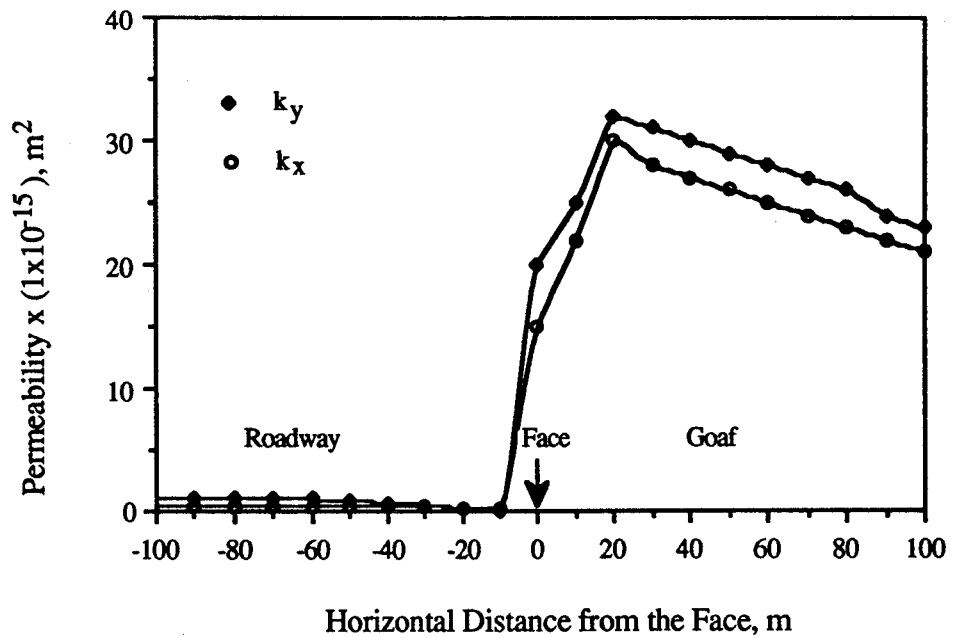
Figure 5.21 Permeability Variations at a Level of 7.5 - 15 m above the
Working Level (Sandstone).
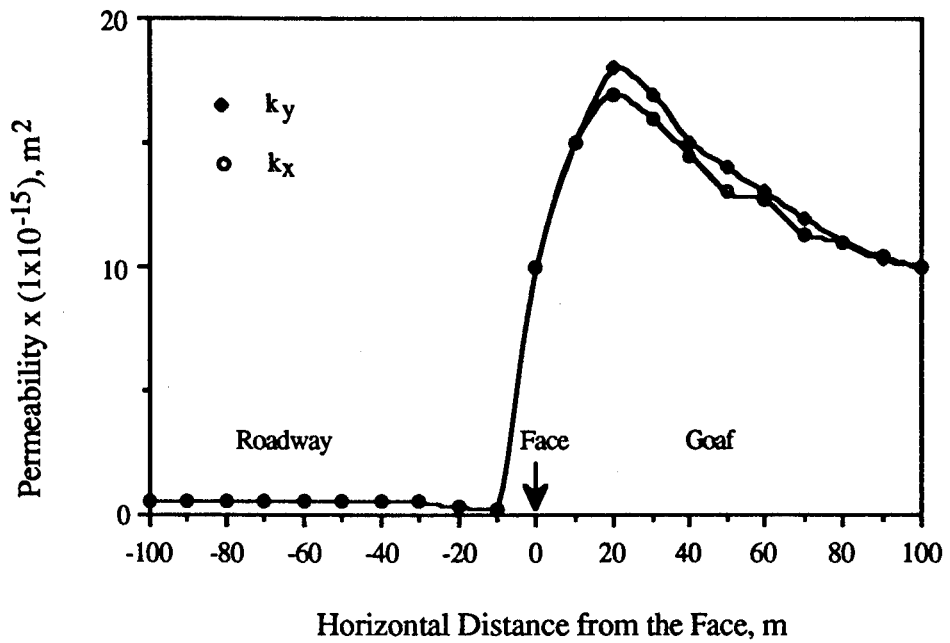
Figure 5.22 Permeability Variations at a Level of 15 - 22.5 m above the Working Level (Sandstone).
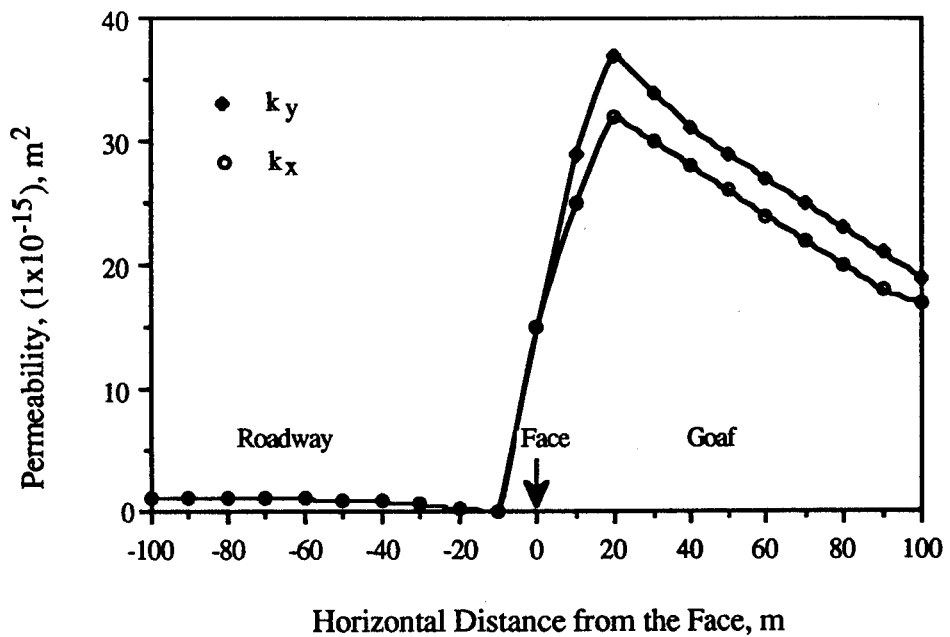
Figure 5.23 Permeability Variations at a Level of 0 - 7.5 m below the Working Level (Sandstone).
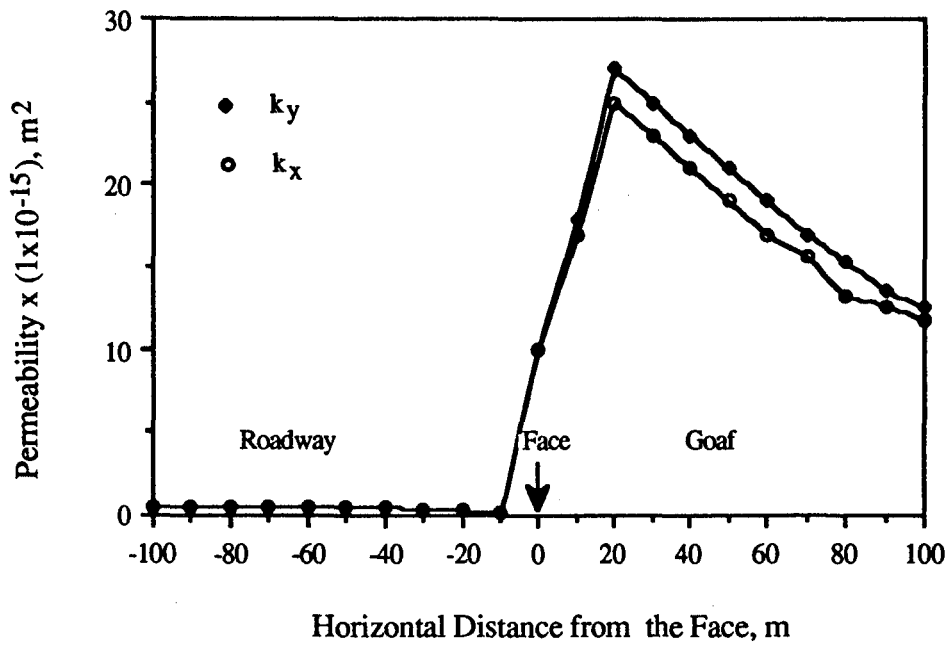
Figure 5.24 Permeability Variations at a Level of 7.5 - 15 m below the Working Level (Sandstone).
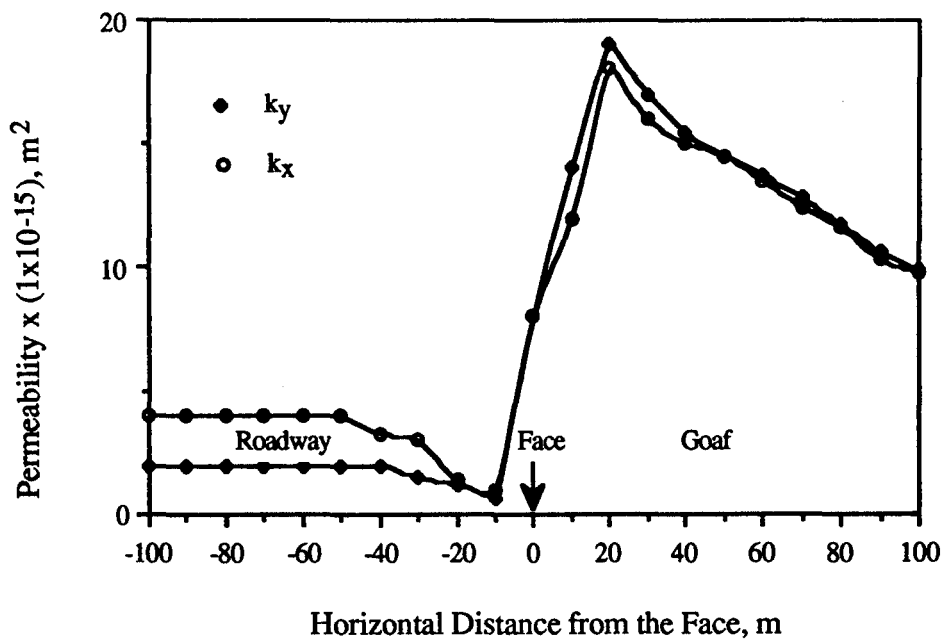
Figure 5.25 Permeability Variations at a Level of 15 - 18 m below the Working Level (Coal).

87

CHAPTER SIX

THE COMPUTATIONAL SOLUTION OF THE
TIME-DEPENDENT GAS FLOW EQUATION
AND THE CALCULATION OF FLUX

6.1 Introduction

The approximate solutions for the time-dependent gas flow equation, equation 3.11, are obtained using finite element analysis to give time-dependent gas pressures. A finite element problem solving package called PAFEC'75 was used for the following;

i.   to obtain gas pressure distribution around a working longwall face,

ii.   to calculate gas flow for roadways,

iii. to simulate methane flow to methane drainage boreholes.

The similarity between the gas flow and heat flow equations enables gas flow problems to be solved using thermal routines from the PAFEC'75 program suite, after suitable modifications.

6.2 The PAFEC'75 Program Package

It is common practice to use existing finite element routines for the solution of equations. This, of course, reduces the amount of work required of users. The PAFEC program package contains thermal routines for the solution of the time-dependent equation for temperature distribution, equation 3.6.

$$\frac{\partial}{\partial x}[\,k\frac{\partial T}{\partial x}\,] + \frac{\partial}{\partial y}[\,k\frac{\partial T}{\partial y}\,] + \frac{\partial}{\partial z}[\,k\frac{\partial T}{\partial z}\,] - c\frac{\partial T}{\partial t} = 0$$

This equation has certain similarities with the time-dependent gas flow equation, equation 3.2, if ϕ ($=P^2$) is set to T, the temperature, and $k_x = k_y = k_z$ to a constant k, the thermal conductivity. This similarity enables the gas flow equation to be solved using the thermal routines from the PAFEC'75 program, after suitable modifications.

Three main original routines of the package required modification to accommodate the relevant differences in the equations to be solved. These were;

i.   element routines,

ii. solution routines,

iii. flux calculation routines.

The PAFEC'75 package divides itself into ten distinct segments which are called 'phases' [44]. At the conclusion of each phase all information required at a later stage is stored in arrays called modules which are then placed on a backing store.

Short descriptions of each phase of the program are given below;

phase 1 = data modules are read in,

phase 2 = pafblocks (element blocks in the mesh) are generated,

phase 3 = the structure itself is drawn,

phase 4 = pre-solutions are derived,

phase 5 = draws input data with applied constraints,

phase 6 = element matrices are generated (permeability),

phase 7 = the system equations are solved (e.g. for temperature ($=\phi$)),

phase 8 = draws output (e.g. temperature),

phase 9 = heat flux equations are solved,

phase 10 = output contour plots are produced.

Therefore, required modifications to the 'element' routines were inserted within phase 6. Similarly, modifications to 'solution' and 'flux calculation' routines were inserted within phases 7 and 9 respectively.

6.3 Modifications to the Element Routines

As noted previously, in the simulation of gas flow through strata adjacent to a working longwall coalface, PAFEC'75 thermal routines were used in which the time-dependent heat flow equation is solved. In such solutions, the thermal conductivity, k, which is the analogue of permeability in the gas flow equation, remains constant throughout the mesh. Solutions may therefore, be regarded as solutions to equation 2.11 with constant permeability (for an isotropic medium). However, in a mining context this situation is far from satisfactory since permeability, which is the main parameter governing gas flow, varies continuously throughout the strata around the mine working. Therefore, the element routines have been modified in order to solve the time-dependent gas flow equation with variable permeability.

In order to model such a situation Keen [12] designed a more flexible element which permitted each of its nodes to have a different permeability. This method, further developed by O'Shaughnessy [22], to achieve an adequate representation of permeability variations in the model, has been extended and improved in the current model. The directional permeability variations with respect to the x-axis of this element is illustrated in figure 6.1 and the listing of program files for element design is also given in appendix 3.

The variable permeability values of the structure are given according to the latest PAFEC'75 manual for running the so called 'transient temperature job', as shown in appendix 4.

each node in the above mesh of elements has its own permeability
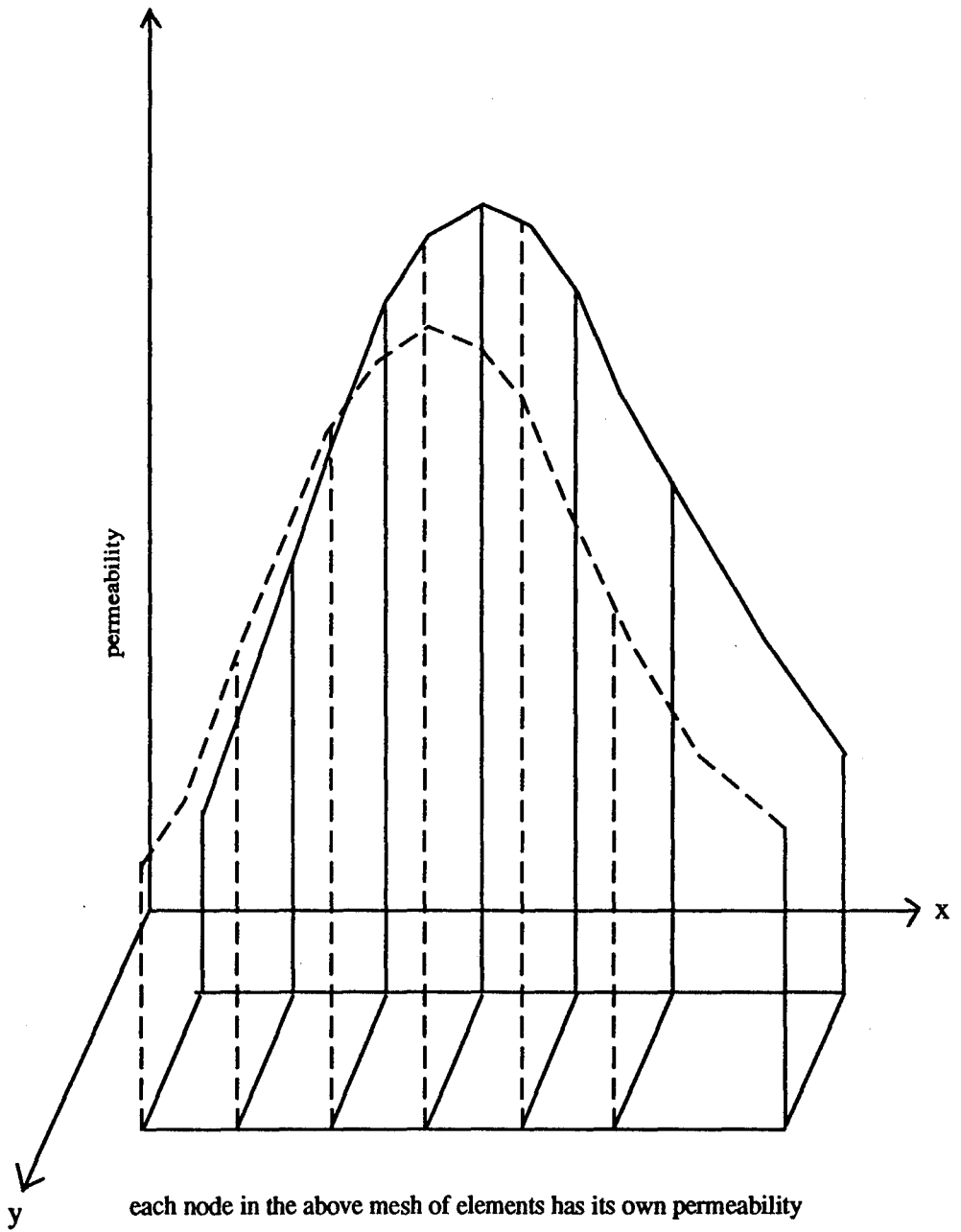
Figure 6.1 Permeability Variation for Isotropic Material (after O'Shaughnessy [22]).

92

Within the PAFEC'75 package a MATERIAL module is available, using this common properties for a group of elements can be defined. These material properties can be as follows;

i. young modulus, E,

ii. poisson's ratio, NU,

iii. mass density, RO,

iv. coefficient of thermal expansion, ALPHA,

v. hysteritic damping factor, MU,

vi. thermal conductivity, k,

vii. specific heat, SH.

From examining the original PAFEC'75 thermal routines, it was realised that the values of porosity, viscosity and permeability, which are the variables of the gas flow equation, could be assigned using, respectively, mass density, specific heat, and thermal conductivity options in the material module of the temperature jobs. To ensure the applicability of equation 2.11 the values of porosity and viscosity were taken to be constant throughout the mesh. These assumptions were considered to be reasonable since the viscosity of methane would not vary greatly for an isothermal process. Secondly, any variation in porosity would be negligible compared with the errors in defining permeability values of the strata.

As can be seen from the data file given in Appendix 4, permeability values for each element are defined in the MATERIAL module. These refer to two tables. The first two digits refer to the number of a table of values for k_x, and the

93

second two to the number of a table of values for k_y. For example, a thermal conductivity of 1020 refers to table 10 and 20 which contain a sequence of values for k_x and k_y respectively. Both the k_x and k_y values must be in a one-to-one correspondence with a series of values of x-coordinates, in the tables. The tables for k_x and k_y were introduced by using the TABLES module, which is documented in the latest PAFEC'75 manual.

As stated before, of the three parameters permeability, porosity and viscosity, it is permeability which has the greatest range for variation. However, permeability should not be allowed to vary by more than two orders of magnitude between one side of an element and another. When this restriction was violated incorrect results were obtained. This restriction was not thought to greatly affect the flexibility of program to accommodate steep permeability gradients.

6.4 Modifications to the Solution Routines

As noted before the PAFEC'75 package contains thermal routines for the solution of the time-dependent heat flow equation, equation 3.6, which yield temperature distributions at any subsequent times. In this equation, temperature, T, corresponds to gas pressure squared, P^2 $(=\phi)$, in the gas flow equation. It is now necessary to introduce a mapping which enables the gas flow equation, equation 3.2, to be solved using the same routines as the heat flow equation. The appropriate mapping is:

94

$$p = +\sqrt{T}$$

so that

$$\frac{\partial T}{\partial t} = \frac{\partial p^2}{\partial t}$$

and hence

$$\frac{\partial T}{\partial t} = 2p \frac{\partial p}{\partial t}$$

As explained in chapter 3, substituting the above relationships into equation 3.2 and minimizing the appropriate functional gives pressure derivatives with respect to time. The resulting matrix equation is (see chapter 3 for a key to the variables) :

$$\frac{[\,M\,]}{2\Delta t} \{\, P^2 \,\}_{t+\Delta t} = \frac{[\,M\,]}{2\Delta t} \{\, P^2 \,\}_t - \{\, P^T \,\}_t [\,S\,] \{\, P^2 \,\}_t$$

From this equation $\{P^2\}_{t+\Delta t}$ can be evaluated to give the time-dependent pressure distribution. The relevant routines of the PAFEC'75 package program needed to be modified, inserting the above equation so that the program produced gas pressures. The listing of the program files producing gas pressure solutions is also given in appendix 5.

In the solution process, all output is obtained in terms of temperature rather than gas pressure, P^2, the pressure values being obtained by taking the positive square root of the corresponding temperature values. Similarly, when supplying input data, known pressure values are squared to ensure their correspondence with the temperature values required for use in the thermal routines of the PAFEC'75 package program.

The next consideration is that of the time-dependence of the boundary conditions. For the purpose of steady-state simulation gas pressure in the source bed is assumed to be constant. However, for the transient flow case, gas pressure in the source bed should change with respect to time. It is reasonable to assume that the pressure in the source bed will gradually decrease as gas migrates towards the roadway, and that this process will continue until a steady-state is reached, when the temporal pressure gradient will be equal to zero. Such a scheme can be applied by use of the THERMAL.SHOCK module of PAFEC'75 wherein a user may specify changes in boundary conditions with respect to time [45].

The program also provides contour drawing facilities for the gas pressure distribution for any desired time intervals together with a list of gas pressure values at each node in the mesh. These contour diagrams were found to be very useful since they displayed the results more clearly than the numerical values.

6.4.1 Determining a Gas Pressure Distribution Using the PAFEC'75 Package

There are two main types of gas pressure calculation. The most straightforward is a steady-state analysis in which the steady pressure distribution is to be found. The description of the problem will include information about gas pressure inputs to the structure and any areas where pressure is prescribed. PAFEC'75 is used to find the gas pressures at all points in the structure where the pressure is unknown [45].

The other type of pressure calculation is the transient case, which usually involves a THERMAL.SHOCK module and a knowledge of how the pressure varies with time is required in this case. A number of solutions are needed. At any point in time it may be supposed that the pressure distribution is known completely. A finite element solution is needed to determine how the pressure will have varied after a short interval of time. It is then possible to obtain the complete temperature distribution at a slightly later time. Thus the analysis proceeds in a series of time steps obtaining a new solution at each time.

The transient pressure solution involves moving forward in time. For the process to begin, pressures are required at an initial time, which for convenience is taken as time t=0. Two possible definitions of the boundary conditions exist; all the initial pressures may be known and be input as data for the problem, or alternatively, the program may have to carry out a steady-state calculation to give an initial pressure field as a prelude to the transient analysis.

6.4.1.1 Steady-State Pressures

For steady-state pressure calculation, the user defines the structure using NODES and either or both of ELEMENTS and PAFBLOCKS modules [30]. The actual elements used are thermal elements. The following modules are used to describe the boundary conditions:

i.   TEMPERATURE, this module gives the pressures at nodes where the pressure is described. Any node which is not mentioned is assumed to be at unknown pressure. The need for a steady-state pressure calculation is signalled in the CONTROL module where a CALC.STEADY.TEMPS statement should be included.

6.4.1.2 Time-Dependent Pressures with Prescribed Initial Pressures

For this type of transient calculation it is assumed that the initial pressure field is completely specified. The following modules are used in transient calculations:

i.   TEMPERATURE, this gives the initial pressure distribution and any node not mentioned is assumed to be at zero pressure.

ii.   THERMAL.SHOCK, this module describes the variations with time of any nodal pressures which are prescribed.

iii.   UNSTEADY.THERMAL.TIMES, this module is used to define the time step and the time at which the final solution is required. The program moves through time calculating the new pressure field at the end of each time step.

For all transient pressure calculations a statement, CALC.TRANS.TEMPS, is required in the CONTROL module. If the initial steady-state is not known, then a steady-state calculation must be performed first. In this case, the TEMPERATURE module is used to describe the boundary conditions in the steady-state. THERMAL.SHOCK and UNSTEADY.THERMAL.TIMES modules perform the subsequent transient pressure calculation. In the CONTROL module there should be both CALC.STEADY.TEMPS and CALC.TRANS.TEMPS statements. An sample data set for a transient pressure distribution is given in appendix 4.

6.5 Modifications to the Flux Calculation Routines

Solving equation 3.2 using the modified thermal routines, a time-dependent gas pressure distribution can be obtained throughout the mesh. These values should then be used to provide gas flow rates, since flow is caused by pressure differences. A mass flux equation was used to calculate methane flow rates in the mesh. The derivation of this equation is given below together with the numerical integration procedure applied.

6.5.1 Derivation of Mass Flux Equation
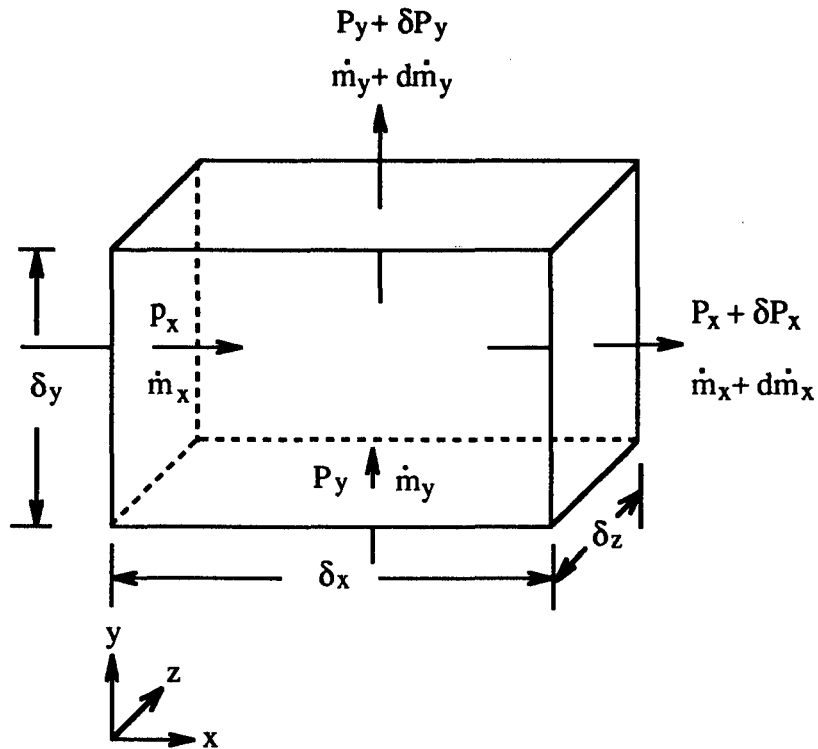
Figure 6.2 Element of Rock with Variable Permeability (after Keen [12]).

Consider an element as shown above. The mass flow rate through a unit volume can be given as:

$$\dot{m} = \rho \; \dot{q} \qquad \qquad \dots [6.1]$$

where $\dot{q}$ is the velocity of the flow, and can be written as [22]:

$$\dot{\underset{\sim}{q}} = \frac{Q}{A} = -\frac{\bar{k}}{\mu} \nabla P \qquad \ldots [6.2]$$

hence

$$\dot{\underset{\sim}{m}} = -\rho \frac{\bar{k}}{\mu} \nabla P \qquad \ldots [6.3]$$

Since methane flow was assumed to obey the 'perfect gas' law:

$$P = \rho \frac{RT}{m_0}$$

and therefore,

$$\rho = \frac{m_0}{RT} P \qquad \ldots [6.4]$$

Substituting equation 6.4 into the equation 6.3, one can obtain the mass flow rate of methane (since the integration is over a surface) across a given bounding surface, c:

$$\int_c \dot{\underset{\sim}{m}} \, ds = -\frac{m_0}{\mu RT} \int_c \{ \bar{k} P \nabla P \} . \underset{\sim}{n} \, ds \qquad \ldots [6.5]$$

where

m_0 = molecular weight of methane,

$\underset{\sim}{n}$ = unit outward normal.

101

Now,

$$P \nabla P = \frac{1}{2} \nabla P^2$$

or

$$P \nabla P = \frac{1}{2} \nabla \phi$$

Hence the equation 6.5 can be re-written:

$$\int_c \dot{m} \, ds = - \frac{m_0}{2\mu RT} \int_c \{ \bar{k} \, \nabla \phi \} . \underset{\sim}{n} \, ds \qquad \ldots [6.6]$$

where $\phi \, (= P^2)$ is the field variable (temperature in PAFEC'75 solutions) and solutions are obtained by the modified PAFEC'75 solution routines.

Considering the boundaries to be parallel to a coordinate axis then in the two dimensional case:

$$\int_{x_0}^{x_1} \dot{m} \, dx = - \frac{m_0}{2\mu RT} \int_{x_0}^{x_1} k_y \frac{\partial \phi}{\partial y} \, dx \qquad \ldots [6.7]$$

or

$$\int_{y_0}^{y_1} \dot{m} \, dy = -\frac{m_0}{2\mu RT} \int_{y_0}^{y_1} k_x \frac{\partial \phi}{\partial x} \, dy \qquad \ldots [6.8]$$

There are many formulas for numerical integration of definite integrals of this form, such as the 'trapezoidal rule' and 'Simpson's rule' [43]. If the trapezoidal rule is employed over successive intervals for a definite integral of the form:

$$\int_{x_0}^{x_n} f(x) \, dx$$

the numerical integration may be given as:

$$\int_{x_0}^{x_n} f(x) \, dx = h \left(\frac{1}{2} f_0 + f_1 + f_2 + \cdots + f_{n-1} + \frac{1}{2} f_n \right) \qquad \ldots [6.9]$$

therefore the mass flow rate of methane (in the y-direction) into a mine roadway using this formula is (equation 6.10):

$$\int_{x_0}^{x_1} \dot{m} \, dx = -\frac{m_0}{2\mu RT} \left\{ h \left(\frac{1}{2} [k_y]_0 [\frac{\partial \phi}{\partial y}]_0 + [k_y]_1 [\frac{\partial \phi}{\partial y}]_1 + \cdots + \frac{1}{2} [k_y]_n [\frac{\partial \phi}{\partial y}]_n \right) \right\}$$

where

$x_0 - x_1$ = length of the roadway,

h = length of the interval.

Similarly, the mass flow rate of methane (in the x-direction) into a borehole can be given as (equation 6.11):

$$\int_{y_0}^{y_1} \dot{m} \, dy = - \frac{m_0}{2\mu RT} \left\{ h \left(\frac{1}{2} [k_x]_0 \left[\frac{\partial \phi}{\partial x} \right]_0 + [k_x]_1 \left[\frac{\partial \phi}{\partial x} \right]_1 + \cdots + \frac{1}{2} [k_x]_n \left[\frac{\partial \phi}{\partial x} \right]_n \right) \right\}$$

where y_0-y_1 is the length of the borehole.

As can be seen from equations 6.10 and 6.11, in order to evaluate the mass flow rate of methane across a given boundary it is necessary to obtain pressure gradients, $d\phi/dx$, $d\phi/dy$ and permeability values, k_x, k_y at that boundary. The pressure gradients which are obtained in the transient temperature calculation phase (phase 7) can be stored as arrays in a backing store for any node in the mesh. These are then used, together with permeability values defined for the relevant nodes, to provide the flux of methane across a given boundary, using equations 6.10 and 6.11. The resultant values are given in kg/s if all other parameters are supplied in SI units. These values should then be divided by the density of methane, 0.7168 kg/m^3, so as to obtain methane flow in m^3/s, which is the usual way of defining methane flow in mining.

A gas flow simulation model has been developed by applying this procedure to particular boundaries, such as roadways and boreholes, and devising routines to perform gas flow calculations. This simulation model will be described in the next chapter.

CHAPTER SEVEN

GAS FLOW SIMULATION MODELS FOR LONGWALL COAL MINING

7.1 Introduction

As explained in the previous chapter, methane flow rates were calculated using equations 6.10 and 6.11 with the thermal routines in the PAFEC'75 package.

From those equations, in order to evaluate the mass flow rate of methane across a given boundary, it is necessary to obtain ϕ gradients and permeability values at that boundary. Gas pressure gradients, $d\phi/dx$, are obtained using modified PAFEC'75 thermal routines, and permeability values can be assigned for each node in the mesh. These values are then used to find the flux of methane across a given boundary (this may be a roadway, the goaf or a borehole), using a trapezoidal integration of the mass flux equations (derived in the previous chapter) on each interval (intervals need not be of equal length).

The next step was to develop a model simulating mining conditions for either retreating or advancing longwall faces and to devise programming routines for this.

7.2 Modelling Technique for a Roadway and Borehole in a Finite Element Mesh

Previous work concerning the flow of methane demonstrated that the shape of a roadway does not significantly affect the flow of methane [22,65]. Keen [12] also showed theoretically that if the diameter of a borehole is not unreasonably large (greater than 0.2 m) nor unreasonably narrow (less than 0.03 m) then diameter should not significantly affect the flow of gas. He suggested that the pattern and the number of boreholes are more important.

Based on the results of these research programs, it was decided that it would be perfectly reasonable to simulate both roadways and boreholes by fixing the pressure at a sequence of nodes in the finite element mesh. Such nodes, which fix the pressure along the boundary, act as a line sink, thus causing gas to flow towards them.

For this modelling technique the pressure at nodes which represent a roadway boundary are fixed at atmospheric pressure throughout the calculations. Similarly, the nodes at the borehole boundary may have any pressure value less than atmospheric to represent applied suction.

In mining practice, boreholes are usually sleeved along part of their length (standpiping), thus rendering this section ineffective as a means of draining gas. Only the open portion of the borehole drains gas and this is therefore termed the 'effective length'. Since the sleeved portion of the borehole is assumed to have

no effect on the flow of gas, it is consequently ignored in the modelling. Hence, any reference to borehole length should be taken as 'effective length' and it is this which is simulated by fixing the pressure on its nodes.

The PAFEC'75 system has no facility for locating any particular boundary. This presents no problem for the case of flow into a roadway as the roadway floor or roof is taken as the x-axis in the rectangular cartesian co-ordinate system. As the roadway boundary was easily located, the required flow rate could be evaluated in a straightforward manner [22]. However, there is no similar co-ordinate restriction on the location of any particular borehole as their positions are generally peculiar to a given simulation. Fortunately, the difficulty was overcome by making the pressure values available in phase 9 so that each node could be examined individually. Those with fixed pressures (characteristic of boreholes) were identified and recorded for use in the borehole flow calculation.

During the research, several different configurations of longwall mining (or stages) have been modelled, these are;

i.   roof or floor strata with vertical boreholes in advance mining,

ii.   roof and floor strata with vertical and inclined boreholes in advance mining,

iii.   retreat mining with inclined boreholes,

iv.   retreat and advance mining with boreholes, crossing multi-layer strata.

7.3 Basic Principles of Methane Drainage

In order to understand the foregoing simulation model, some basic knowledge is required about methane drainage. Methane drainage is the process of removing gas contained in the coal seam and surrounding strata through pipelines. The principal objective of methane drainage is the improvement of safety by reducing the methane concentration in the ventilated air. Methane drainage is expected to capture as much of the methane as possible before it enters the mine ventilation. In order to achieve this, the drainage system should be designed considering the potential drainage zones around longwall faces.

In general, small-diameter (51 to 64 mm) boreholes are drilled from the return airways of longwall faces to intercept the overlying strata at an angle of 30 to 40° from vertical, parallel in plan view to the line of the face, and also inclined over the goaf. Holes drilled downward into the floor strata also sometimes provide appreciable flows of gas. The depth of these holes is generally 40 to 50 m, with a spacing of 18 to 27 m. In order to minimize the entry of air or 'air leakage' into the drainage system, a 76 mm diameter standpipe is inserted into the mouth of the hole and grouted in with cement. All the boreholes are connected to a main drainage range, typically 152 to 203 mm in diameter. Exhausters are used to maintain a suction of 0.5 to 0.98 KPa to overcome the resistance of pipeline to gas flow and improve gas production [66]. The suction pressure created by these exhausters is not carried to the end of borehole because of the pressure losses. Therefore, at the end of the borehole the borehole pressure is assumed to be slightly smaller than atmospheric [67].

7.4 The Simulation of Roof or Floor Strata with Vertical Boreholes in Advance Mining, Stage-1

The first stage of the model, using the integration procedure outlined in chapter 6 on particular boundaries, was only capable of simulating either the roof or the floor of the working horizon. In other words, the total calculated gas flow rates through the roadway could only represent the gas emission from either roof or floor strata, but not the total emission. For the finite element mesh generation 8-noded temperature calculation element type, which is called 39210 by PAFEC, is used as shown in figure 7.1 together with the restriction on its shape.
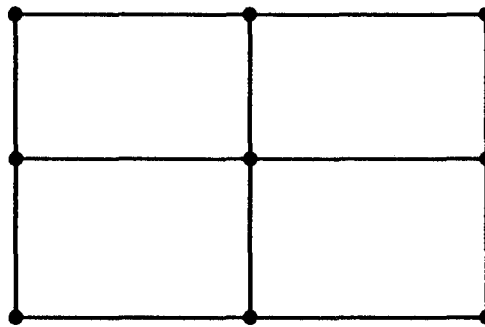
R < 15

R = length of longest side / length of shortest side

Figure 7.1 8-Noded Temperature Calculation Element and its Restriction.

In this stage, the pressure at nodes which represent a roadway boundary were fixed at atmospheric pressure, while the nodes at the borehole boundary were given suction pressures (less than atmospheric) throughout the calculations. The definition of the boundary conditions for the model was found to be very important as the subsequent pressure distribution would depend heavily on these values (see chapter 6.4.1). In this stage, the roadway length could not be changed (it was taken as 100 m) and it was only possible to define fixed length boreholes, vertically drilled from a roadway.

The output has been devised so as to produce methane flow rates for each interval as well as the cumulative methane emission over the roadway length. Drainage values are also given for each individual borehole and the total drainage system.

7.5 The Simulation of Roof and Floor Strata with Vertical and/or Inclined Boreholes in Advance Mining, Stage-2

As an adequate simulation, the first stage of the model was not satisfactory because of its restrictions as explained before. Therefore, the next step was to design another model which would be more flexible. This would allow the definition of boreholes varying in angle and length, and also of a variable roadway length. Moreover, this new trial had to produce the results in terms of known quantities, rather than relative numbers as was the case in the first stage. These objectives were achieved by redevising the relevant routines in the gas flow calculation. Since all the equation constants are inserted within the solution process in this model, it is only necessary to supply the other

110

parameters in the correct units to obtain methane flow rates in m^3/s or l/s. The exponents of very small and large quantities were inserted within the program for ease of data entry (e.g. permeability = n$\times$10^{-15}, gas pressure squared = n$\times$10^{10}, and viscosity = n$\times$10^{-5}). In the second stage of the model, the routines have been changed so that they can recognize whether the nodes are in the floor or roof strata and calculate the gas flow rates separately to obtain a reasonable simulation of the total strata emissions. To achieve this, negative y-coordinates were given for nodes in the floor strata, whereas the coordinates of roof strata nodes were positive.

Definition of inclined boundaries has been made possible by employing a different element type, the '6-noded temperature calculation element', 39110 (see figure 7.2), while the '8-noded element' type could be used for vertical and horizontal boundaries. Employing the 6-noded element type, it is always possible to arrange borehole direction and length in the roof or floor strata as desired (figure 7.3). In this model more informative output displays were obtained by re-arranging the routines.
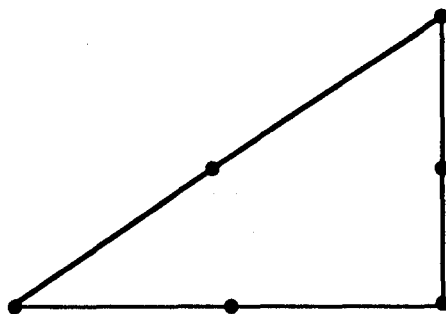
25 < A < 155

A = angle between chords across any adjacent element sides

Figure 7.2 6-Noded Temperature Calculation Element and its Restriction.

roof borehole boundaries

roof strata

roadway boundary →

floor strata

floor borehole boundaries
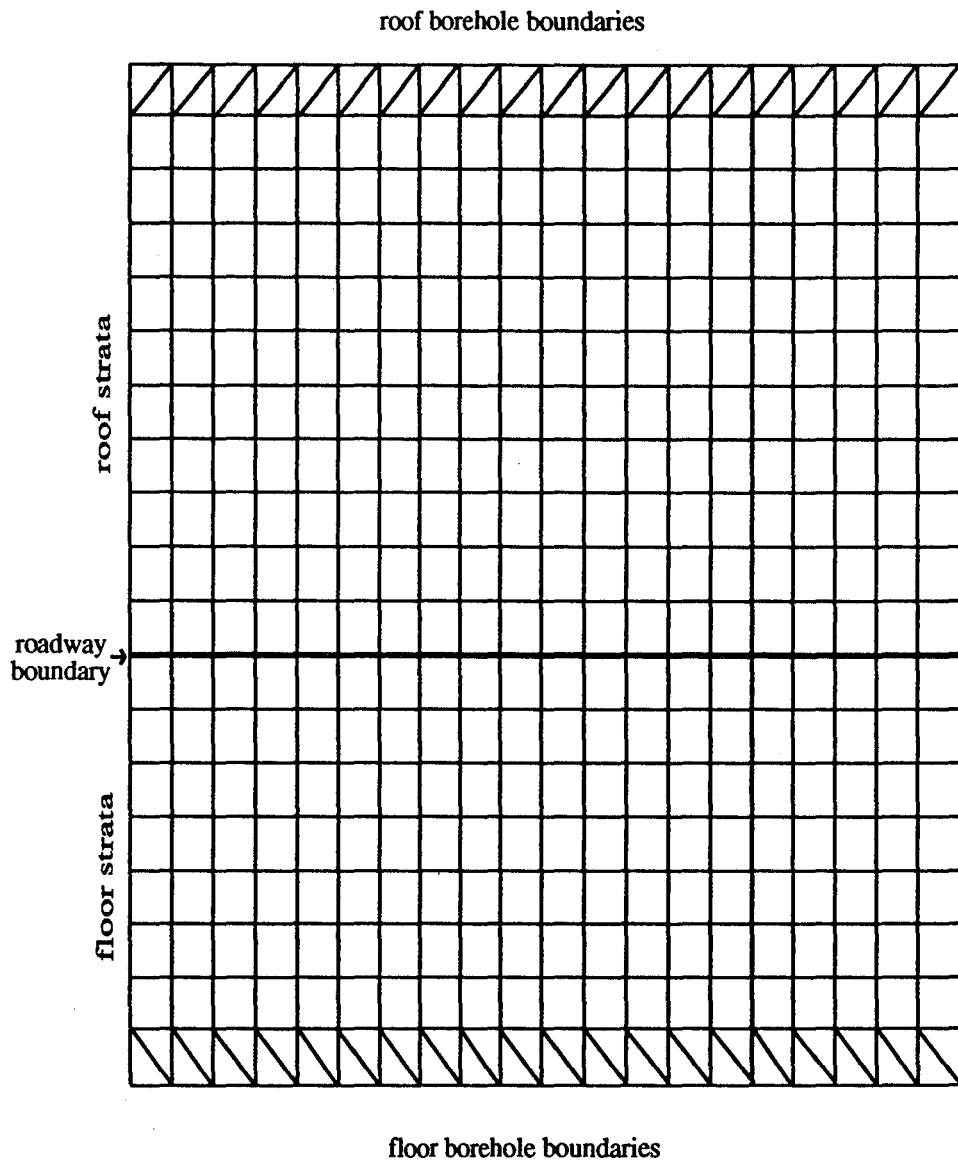
Figure 7.3 Advance Mining Model with Inclined Borehole Boundaries.

7.6 Retreat Mining with Inclined Boreholes, Stage-3

The second model could be used to simulate gas flow for an advancing longwall face. However, it was necessary to modify the model for retreating face conditions, considering both goaf emission and emission to the roadway. This was achieved by taking the coal face as the base line, while the nodes in the roof and floor strata above and below the roadway or goaf will have characteristic coordinates so that the related routines calculate the methane flow separately and combine them later to give the total return airway emission. Output display has also been changed to show cumulative methane flow rates (as well as flow rates for every roadway or goaf interval). This type of display is advantageous in that it shows each section's contribution to overall methane levels. In this third model, special care must be taken to match the nodes to the base directions when defining the structure (figure 7.4), as follows (appendix 4):

i.   The nodes in the roof have positive y-coordinates, while the floor nodes have negative values.

ii. The nodes in the goaf area have positive x-coordinates, while the nodes in the roadway area have negative values.

The flow of methane to the goaf area is then added to the roadway values to give a total return airway emission rate, however, an option has been provided, whereby the emission from goaf to the roadways can be reduced by a given percentage. This option allows account to be taken of methane which is contained within the goaf but does not appear in the ventilating air.

113

roadway boundary face line goaf boundary

roof strata

floor strata
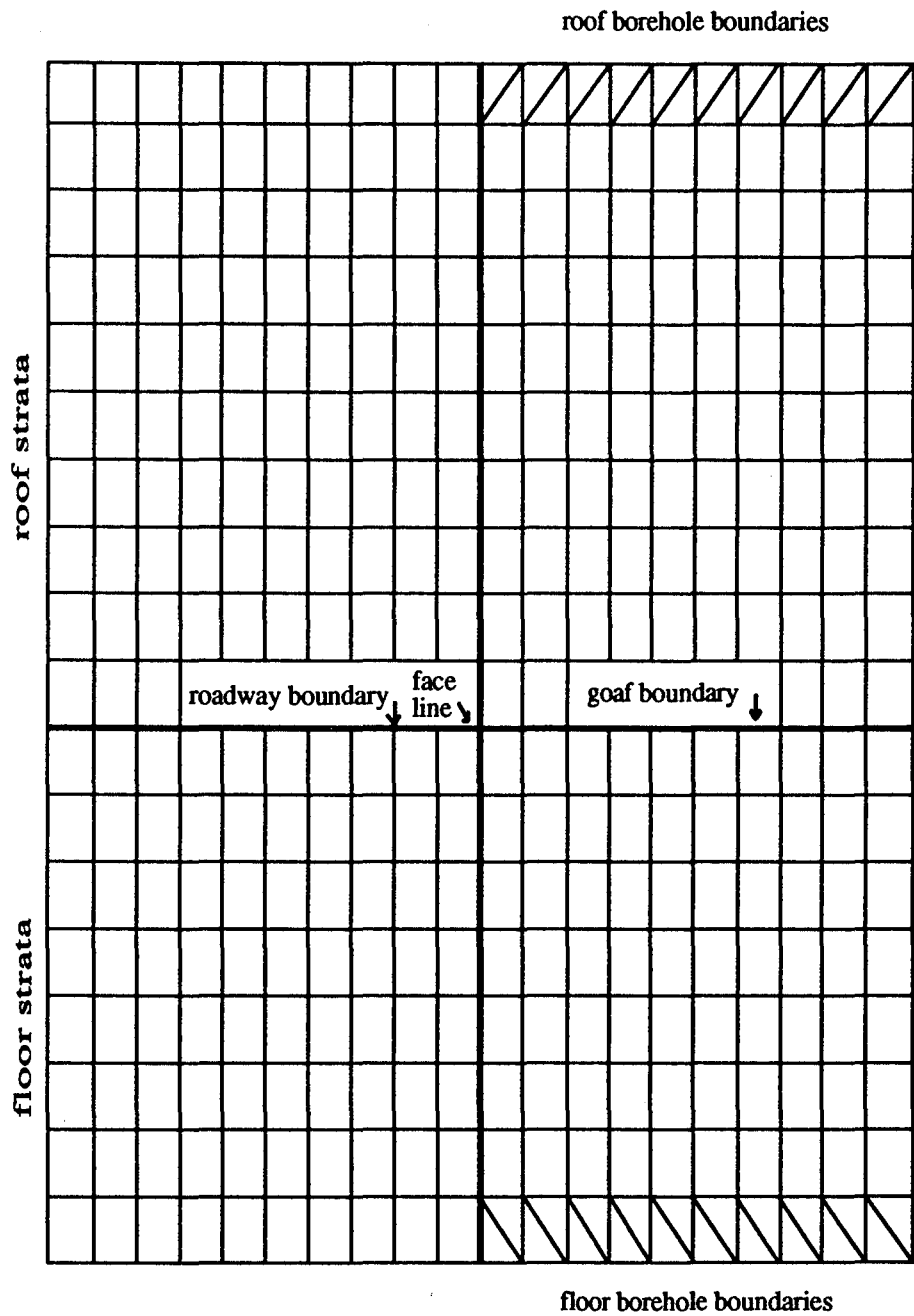
Figure 7.4 Retreat Mining Model with Inclined Borehole Boundaries.

114

In this model, it is possible to define inclined boreholes which can be drilled from the roadway through the area above and below the goaf. The length and the angle of boreholes can be defined as desired, arranging the relevant element's shape.

7.7 Retreat and Advance Mining with Boreholes, Crossing Multi-Layer Strata, Stage-4

In practice, drainage boreholes drilled from the roadway or goaf may cross different types of strata including coal seams. However, in the previous model, borehole boundaries could only be defined so as to cross one type of strata. This was far from satisfactory. The relevant routines have been modified to define different material properties for different strata and to add up the flow rates calculated for each section to give the total drainage values. After a series of tests, these modifications have been proved to be successful from a mathematical and programming point of view.

The final form of the model is capable of simulating any configuration outlined above. The relevant program listing is given in appendix 6.

CHAPTER EIGHT

RESULTS OF TIME-DEPENDENT GAS FLOW SIMULATION

8.1 Introduction

This chapter is concerned with the results obtained from the simulation of two-dimensional time-dependent gas flow through strata adjacent to a moving longwall coal face. Several gas flow analyses were carried out using the latest form of the model for advancing and retreating types of mining as explained in the previous chapter. The aim of this was to determine whether the model actually produces realistic results.

In these analyses, methane emission rates to a roadway were predicted for a given set of conditions without drainage. Then, for the same conditions, the model was tested with several different drainage configurations to show the effect of drainage on gas flow into a roadway. Methane flow rates were predicted for different boundary gas pressures and for the same boundary pressure changing the permeability values of strata by some order. The sensitivity of the model to variations in parameters such as borehole pressure, length and spacing was also investigated. Permeability values for different strata sections have been assigned according to the stress analysis carried out on similar geological models, and previous work on gas flow through strata adjacent to a moving longwall coal face.

8.2 Results of Gas Flow Analysis

The geology and the simplified finite element mesh of the models used in the gas flow analysis are shown in figures 8.1 and 8.2. The permeability values of each strata section were firstly kept constant in order to find out the effect of the defined boundary gas pressures. Then they were increased in magnitude to see the resultant effects whilst keeping the gas pressure constant. In order to ensure the applicability of the time dependent gas flow equation, the values of porosity and viscosity were also taken to be constant (see appendix 4 for data preparation for a gas flow analysis).

Methane flow rates into a roadway were calculated for the advancing and retreating types of longwall mining with and without applying drainage. The results obtained from the simulation of advance and retreat mining represent completely different sets of mining conditions and therefore should not be used for making a direct comparison of the potential methane emission from advance and retreat coal faces. The retreat model represents the 9's Great Row retreating face of Silverdale Colliery and the advancing model represents 505's Yard Ragman advancing face of Florence Colliery. The depth of mining of 9's Great Row is 800 m and its face length is 220 m. Face production averages 20,000 tonnes/week with retreat rates of up to 35 m per week. The face in Florence Colliery is located at a depth of 900 m with a face length of 250 m. Face production in this face averages 14,000 tonnes/week with advance rates of up to 20 m per week.

The methane drainage borehole layout for the return gate on 9's face consists of 46 m long holes, angled over the goaf at 70° - 80° and at 6 - 8 m spacings. The boreholes are standpiped for the first 18 m and the drained gas is removed by two 250 mm diameter pipe ranges. The methane drainage borehole layout for the return gate on the 505's face comprises of 65 m long holes, angled over the face at 55° - 70° and at 10 m spacings. The boreholes are standpiped for the first 15 m and the drained gas is removed by two 250 mm diameter pipe ranges.

Boundary gas pressures (source pressures) of 8×10^5 N/m^2, 9×10^5 N/m^2, and 10×10^5 N/m^2 were given for each case considered. In the subsequent gas flow analysis, permeability values of each strata section were increased by 10 %, 20 %, and 50 % successively while keeping the boundary gas pressure constant at 10×10^5 N/m^2. The results obtained from these analyses are summarised in tables 8.1 to 8.6 and in figures 8.3 to 8.20. Contour plots of the gas pressure distribution (for a source pressure of 10×10^5 N/m^2) with and without drainage are also given in figures 8.21 to 8.24. An example output display obtained from a gas flow analysis is given in appendix 7.
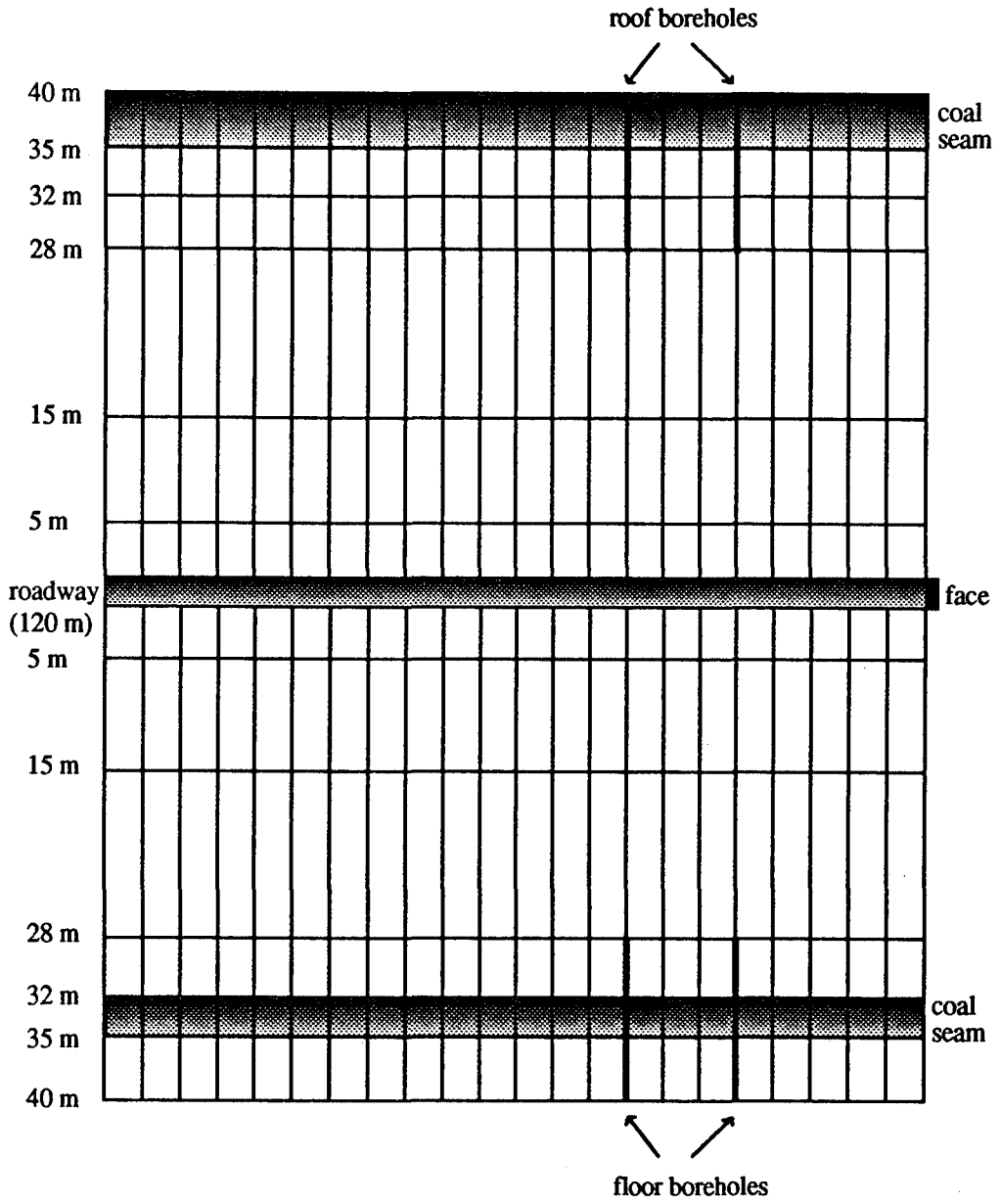
Figure 8.1 Two Dimensional Advancing Longwall Modelling with
Vertical Boreholes.

119
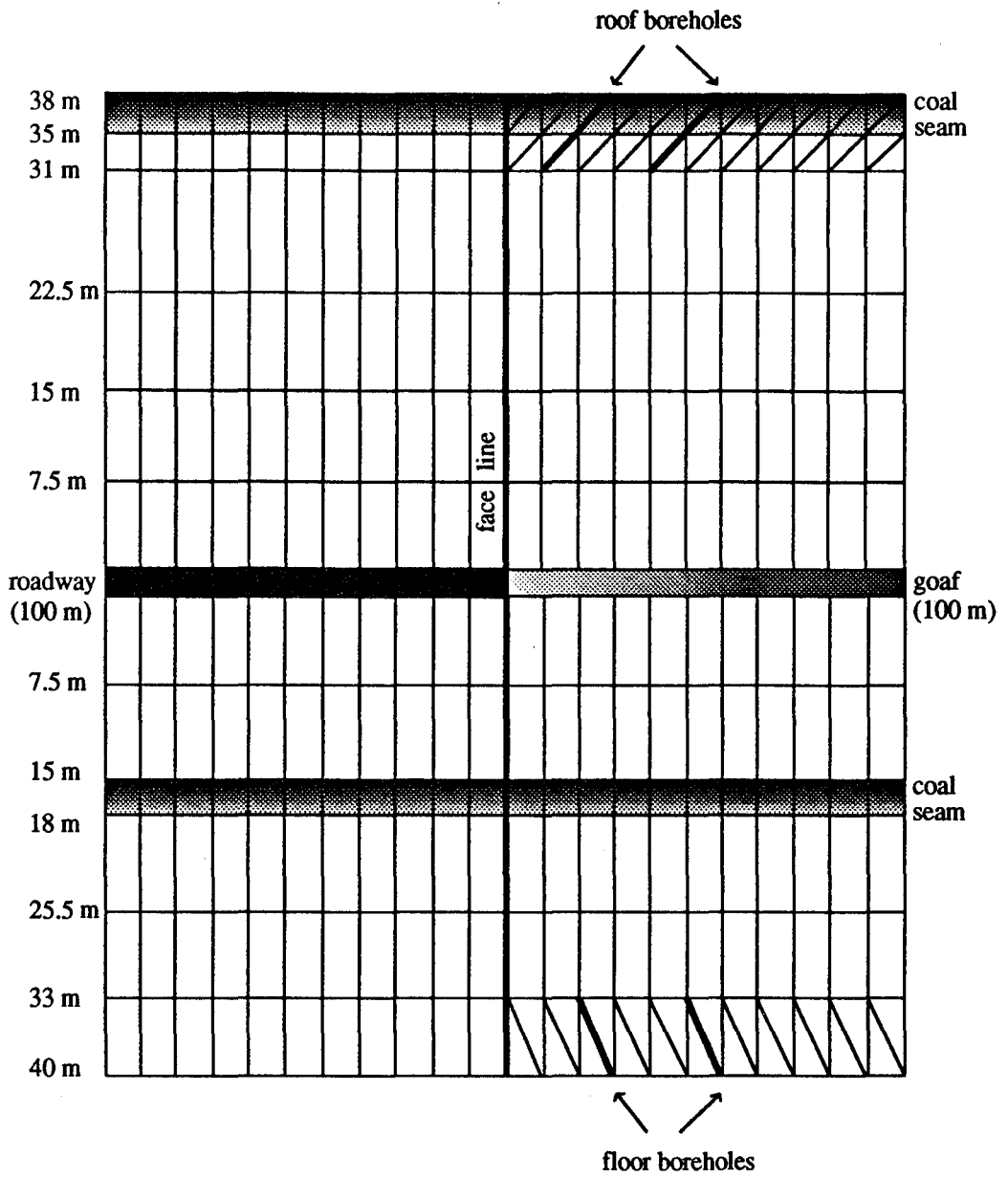
Figure 8.2 Two Dimensional Retreating Longwall Modelling with Inclined Boreholes.

Mining Type	Retreat Longwall	Advance Longwall
Methane Flow into Roadway from Roof Strata, l/s	17.06 12.88*	124.72 87.56*
Methane Flow into Roadway from Floor Strata, l/s	12.23 10.24*	76.12 53.26*
Methane Flow into Goaf from Roof Strata, l/s	206.71 89.58*	—
Methane Flow into Goaf from Floor Strata, l/s	70.22 38.02*	—
Total Return End Methane Flow, l/s	306.21 150.72*	200.84 140.82*

* with Drainage

Table 8.1   Results of Methane Flow Prediction for Retreat and Advance Models (Boundary Gas Pressure was Taken as 8×10^5 N/m^2).

Mining Type	Retreat Longwall	Advance Longwall
Methane Flow into Roadway from Roof Strata, l/s	21.54 16.27*	158.36 111.16*
Methane Flow into Roadway from Floor Strata, l/s	15.53 13.02*	96.64 67.59*
Methane Flow into Goaf from Roof Strata, l/s	262.31 113.45*	—
Methane Flow into Goaf from Floor Strata, l/s	89.15 48.27*	—
Total Return End Methane Flow, l/s	388.54 191.02*	255.00 178.76*

* with Drainage

Table 8.2   Results of Methane Flow Prediction for Retreat and Advance Models (Boundary Gas Pressure was Taken as 9×10^5 N/m^2).

Mining Type	Retreat Longwall	Advance Longwall
Methane Flow into Roadway from Roof Strata, l/s	26.58 20.04*	195.95 137.62*
Methane Flow into Roadway from Floor Strata, l/s	19.22 16.15*	119.56 83.65*
Methane Flow into Goaf from Roof Strata, l/s	324.38 139.92*	—
Methane Flow into Goaf from Floor Strata, l/s	110.31 59.72*	—
Total Return End Methane Flow, l/s	480.49 235.83*	315.51 221.27*

* with Drainage

Table 8.3 Results of Methane Flow Prediction for Retreat and Advance Models (Boundary Gas Pressure was Taken as 10×10^5 N/m^2).

Mining Type	Retreat Longwall	Advance Longwall
Methane Flow into Roadway from Roof Strata, l/s	29.19 22.05*	215.52 151.40*
Methane Flow into Roadway from Floor Strata, l/s	21.15 17.77*	131.58 92.17*
Methane Flow into Goaf from Roof Strata, l/s	355.84 152.95*	—
Methane Flow into Goaf from Floor Strata, l/s	121.64 65.80*	—
Total Return End Methane Flow, l/s	527.82 258.57*	347.10 243.57*

* with Drainage

Table 8.4 Results of Methane Flow Prediction with 10 % Permeability Increase (Boundary Gas Pressure was Taken as 10×10^5 N/m^2).

Mining type	Retreat Longwall	Advance Longwall
Methane Flow into Roadway from Roof Strata, l/s	31.89 24.05*	235.14 165.14*
Methane Flow into Roadway from Floor Strata, l/s	23.03 19.38*	162.53 119.11*
Methane Flow into Goaf from Roof Strata, l/s	389.40 168.00*	—
Methane Flow into Goaf from Floor Strata, l/s	131.02 71.49*	—
Total Return End Methane Flow, l/s	575.34 282.92*	397.67 284.25*

* with Drainage

Table 8.5   Results of Methane Flow Prediction with 20 % Permeability Increase (Boundary Gas Pressure was Taken as 10×10^5 N/m^2).

Mining Type	Retreat Longwall	Advance Longwall
Methane Flow into Roadway from Roof Strata, l/s	39.87 30.06*	294.21 206.71*
Methane Flow into Roadway from Floor Strata, l/s	28.81 24.24*	179.29 125.43*
Methane Flow into Goaf from Roof Strata, l/s	486.41 209.78*	—
Methane Flow into Goaf from Floor Strata, l/s	166.74 90.04*	—
Total Return End Methane Flow, l/s	721.83 354.12*	473.50 332.14*

* with Drainage

Table 8.6   Results of Methane Flow Prediction with 50 % Permeability Increase (Boundary Gas Pressure was Taken as 10×10^5 N/m^2).

The results obtained from the tests have shown good agreement with those anticipated from physical considerations. However, it is believed that the reliability of the model can be improved by supplying better field data, mainly gas pressure values of strata boundaries, and permeabilities of strata with respect to a moving coal face.

As seen from the results given by tables 8.1 to 8.6, methane flow rates were highly affected by changing the parameters such as boundary gas pressure and strata permeabilities by given magnitudes. It is therefore, necessary to define these parameters as close as possible to the real values in order to achieve satisfactory results from the prediction model.

The following figures give predicted methane flow rates obtained from the advancing and the retreating models with and without drainage for boundary gas pressures of 8×10^5 N/m^2, 9×10^5 N/m^2, and 10×10^5 N/m^2. Methane drainage was modelled by defining two roof and two floor boreholes. It is worth noting again that the two models refer to two different sets of mining conditions and so the predicted flow rates should not be compared. These results are shown in figures 8.3 to 8.20. Contour plots of the gas pressure distribution with and without drainage (for a source pressure of 10×10^5 N/m^2) are also given in figures 8.21 to 8.24.
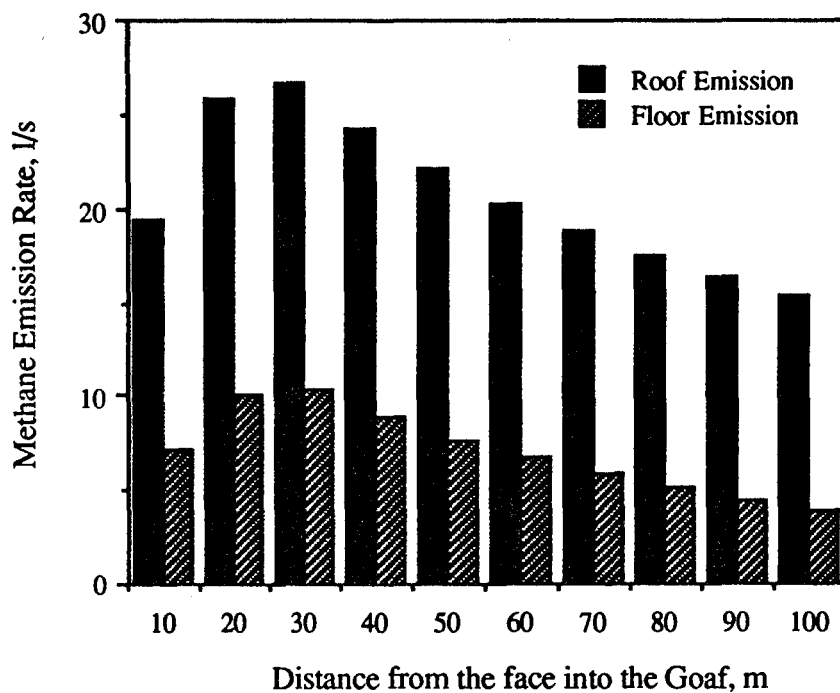
Figure 8.3 Methane Emission Rates to the Goaf in the Retreat Model with no Drainage (Boundary Gas Pressure = 8×10^5 N/m^2).
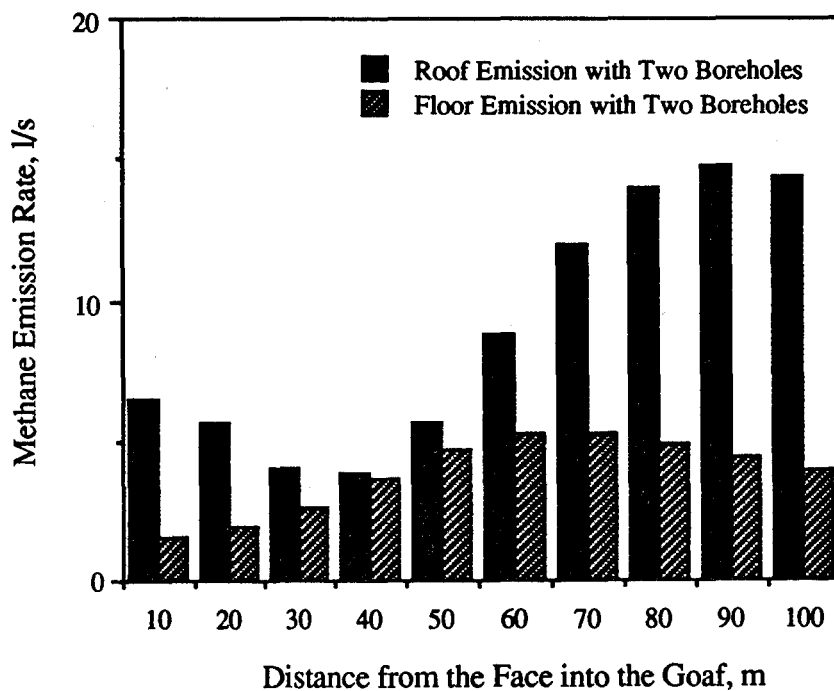
Figure 8.4 Methane Emission Rates to the Goaf in the Retreat Model with Drainage (Boundary Gas Pressure = 8×10^5 N/m^2).

125
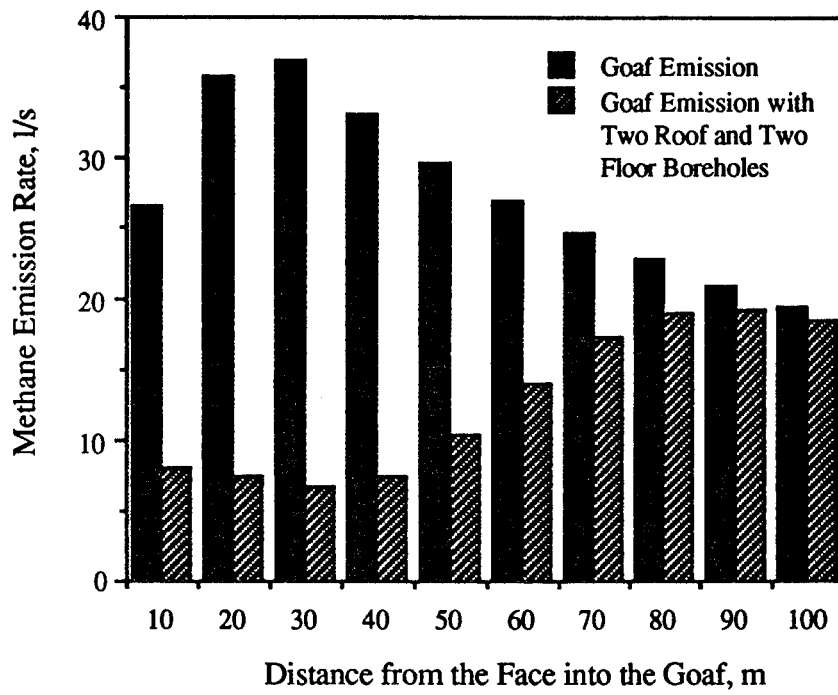
Figure 8.5 Goaf Emissions with and without Drainage in the Retreat Model (Boundary Gas Pressure = 8×10^5 N/m^2).
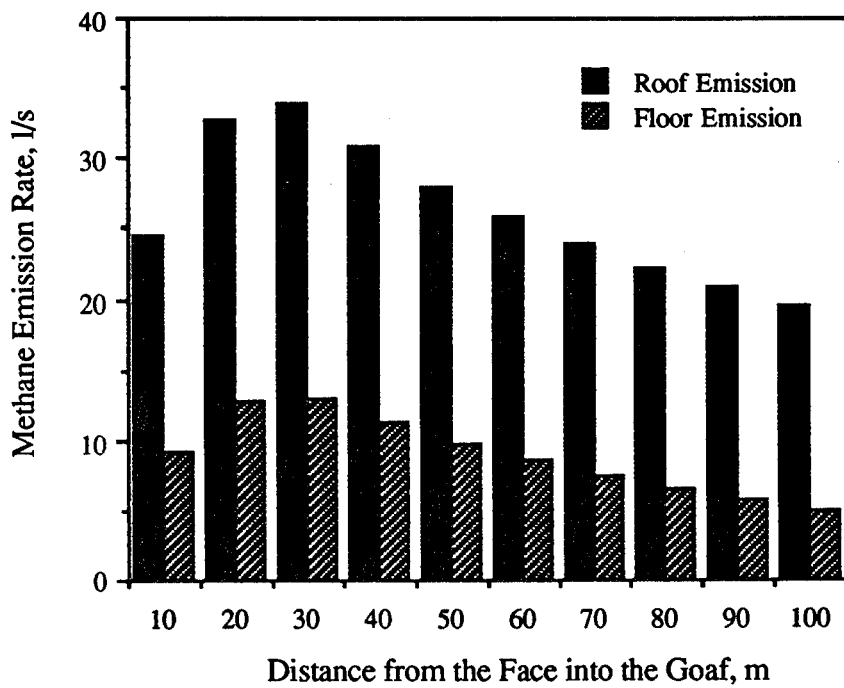
Figure 8.6 Methane Emission Rates to the Goaf in the Retreat Model with no Drainage (Boundary Gas Pressure = 9×10^5 N/m^2).
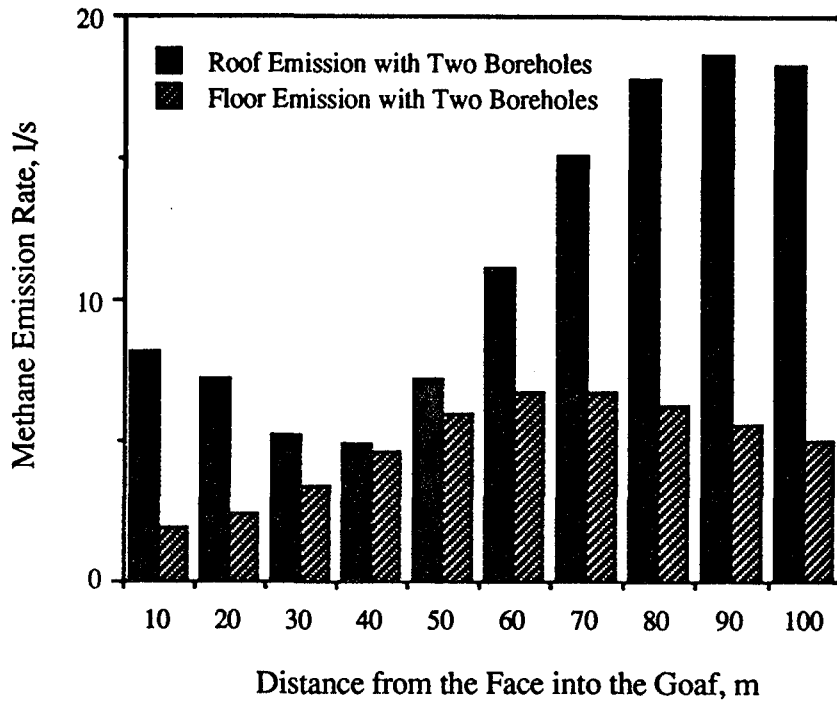
Figure 8.7 Methane Emission Rates to the Goaf in the Retreat Model with Drainage (Boundary Gas Pressure = 9×10^5 N/m^2).
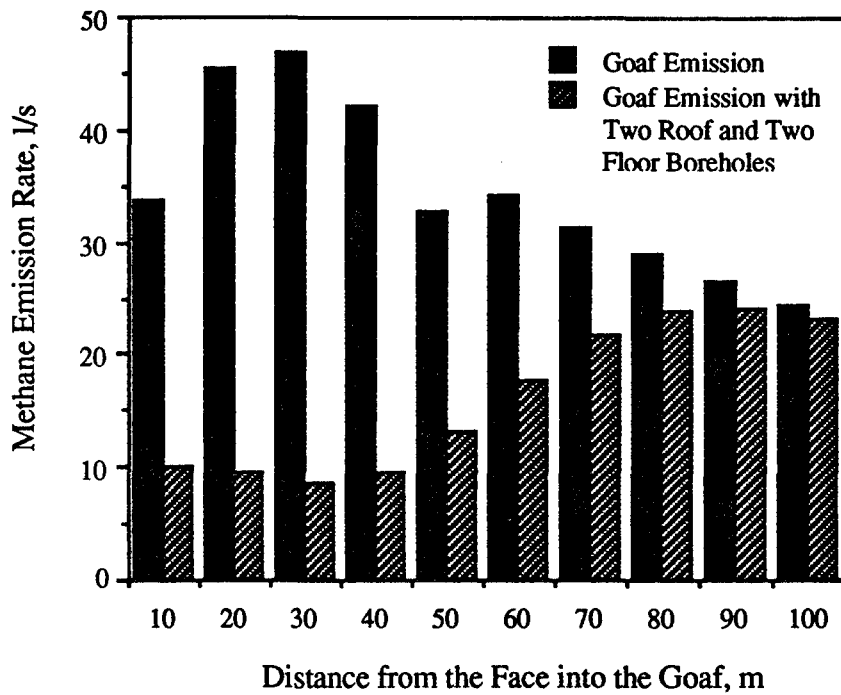
Figure 8.8 Goaf Emissions with and without Drainage in the Retreat Model (Boundary Gas Pressure = 9×10^5 N/m^2).
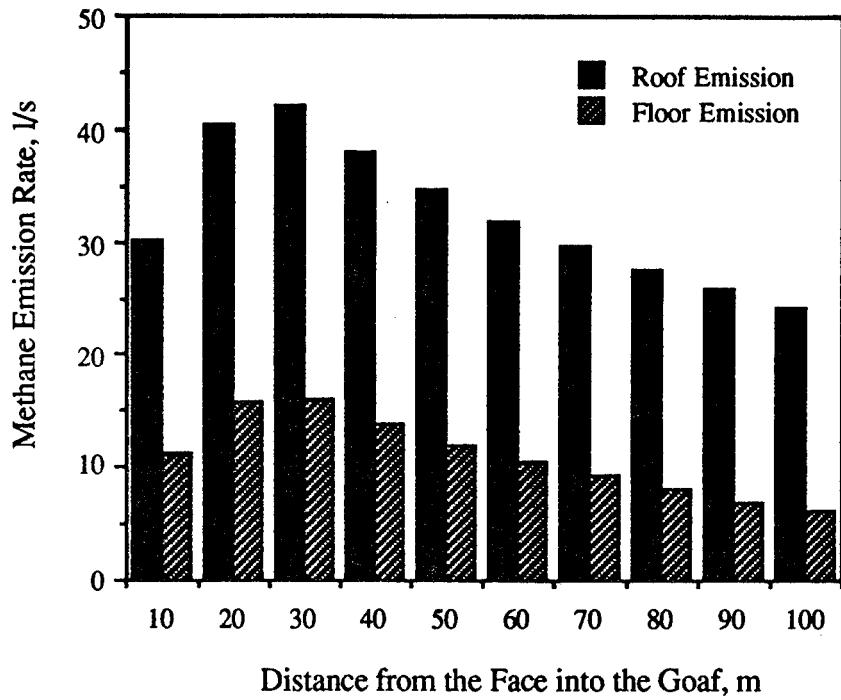
Figure 8.9 Methane Emission Rates to the Goaf in the Retreat Model with no Drainage (Boundary Gas Pressure = 10×10^5 N/m^2).
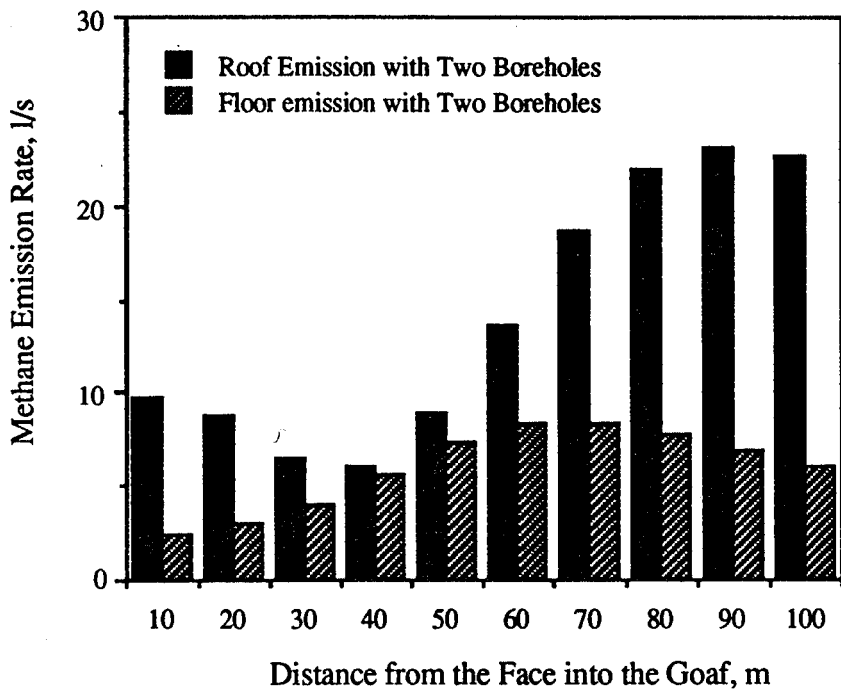
Figure 8.10 Methane Emission Rates to the Goaf in the Retreat Model with Drainage (Boundary Gas Pressure = 10×10^5 N/m^2).
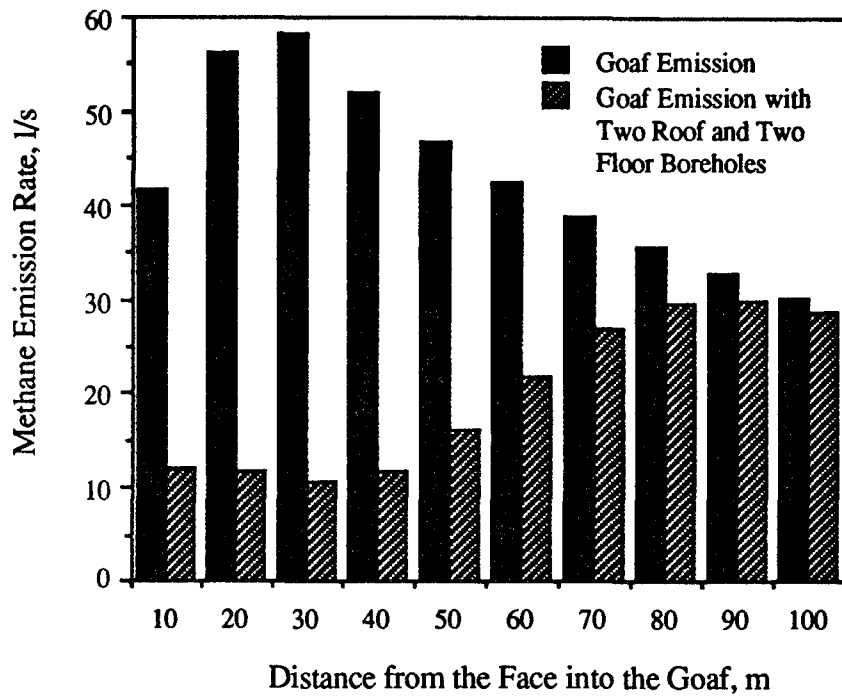
Figure 8.11 Goaf Emissions with and without Drainage in the Retreat Model
(Boundary Gas Pressure = 10×10^5 N/m^2).
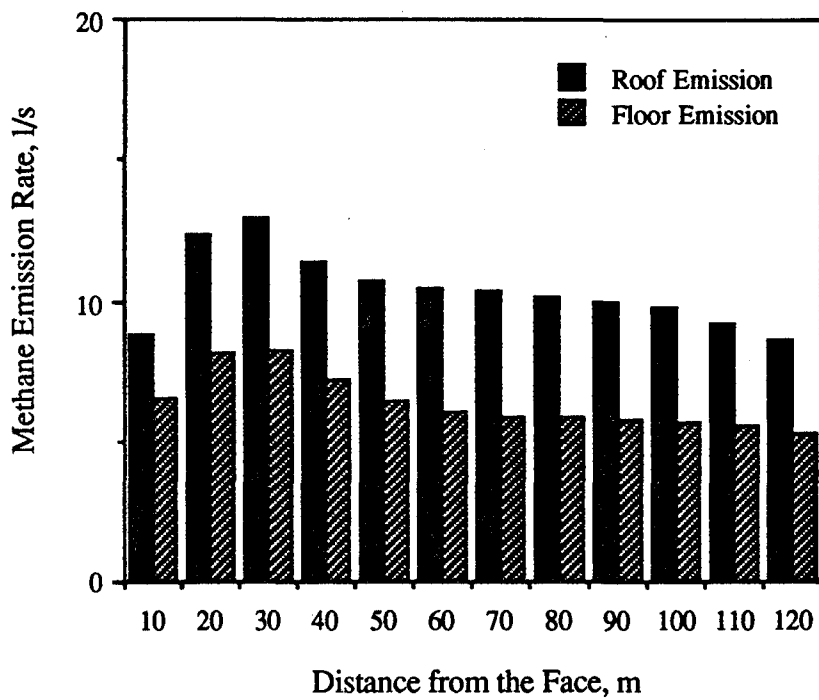
Figure 8.12 Methane Emission Rates to the Roadway in the Advance Model
with no Drainage (Boundary Gas Pressure = 8×10^5 N/m^2).
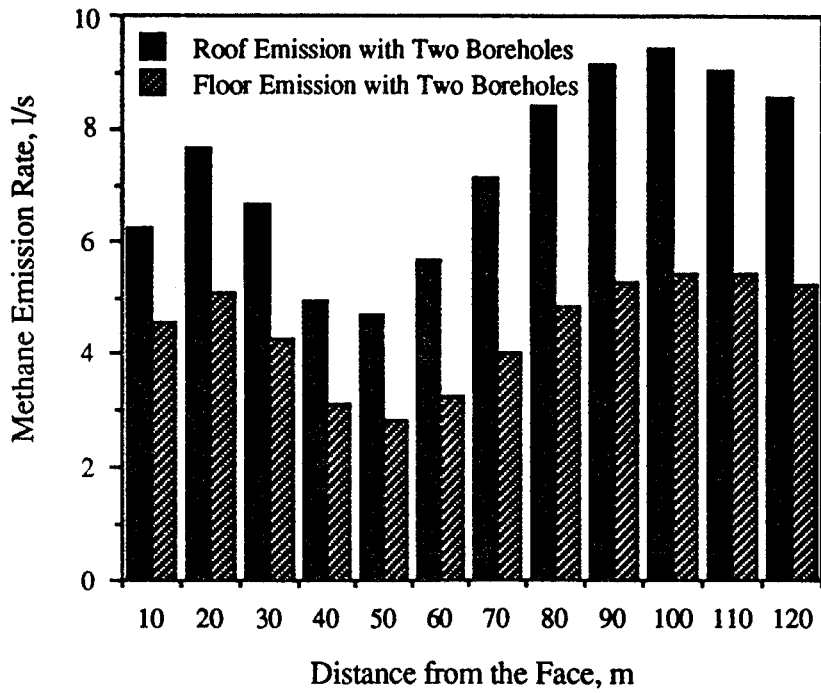
Figure 8.13 Methane Emission Rates to the Roadway in the Advance Model with Drainage (Boundary Gas Pressure = 8×10^5 N/m^2).
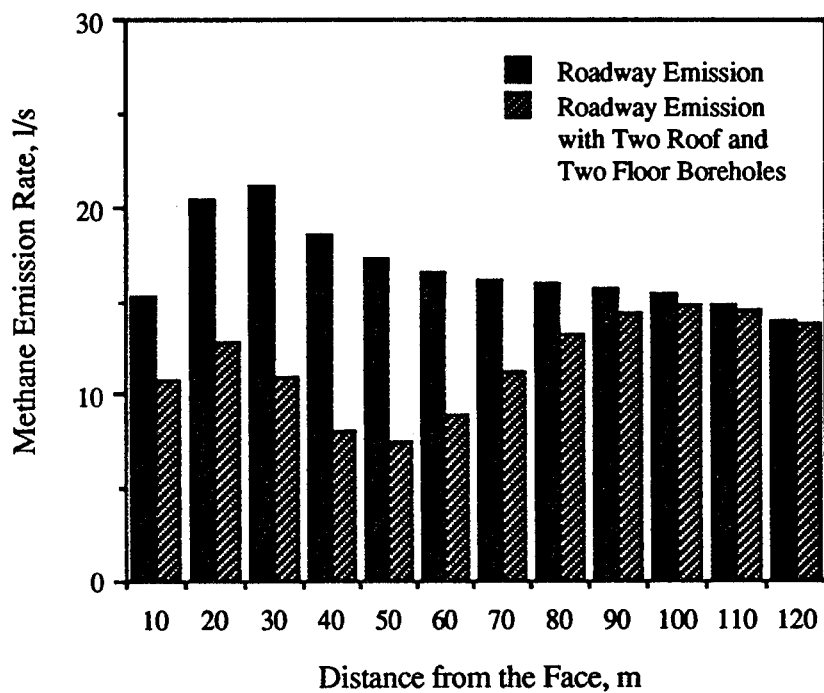
Figure 8.14 Roadway Emissions in the Advance Model with and without Drainage (Boundary Gas Pressure = 8×10^5 N/m^2).
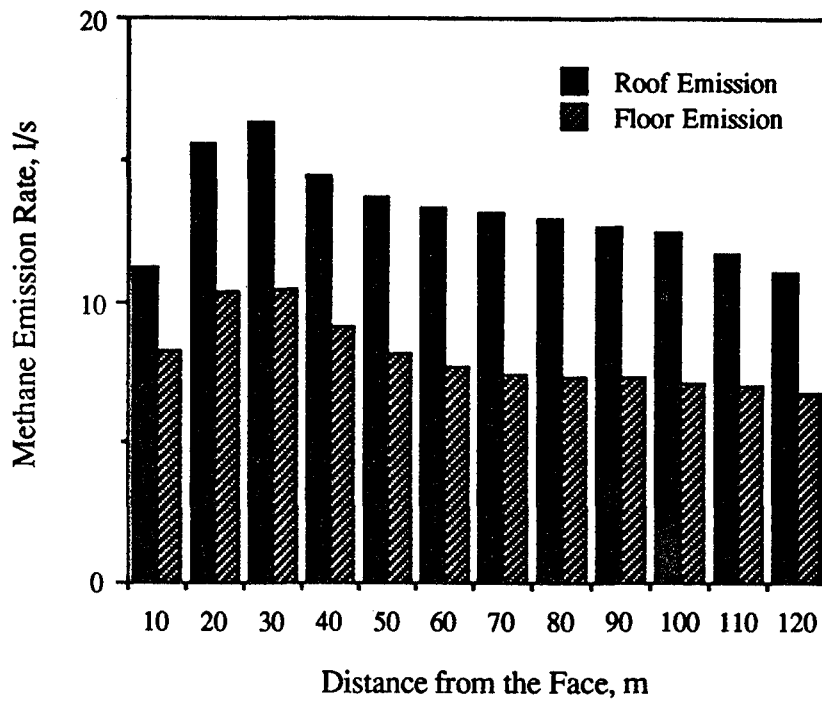
Figure 8.15 Methane Emission Rates to the Roadway in the Advance Model
with no Drainage (Boundary Gas Pressure = $9{\times}10^5$ N/m^2).
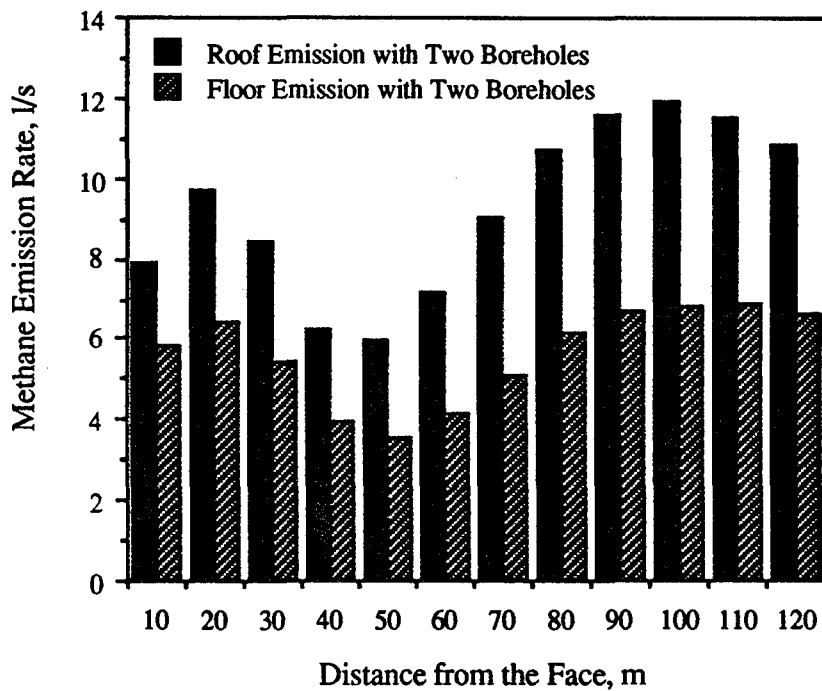
Figure 8.16 Methane Emission Rates to the Roadway in the Advance Model
with Drainage (Boundary Gas Pressure = $9{\times}10^5$ N/m^2).

131
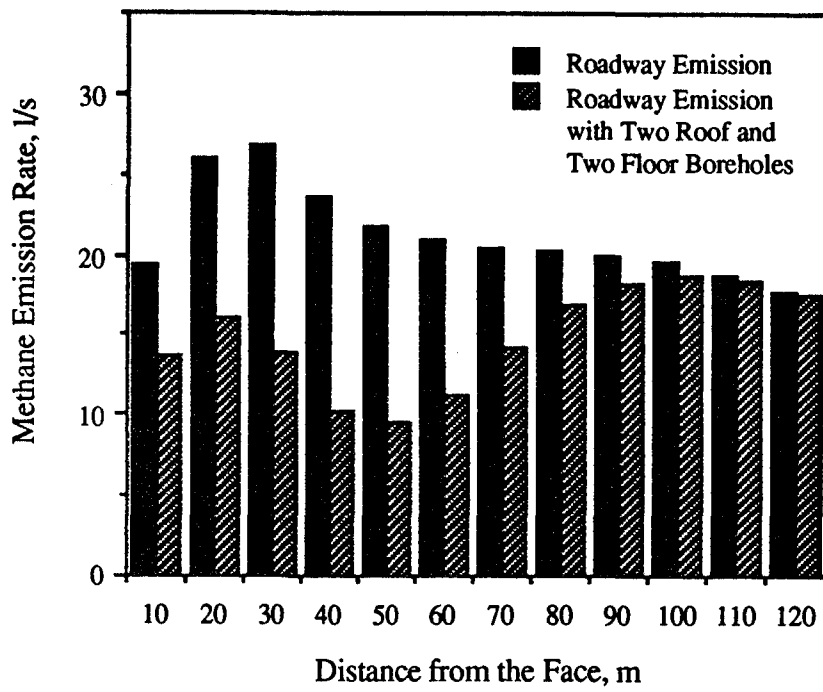
Figure 8.17 Roadway Emissions in the Advance Model with and without Drainage (Boundary Gas Pressure = 9×10^5 N/m^2).
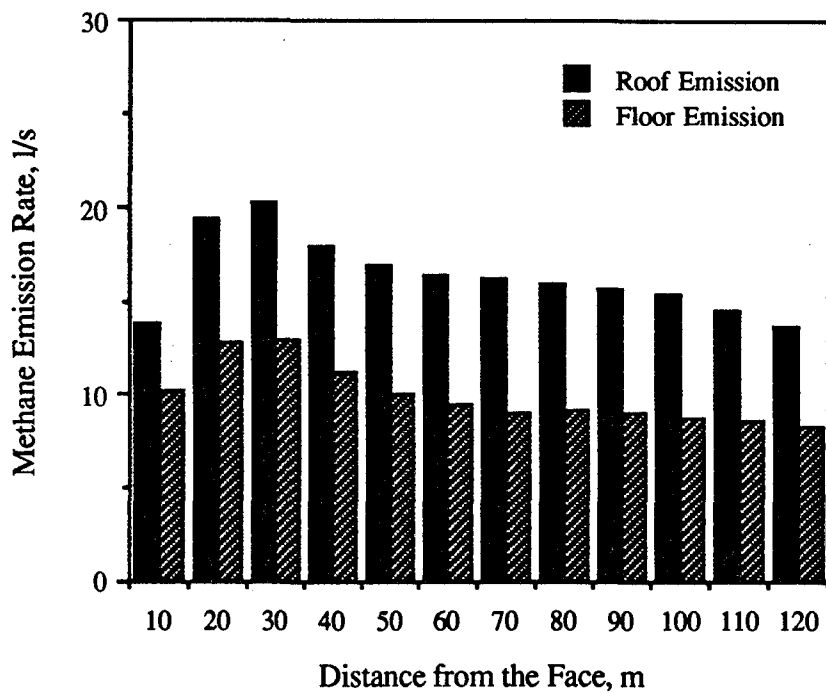
Figure 8.18 Methane Emission Rates to the Roadway in the Advance Model with no Drainage (Boundary Gas Pressure = 10×10^5 N/m^2).
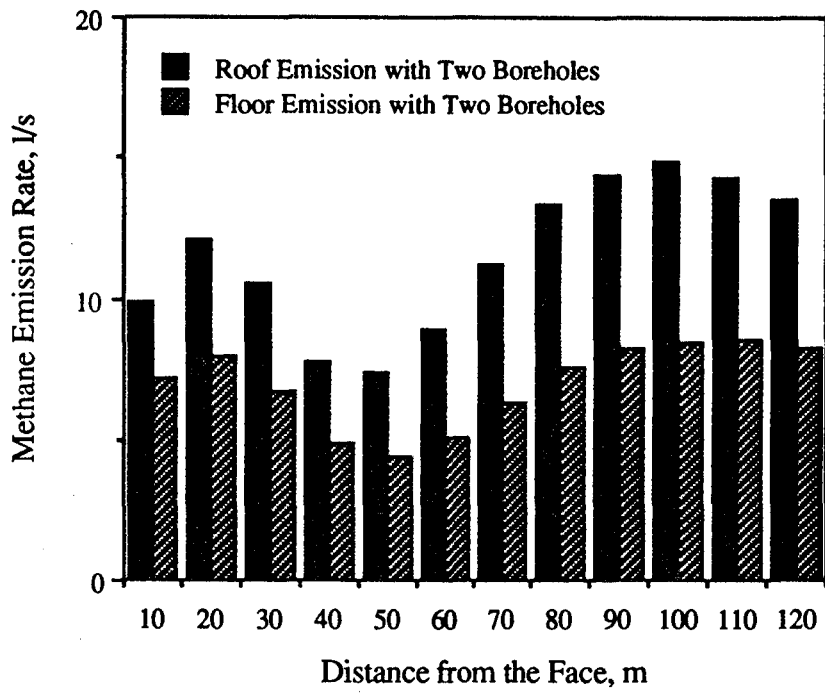
Figure 8.19 Methane Emission Rates to the Roadway in the Advance Model with Drainage (Boundary Gas Pressure = 10×10^5 N/m^2).
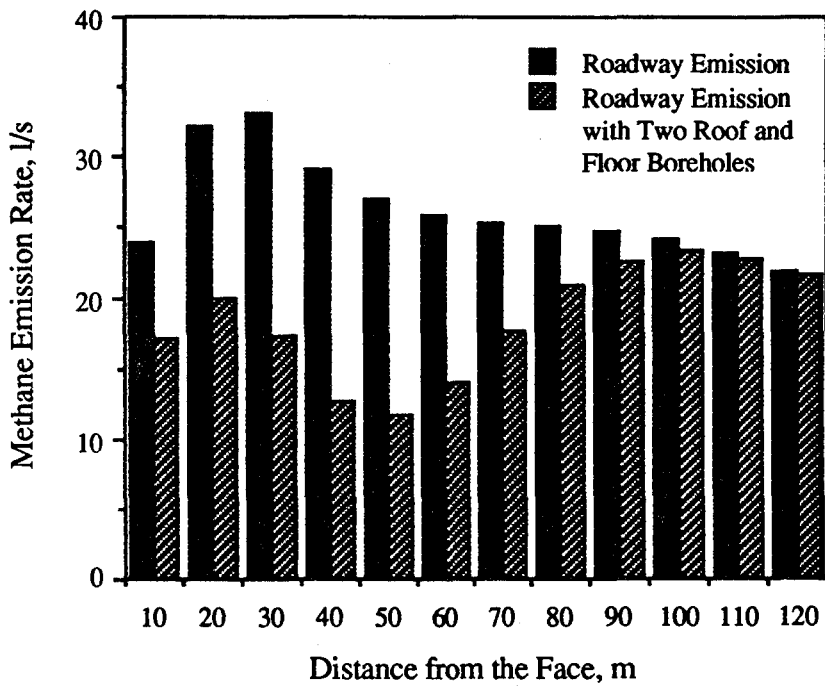
Figure 8.20 Roadway Emissions in the Advance Model with and without Drainage (Boundary Gas Pressure = 10×10^5 N/m^2).

Temp Field /10	
A	0.19
B	0.27
C	0.35
D	0.43
E	0.51
F	0.58
G	0.66
H	0.74
I	0.82
J	0.89
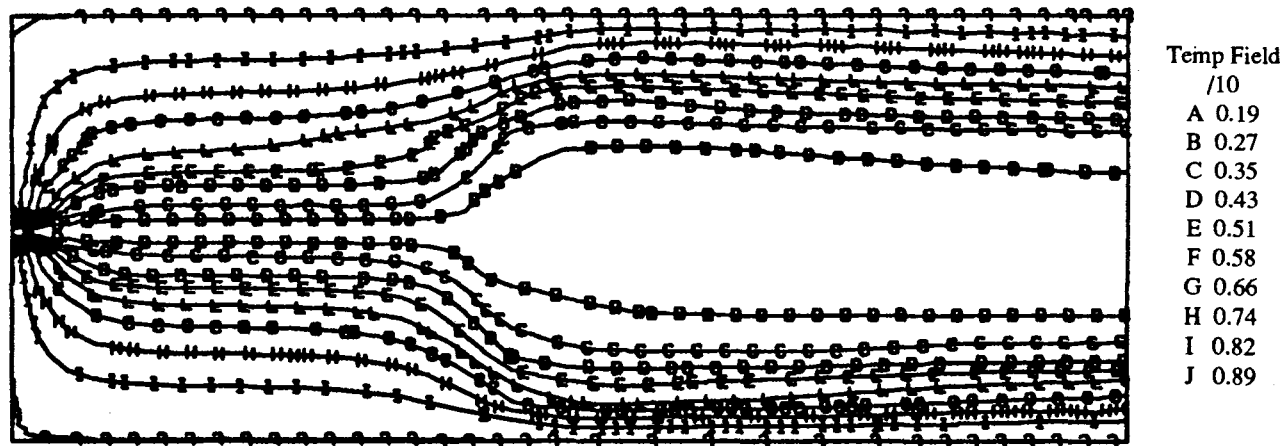
Figure 8.21 Gas Pressure Distribution in the Retreat Model.

Temp Field
/101
A 0.19
B 0.27
C 0.35
D 0.43
E 0.51
F 0.58
G 0.66
H 0.74
I 0.82
J 0.89

Figure 8.22 Gas Pressure Distribution with Drainage in the Retreat Model.

Temp
Field
/10
A 0.19
B 0.27
C 0.35
D 0.43
E 0.51
F 0.58
G 0.66
H 0.74
I   0.82
J   0.89
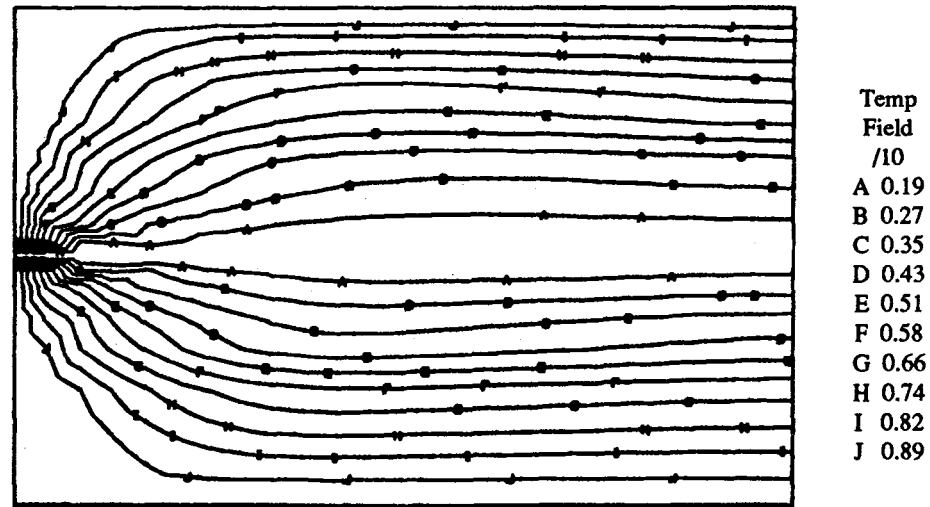
Figure 8.23 Gas Pressure Distribution in the Advance Model.

Temp Field
/10
A 0.19
B 0.27
C 0.35
D 0.43
E 0.51
F 0.58
G 0.66
H 0.74
I 0.82
J 0.89
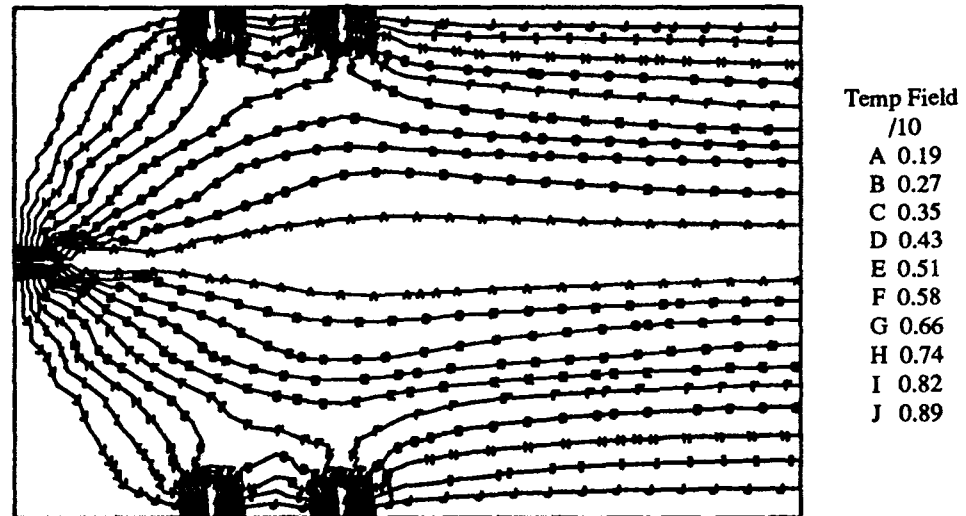
Figure 8.24 Gas Pressure distribution with Drainage in the Advance Model.

8.3 Sensitivity Tests

Several sensitivity tests were carried out to investigate the effects on methane flow of varying;

i.   borehole length,

ii. borehole pressure,

iii. borehole spacing.

During the simulations gas pressure in the source beds was kept at a constant value of 10×10^5 N/m^2 throughout the time-period considered. The length of roadway was also taken as a constant 120 m for an advancing longwall model. Boreholes are considered to be drilled from the roadway into the roof and floor strata vertically. An attempt was made to define realistic boundary conditions and permeability values for strata in the program.

8.3.1 Results of Varying Borehole Length

Three different effective borehole lengths of 5 m, 8 m and 12 m were successively used for the two roof and two floor boreholes (drilled vertically from the roadway at 30 m and 50 m away from the face) in an advance model. The other parameters were taken as constant e.g. borehole spacing was fixed at 20 m, boundary gas pressure and borehole pressure were taken as 10×10^5 N/m^2 and 0.9×10^5 N/m^2 respectively. The results are summarised in table 8.4.

Borehole Length, m	5.00	8.00	12.00
Methane Flow into Roadway from Roof Strata, l/s	137.62	131.34	120.26
Methane Flow into Roadway from Floor Strata, l/s	83.65	79.18	73.35
Drainage from the First Roof Borehole, l/s	252.84	292.05	296.90
Drainage from the Second Roof Borehole, l/s	240.02	277.88	281.15
Drainage from the First Floor Borehole, l/s	166.25	205.40	213.11
Drainage from the Second Floor Borehole, l/s	149.83	182.95	185.98

Table 8.7   Methane Flow into Roadway and Borehole for Various Borehole Lengths.

As seen from table 8.4, as borehole length increases, gas flow into boreholes increases, whereas gas emission to the roadway decreases.   This result, of course, confirms the practical observations seen in mining operations.

8.3.2 Results of Varying Borehole Pressure

In order to investigate the effect of borehole pressure on gas flow from strata, several different borehole pressures were given to two roof and two floor boreholes using the same geological model, the other parameters being constant (borehole length is taken as 5 m, spacing is 20 m, boundary source pressure is 10×10^5 N/m^2) and the results were:

Borehole Pressure, N/m^2	0.95×10^5	0.9×10^5	0.8×10^5
Methane Flow into Roadway from Roof Strata, l/s	137.68	137.62	137.50
Methane Flow into Roadway from Floor Strata, l/s	83.69	83.65	83.58
Drainage from the First Roof Borehole, l/s	252.41	252.84	253.66
Drainage from the Second Roof Borehole, l/s	239.58	240.02	240.87
Drainage from the First Floor Borehole, l/s	165.95	166.25	166.83
Drainage from the Second Floor Borehole, l/s	149.50	149.83	150.44

Table 8.8   Effect of Varying Borehole Pressure on Methane Flow.

As shown in the results, decreasing borehole pressure (or applying higher suctions) increased gas flow to the borehole and reduced the methane flow into the roadway as expected.   However, the changes were small, i.e. for borehole

140

pressure differences of 5 KPa, gas flow from the strata to the boreholes was not changed by more than 0.2 %. Therefore, it can be concluded that increasing suction does not have any value in terms of increasing drainage production, according to the test results produced by the model.

8.3.3 Results of Varying Borehole Spacing

Three different borehole spacings, 10 m, 20 m, and 30 m, were given for the two roof and two floor boreholes in an advancing longwall model. In these tests borehole effective length was fixed at 5 m and borehole pressure was given as 0.9×10^5 N/m^2. The results are summarized in table 8.6.

From the results seen in table 8.6, it can be concluded that as the spacing increases, drainage from individual boreholes increases and therefore methane flow to the roadway decreases for the simple model used. Closer spacing reduces the pressure gradients between the boreholes and causes less methane capture, but the total capture would be increased due to there being more boreholes. However, in widely spaced patterns, the total drainage from a given length of roadway decreases. In practice the borehole spacing and the total drainage for a given roadway length should be optimized.

Borehole Spacing, m	10	20	30
Methane Flow into Roadway from Roof Strata, l/s	149.30	137.62	134.31
Methane Flow into Roadway from Floor Strata, l/s	89.49	83.65	81.65
Drainage from the First Roof Borehole, l/s	200.98	252.84	288.42
Drainage from the Second Roof Borehole, l/s	191.07	240.02	272.20
Drainage from the First Floor Borehole, l/s	132.01	166.25	187.42
Drainage from the Second Floor Borehole, l/s	119.48	149.83	168.95

Table 8.9 Effect of Borehole Spacing on Methane Flow into Boreholes.

From these tests it can be seen that the position of the borehole is most important in obtaining higher drainage, in other words, the borehole must be drilled into the higher gas pressure distribution or higher permeability regions to maximize drainage.

CHAPTER NINE

CONCLUSIONS

9.1 Summary of the Research

This thesis describes an application of numerical methods for the prediction of strata methane flow into mine workings around a moving longwall face employing methane drainage. This method of methane prediction was achieved by solving the time-dependent gas flow equation using finite element analysis to give time-dependent gas pressures. Having obtained the gas pressure distribution throughout the finite element mesh, a mass flow equation was introduced to calculate methane flow rate for a given boundary. A computer program for methane prediction was then developed by devising appropriate modifications and additions to a finite element package originally written for heat flux calculations by PAFEC Limited. Stress analysis was also carried out in order to provide an understanding of stress fields around a longwall face to evaluate the induced permeabilities which are of the greatest importance to the reliability of such a methane prediction. This thesis can be sub-divided into the following sections:

i.   A review about methane, methane flow, and the current knowledge on the mathematical prediction methods are given in chapter 1.

ii.   The time-dependent gas flow equation for anisotropic porous media with variable permeability was derived with certain assumptions in chapter 2.

iii. Possible numerical solution methods of the time-dependent gas flow equation were discussed and finite element solutions were given in chapter 3.

iv.   Stress-permeability relationships for coal strata were given due to its importance in such a prediction method in chapter 4.

v.   Stress analysis using the finite element method and the method of induced permeability assessment under these stress conditions were given in chapter 5.

vi.   Modifications were introduced to the PAFEC'75 system in order to obtain approximate solutions of the time-dependent gas flow equation and a mass flux equation was derived to perform gas flow calculations in chapter 6.

vii. Routines were developed to perform gas flow calculations into a roadway and borehole for either retreat or advance longwall mining in chapter 7.

viii. The results obtained from the simulation of different longwall conditions were given in chapter 8.

9.2 The Main Conclusions

The most important conclusion of the research is that the methane prediction model which has been developed, has been found to be extremely versatile in the analysis of strata gas flow around a moving longwall coal face. Since the program allows rapid variations in permeability and gas pressures with time, the actual conditions can be modelled for reliable prediction of methane emission into a roadway. Although this is a two dimensional simulation, the modelling of methane drainage systems considered has produced reasonable results. The results, for example, have proven that:

i. The accuracy of the prediction mainly depends upon the values defined for permeability and time dependent gas pressures at the boundaries.

ii. The application of methane drainage has a great effect in reducing methane flow into roadways.

iii. Roof drainage is more effective than floor drainage since roof strata is more disturbed and thus has higher permeabilities.

iv. Increasing borehole effective length has a positive effect on both increasing borehole drainage and reducing gas flow into the roadway.

v. Increasing borehole pressure by means of applying higher suction pressure has almost negligible effect on gas flow from strata into a borehole. The application of higher suction pressure may only increase

the flow rate from the borehole due to air leakage, however, strata gas flow to the borehole is not significantly changed.

vi. Increasing borehole spacing has resulted in increased drainage from individual boreholes.   Closer spacing reduces the gas pressure gradients between the boreholes and causes less methane capture, but the total capture would be increased for a given roadway length due to there being more boreholes.

vii. From the drainage simulation tests it can be seen that the position of the borehole is the most important aspect to consider in obtaining higher drainage, in other words, the borehole must be drilled into the higher gas pressure distribution or higher permeability regions to maximise drainage.

The results obtained from the tests have shown good agreement with those anticipated from physical considerations.   However, the reliability of the model can be improved by supplying better field data.   It is widely believed that methane flow through strata is mainly controlled by the permeability of the formations concerned, which result from stress disturbances caused by mining activities.   Therefore, it is important to note that the stress-permeability behaviour of coal or coal measure strata is the key to any simulation attempt of methane flow.   This requires a link between the disciplines of mine ventilation and rock mechanics.   If such a link were achieved it would provide a better overall understanding of the physical events occurring during longwall mining.

9.3 Possible Topics for Future Research

9.3.1 Type of Flow

As stated in chapter 1, in order to achieve the gas flow simulation several assumptions had to be made, one of which was to consider the gas flow to be pure (i.e. not a mixture of gases) and single phase. This assumption is not believed to alter the accuracy of flow prediction into a roadway. However, in the case of borehole simulation, it may be necessary to consider air leakage from the roadway into a borehole. In fact, the present model simulates the gas flow from the strata to borehole boundaries ignoring air flow through boreholes, which is not the case in reality. Therefore, for better drainage simulation, air flow should be considered together with methane flow. This requires the simulation of a mixed-flow regime in which the constituents will be methane and air.

9.3.2 Three Dimensional Simulation

Two dimensional simulation does not create many problems for gas flow simulation into a roadway. However, it is desirable to use a three dimensional simulation method for drainage systems since they are normally drilled in various directions from the roadway axis. In this case element routines should be extended to three dimensions to allow permeability definition in the third dimension as well. However, problems would arise in practice due to the present upper limit on the number of elements that can be accommodated.

9.3.3 Further Research into Stress-Permeability Relationships of Strata and Fracture Mechanism

It is obvious that many parts of the mining area, especially the roof of the working level, are subject to some degree of failure. Most of the gas flow occurs through this failed area around the face. Therefore, virgin or pre-failure permeability cannot represent the actual flow characteristics of strata to gas flow. It is also possible that fractures may play a more dominant role in gas flow than strata permeabilities in this area. This indicates the importance of the work on the mechanism of strata fracturing in gas flow simulation. Apart from this, in any geological cross-section the thickness of coal measure strata through which gases pass is much larger than the total thickness of coal seams. This necessitates, the knowledge of post-failure stress-permeability behaviour of coal measure strata as well as those of coal seams.

In order to make better use of the gas flow simulation model, considerable time has been spent in finding reliable data, especially for coal measure strata, on the stress-permeability relationship, including the post-failure relationship. In fact, there has been some research for coal, and coal measure rocks up to failure, but none for coal measures after failure. All gas emissions in the model are considered to be from strata other than the coal seam being worked, and since changes in permeability after failure are more significant than pre-failure changes, this is taken into account by the simulation. The above indicates the need for research into the post-failure stress-permeability relationship and fracture mechanism for coal measure rocks. This would not only improve the understanding of gas flow phenomenon through strata affected by underground mining, but would also improve the reliability of the current model.

9.3.4 Determining Time-Dependent Gas pressures Around a Moving Longwall Face

It is obvious that predicted flow rates are the product of initial gas pressure values defined for the boundaries of the mining model. In order for the program to calculate the transient gas pressure distribution, all the initial boundary pressures and the changes in these pressures with time should be known, and be input as data for the simulation. This is especially important in the vicinity of a borehole where the pressure changes are more rapid and substantial, causing sudden high flow rates at the beginning and lower gas flow later on. Therefore, more data should be available for the definition of time-dependent gas pressure boundaries with respect to a moving longwall face and around a producing borehole.

ACKNOWLEDGEMENT

150

REFERENCES

1. MINES AND QUARRIES ACT, " The Law Relating to Safety and Health in Mines and Quarries. Part 1 The Act, Part 2 Regulations ", HMSO, 1954.

2. THE MINE VENTILATION SOCIETY OF SOUTH AFRICA, " Environmental Engineering in South African Mines ", Cape Town, 1982.

3. COWARD, H. F., JONES, G. W., " Limits of Flammability of Gases and Vapours ", US Bureau of Mines, Bulletin No. 503, 1952.

4. HARPALANI, S., McPHERSON, M.J., " Retention and Release of Methane in Underground Coal Workings ", International Journal of Mining and Geological Engineering, Vol. 4, No. 3, 1986, pp 217-233.

5. IEA COAL RESEARCH, " Methane Prediction in Coal Mines ", IEA, 1978, 77 p.

6. YEREBASMAZ, G., " An Investigation into the Flow of Methane through Coal Samples ", M.Phil. Thesis, University of Nottingham, 1981.

7. JOLLY, D.C., MORRIS, L.H., HINSLEY, F.B., " An Investigation into the Relationship Between the Methane Sorption Capacity of Coal and Gas Pressure ", Mining Engineer, Vol. 127, No. 94, July 1968, pp 539-548.

8. PATCHING, T.H., " The Retention and Release of Gas in Coal - A Review ", CIM Bulletin, Vol. 63, No. 703, 1970, pp 1302-1308.

9. BIELICKI, R.J., PERKINS, J.H., KISSELL, F.N., " Methane Diffusion Parameters for Sized Coal Particles. A measuring apparatus and some provisional results ", US Bureau of Mines, Report of Investigation, RI 7697, 1972, 15pp.

10. LANGMUIR, I., " The Constitution and Fundamental Properties of Solids and Liquids ", Journal of American Chemical Society, Vol. 38, 1916, pp 2221-2295.

11. BRUNNAUER, S., EMMET, P.H., TELLER, E., " Adsoption of Gases in Multi-Molecular Layers ", Journal of American Chemical Society, Vol. 60, 1938, pp 309-319.

12. KEEN, T.F., " The Simulation of Methane Flow in Carboniferous Strata" Ph.D. Thesis, University of Nottingham, Oct. 1977.

13. KISSEL, F.N., McCULLOCH, C.M., ELDER, C.H., " The Direct Method of Determining Methane Content of Coalbeds for Ventilation Design ", US Bureau of Mines, Report of Investigation, RI 7767, May 1973, 22 p.

14. KIM, A.G., " Estimating Methane Content of Bituminous Coalbeds from Adsorption Data ", US Bureau of Mines, Report of Investigation, RI 8245, 1977, 22 p.

15. HARPALANI S., McPHERSON M.J., " An Experimental Investigation to Evaluate Gas Flow Characteristics of Coal ", 4th International Mine Ventilation Congress, Queensland, July 1988, pp 175-182.

16. DUNMORE, R., " A Theory of Emission of a Mixture of Methane and Ethane from Coal ", International Mine Ventilation Congress, Johannesburg, 1975, 7 p.

17. KISSELL, F.N., EDWARDS, J.C., " Two-Phase Flow in Coalbeds ", US Bureau of Mines, Report of Investigation, RI 8066, 1975, 22 p.

18. DARCY, H., " Les Fontaines Publiques de la Ville de Dijon ", V. Dalmont, Paris, 1856.

19. OWILI-EGER, A.S.C., RAMANI, R.V., " Mathematical Modelling of Methane Flow in Mines ", Proceedings of the 12th International Symposium on the Application of Computing and Mathematics in Mining Industry, Published by Colorado School of Mines, Vol.2, Section G, 1974, pp 218-229.

20. ADZUMI, H., " On the Flow of Gases through a Porous Wall ", Bulletin of Chemical Society of Japan, Vol. 12, No. 6, June 1937, pp 304-312.

21. KLINKENBERG, L. J., " The Permeability of Porous Media to Liquids and Gases ", Drilling and Production Practice, Published by the American Petroleum Institute, 1941, pp 200-211.

22. O'SHAUGHNESSY, S.M., " The Computer Simulation of Methane Flow Through Strata Adjacent to Working Longwall Coal Faces ", Ph.D. Thesis, University of Nottingham, May 1980.

23. VUTUKURI, V.S., LAMA, R.D., " Environmental Engineering in Mines ", Cambridge University Press, 1986, 504 p.

24. MORDECAI, M., MORRIS, L.H., " The Effect of Stress on the Flow of Gas through Coal Measure Strata ", Trans. Institute of Mining Engineers Vol.133, 1974, pp 435-443.

25. DUNMORE, R., " Gas Flow through Underground Strata ", Mining Engineer, Vol. 128, No. 100, Jan 1969, pp 193-199.

26. RICHARDS, M.J., " An Investigation into the Movement of Firedamp from the Strata in the Region of Working Longwall Faces ", Ph.D. Thesis, University of Nottingham, 1975.

27. GUNTHER, J., " Investigation of the Relationship Between Coal and the Gas Contained in It ", Revue de L'industrie Minerale, Vol. 47, No.10, 1965, 693 p.

28. RILEY, P.A., " An investigation into the Changes of Stress and Release of Methane from Longwall Coal Faces ", Ph.D. Thesis, University of Nottingham, 1986.

29. MUCHNIC, S.V., " Feasibility Combined Determination of the Natural Residual Methane Content of a Coal Seam, the Methane Pressure in the Seam, the Sorption Isotherms and the Gas Emission Kinetics ", Soviet Mining Science, Vol. 11, No.6, 1975, pp 759-762.

30. MUCHNIC, S.V., " Emission of Methane from Coal ", Soviet Mining Science, Vol. 11, No.1, 1975, pp 91-94.

31. SCHEIDEGGER, A. E., " The Physics of Flow Through Porous Media" University of Toronto Press, Revised Edition, 1963.

32. HUBBERT, M.K., " Darcy's Law and the Field Equations of the Flow of Underground Fluids ", Transactions of AIME, Petroleum Branch, Vol. 207, 1956, pp 222-239.

33. NUTTING, P.G., " Physical Analysis of Oil Sands ", Bulletin of American Association of Petroleum and Geology, Vol. 14, 1930, pp 1337-1349.

34. KNUDSEN, M., " Die Gezetze der Molekularstromung und der inneren Reinbungsstromung der Gase durch Rohren ", Annalen der Physik, Vol.28, Leipzig, 1909, pp 75-130.

35. SOWIER, T.S., " Steady-State and Non-Steady-State Flows of Compressible Fluids through Sorptive Porous Media ", Ph.D. Thesis, University of Nottingham, Oct. 1973.

36. KING G.R., ERTEKIN T.M., " A Survey of Mathematical Models Related to Methane Production from Coal Seams, Part I: Emprical and Equilibrium Sorption Models ", Proceedings of the 1989 Coalbed Methane Symposium, The University of Alabama/Tuscaloosa, April 17-20, 1989, pp 125-138.

37. KING G.R., ERTEKIN T.M., " A Survey of Mathematical Models Related to Methane Production from Coal Seams, Part II: Non-Equilibrium Sorption Models ", Proceedings of the 1989 Coalbed Methane Symposium, The University of Alabama/Tuscaloosa, April 17-20, 1989, pp 125-138.

38. FEDEROV, A.V., GORBACHEV, A.I., SOMOV, G.I., " Exact Solution to the Problem of Inflow of Gas into a Borehole under Conditions of Quasilinear Isothermal Non-Equilibrium Filtration ", Fiziko-Teknickeskie Problemy Razrabolki Poleznykh Iskopaehykh, No. 6, Nov.-Dec. 1976.

39. KOVALEV, Y.M., KUZNETSOV, S.M., " Filtration of Gas in a Coal Seam Being Worked in the Presence of Diffusion Desorption ", Fiziko-Teknickeskie Problemy Razrabolki Poleznykh Iskopaehykh, No. 6, Nov.-Dec. 1974.

40. PINDER, G.F., GRAY, W.G., " Finite Element Simulation in Surface and Subsurface Hydrology ", Academic Press, 1977.

41. ZIENKIEWICZ, O.C., " The finite Element Method in Engineering Science ", McGraw-Hill Book Co., 1971.

42.   ZIENKIEWICZ, O.C., " Introductory Lectures on the finite Element Method ", Springer-Verlag, Vienna, N.Y., June 1972.

33.   WYLIE, C.R., BARRETT, L.C., " Advanced Engineering Mathematics " McGraw-Hill Book Co., 1985.

44.   PAFEC LIMITED, " PAFEC'75 Theory and Results ", Nottingham, 1977.

45.   PAFEC LIMITED, " PAFEC'75 Data Preparation ", Nottingham, 1978.

46.   McPHERSON, M.J., " The Occurence of Methane in Mine Workings ", Journal of Mine Ventilation Society of South Africa, Vol. 28, No. 8, 1975, pp 118-128.

47.   DURUCAN, S., " An Investigation into the Stress-Permeability Relationships of Coals and Flow Patterns Around Working Longwall Faces ", Ph.D. Thesis, University of Nottingham, Oct. 1981.

48.   FATT, I., DAVIS, D.H., " Reduction in Permeability with Overburden Pressure ", Transactions of AIME, Petroleum Branch, Vol. 195, 1952, 329 p.

49.   PATCHING, T.H., " Variations in the Permeability of Coal ", Proceedings of 3rd Rock Mechanics Symposium, University of Toronto, Jan. 1965, pp 185-199.

50. MORDECAI, M., " An Investigation into the Effect of Stress on Permeability of Rock Taken from Carboniferous Strata ", Ph.D. Thesis, University of Nottingham, 1971.

51. SOMERTON, W.H., SOYLEMEZOGLU, I.M., DUDLEY, R.C., " Effect of Stress on Permeability of Coal ", International Journal of Rock Mechanics Mining Science Geomechanics Abstracts, Vol.12, 1975, pp 129-145.

52. GAWUGA, J.K., " Flow of Gas Through Stressed Carboniferous Strata ", Ph.D. Thesis, University of Nottingham, 1979.

53. EDWARDS, J.S., DURUCAN, S., RILEY, P.A., " Preliminary Report on Methane Drainage Enhancement at Silverdale Colliery ", University of Nottingham, 1987.

54. DURUCAN, S., EDWARDS, J.S., " The Effects of Stress and Fracturing on Permeability of Coal ", Mining Science and Technology, 1986, pp 205-216.

55. DURUCAN, S., " Private Communications ", Department of Mineral Resources Engineering, Imperial College of Science, Technology and Medicine, London, 1991.

56. WHITTAKER, B.N., " An Appraisal of Strata Control Practice ", Transactions of the Institute of Mining Engineers, Vol. 166, 1974, pp 9-24.

57. HOEK, E., BROWN, E.T., " Underground Excavations in Rock ", Institutions of Mining and Metallurgy, London, 1982, 528 p.

58. JEAGER, J.C., COOK, N.G.W., " Fundamentals of Rock Mechanics ", Chapman & Hall, London, 1976, 585 p.

59. GRIFFITH, A.A., " Theory of Rupture ", Proceedings of 1st International Conference on Applied Mechanics, Delft, 1924, pp 55-64.

60. WHITTAKER, B.N., REDDISH, D.J., " Subsidence, Occurence, Prediction and Control ", Developments in Geotechnical Engineering 56, Elsevier Science Publishers, 1989, 528 p.

61. REDDISH, D.J., " The Modelling of Rock Mass Behaviour Over Large Excavations Using Non-Linear Finite Element Techniques ", Mining Department Magazine, University of Nottingham., Vol. No. XLI 1989, pp 93-102.

62. UNVER, B., " Closure in Longwall Access Roadways ", Ph.D. Thesis, University of Nottingham, Aug. 1988.

63. WILSON, A.H., " The Stability of Underground Workings in the Soft Rocks of the Coal Measures ", Ph.D. Thesis, University of Nottingham, 1980.

64. FITTZPATRICK, D.J., " Modelling of Mining Subsidence Mechanisms and Prediction of Ground Movements ", Ph.D. Thesis, University of Nottingham, 1987.

65. GIBSON, K.L., " The Computer Simulation of Climatic Conditions in Underground Mines ", Ph.D. Thesis, University of Nottingham, 1976.

66. HOWARD, L.H., " Mine Ventilation and Air Conditioning ", John Wiley & Son , 1982.

67. RILEY, P.A., " Private Communications ", Department of Mining Engineering, University of Nottingham, 1990-91.

APPENDIX 1 GENERALIZED SECTION OF SILVERDALE COLLIERY

Seam	Thickness
	29 m
Spencroft	
	30.5 m
Great Row	
Channel Row	14.6 m
	134.7 m
Winghay	
	89.3 m
Rowhurst	
	189 m
Moss	
	22.6 m
Five Feet	
Yard	15.8 m
	35.7 m
Hams	
	67.1 m
Ten Feet	
	23.8 m
Bowling Alley	
Holly Lane	17.1 m
Hard Mine	18.3 m
New Mine	18.9 m
	58.2 m
Banbury	
	39 m
Cockshead	
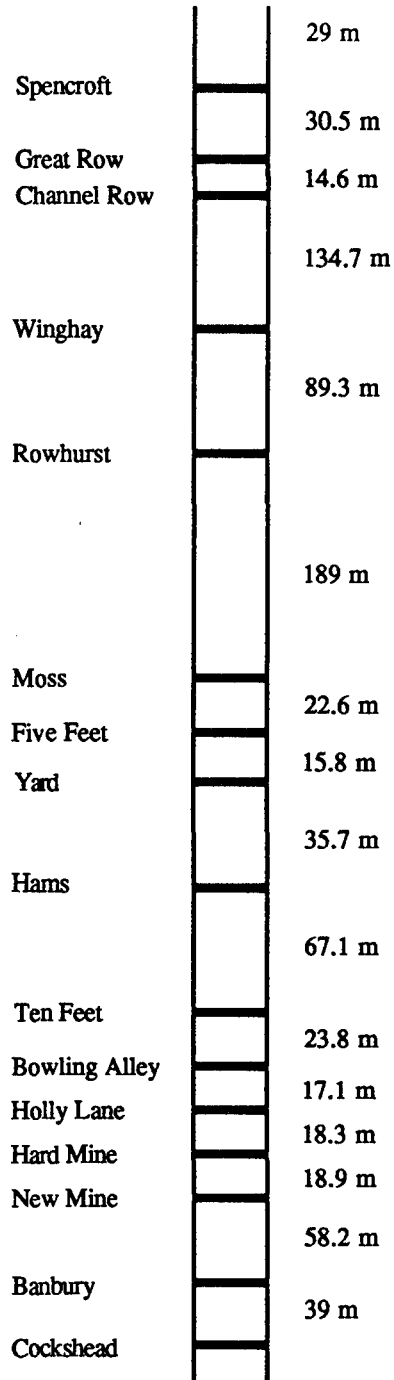
APPENDIX 2 DATA USED IN STRESS ANALYSIS


```
RPAFEC(RUNNAME=STRESS)
----
CONTROL
PLANE.STRAIN
STRESS
TOLERANCE=10E-1
PIGS.STRESS.FILE
FULL.CONTROL
PHASE=1,2,4
PHASE=6
PHASE=7
PHASE=8
PHASE=9
PHASE=10
SAVE
STOP
CONTROL.END
NODES
```

NODE.NUMBER	X	Y
1	0	800
2	100	800
3	0	440
4	100	440
5	0	385
6	100	385
7	0	140
8	100	140
9	0	100
10	100	100
11	0	70
12	100	70
13	0	63
14	100	63
15	0	61
16	100	61
17	0	54
18	100	54
19	0	47
20	100	47
21	0	42
22	100	42
23	0	38
24	100	38
25	0	34
26	100	34
27	0	32
28	100	32
29	0	31
30	100	31
31	0	30
32	50	30

33	100	30
34	0	27
35	50	27
36	100	27
37	0	26
38	100	26
39	0	25
40	100	25
41	0	23
42	100	23
43	0	20
44	100	20
45	0	15
46	100	15
47	0	12
48	100	12
49	0	6
50	100	6
51	0	0
52	100	0

GRAPH
TOLERANCE=0.1

FRAME	GRAPH	TYPE	LENGTH	HEIGHT	LIST
C MAX PRINCIPAL STRESSES,ROOF LEVELS					
1	1	20	20	10	17 18
2	2	20	20	10	19 20
3	3	20	20	10	21 22
4	4	20	20	10	23 24
5	5	20	20	10	25 26
6	6	20	20	10	27 28
7	7	20	20	10	29 30
C MAX PRINCIPAL STRESSES,FLOOR LEVELS					
8	8	20	20	10	37 38
9	9	20	20	10	39 40
10	10	20	20	10	41 42
11	11	20	20	10	43 44
12	12	20	20	10	49 50
C MIN PRINCIPAL STRESSES,ROOF LEVELS					
13	13	21	20	10	17 18
14	14	21	20	10	19 20
15	15	21	20	10	21 22
16	16	21	20	10	23 24
17	17	21	20	10	25 26
18	18	21	20	10	27 28
19	19	21	20	10	29 30
C MIN PRINCIPAL STRESSES,FLOOR LEVELS					
20	20	21	20	10	37 38
21	21	21	20	10	39 40
22	22	21	20	10	41 42
23	23	21	20	10	43 44
24	24	21	20	10	49 50

PAFBLOCKS

BLOCK	TYPE	ELEMENT	PROPERTY	N1	N2	TOPOLOGY
1	1	36210	1	1	2	3 4 1 2
2	3	36110	1	3	1	5 6 3 4
3	1	36210	1	3	2	7 8 5 6

4	3	36110	1	4	3	9	10	7	8
5	3	36110	1	5	4	11	12	9	10
6	3	36110	1	6	5	13	14	11	12
7	1	36210	2	6	2	15	16	13	14
8	1	36210	1	6	2	17	18	15	16
9	3	36110	1	7	6	19	20	17	18
10	3	36110	1	8	7	21	22	19	20
11	1	36210	1	8	2	23	24	21	22
12	1	36210	1	8	2	25	26	23	24
13	3	36110	1	9	8	27	28	25	26
14	1	36210	1	9	2	29	30	27	28
15	1	36210	1	9	2	31	33	29	30
16	1	36210	2	8	2	34	35	31	32
17	1	36210	1	9	2	37	38	34	36
18	1	36210	1	9	2	39	40	37	38
19	3	36110	1	9	8	39	40	41	42
20	1	36210	1	8	2	43	44	41	42
21	1	36210	1	8	2	45	46	43	44
22	3	36110	2	8	7	45	46	47	48
23	3	36110	1	7	6	47	48	49	50
24	3	36110	1	6	5	49	50	51	52

MESH

REFERENCE	SPACING
1	4
2	1
3	6
4	8
5	10
6	20
7	25
8	50
9	100

PLATES.AND.SHELLS

PLATE.NUMBER	MATERIAL.NUMBER	THICKNES
1	1	1
2	1	1
3	1	1
4	1	1
5	1	1
6	1	1
7	2	1
8	1	1
9	1	1
10	1	1
11	1	1
12	1	1
13	1	1
14	1	1
15	1	1
16	2	1
17	1	1
18	1	1
19	1	1
20	1	1
21	1	1
22	2	1

```
        23                        1                      1
        24                        1                      1
MATERIAL
MATERIAL.NUMBER           E              NU              RO
        1                30E09          0.35            2400
        2                3.3E09         0.28            1300
RESTRAINTS
NODE.NUMBER              PLANE              DIRECTION
       51                  1                      1
       51                  2                      2
       52                  1                      1
GRAVITY
LOAD    XGVALUE    YGVALUE    ZGVALUE    AXIS
  1        0.0       -1          0.0        2
IN.DRAW
TYPE                    INFO
  2                     237
OUT.DRAW
PLOT
20
30
31
END.OF.DATA
++++
```

```
      SUBROUTINE R39010 (GVALS,UX,UY,UR,A,AINV,CNDS,
     +          PV,PXI,PETA,Q,QQ,EE,X,Y,R,IERN,INE,II)
C-COMMENT------------------------------------------
C
C COMMON CODE FOR ISOPARAMETRIC 2-D HEAT CONDUCTION
C ELEMENTS R39100 R39110 R39200 R39210
C (ORTHOTROPIC MATERIAL VERSIONS - R39105, R39115,
C R39205, R39215)
C------------------------------------------------
C                        R39010
C INITIALISE BASE D09500.R14000 STORE SE
C BASE INTEGERS R09720...R39005 TRANSFORM SE TO NODAL
C GAUSS D13100..........R39006 COORDINATES
C POLYNOMIAL D35091......R39011 PROPERTIES
C                        (R39031 ORTHOTROPIC KERNEL)
C               ......R39018 KERNEL
C                        (R39038 ORTHOTROPIC KERNEL)
C NOTE-Q,R,AND UR IN ARGUMENT LIST REDUNDANT-NOT USED
C-COMMENT END------------------------------------
      DOUBLE PRECISION   GVALS(II,2),UX(INE),UY(INE),
     +  PV(INE),A(INE,INE),AINV(INE,INE),CNDS(INE,3),
     +  PETA(INE),Q(INE,INE),QQ(INE,9),R(INE),X(INE),
     +  Y(INE), DCA(3,3), AJ(2,2), UR(INE), PXI(INE),
     +  EE(2,INE),RKLAM(3),YV,CBB,DET,CA,CB,CE,TH,RK,
     +  THO,SH,XI,ETA
C-Insert by I.G.Ediz-------------
C
      DOUBLE PRECISION SCAL(1,1),UKX(8),UKY(8),RKX(8)
     +          ,RKY(8), RKXA(8), RKYA(8), RKXG, RKYG
     DIMENSION  TKX(30), TKY(30)
     INTEGER    TX(30),  XTABLE
C
C-End of insert-----------------
C-WORK(36) HAS BEEN REPLACED BY CDS(8,3)-I.G.Ediz----
      DIMENSION   IDG(6),  ISIDNO(2,4),  ISIDCO(2,4)
     +          ,SDCA(3,3),  CDS(8,3),  SURHES(3,4)
     COMMON/IBASE/IBASE(1500)
     COMMON / MAGNL / IGAUS,ICONV,MAGM1,MAGM2,MAGM3
     COMMON BASE(33000)
C-SET DYNAMIC MODULE NUMBER FOR TRANSPORT PARAMETERS
     DATA IDYNMD/12/
C-Insert by I.G.Ediz--------------
C
     IELE=IBASE(12)
C
C-End of insert-------------------
     INIT = 0
     ISURF = 0
     IMAG = I09891( 89 )
C-PUT GAUSS ORDER INTO COMMON BLOCK SO THAT  EXTRA
C-STORAGE CAN BE ALLOCATED FOR CONDUCTIVITY MATRIX
```

```
      IGAUS = II
      MAGNL = 0
      IF( IMAG.EQ.1.AND.IBASE(33).NE.0) MAGNL=1
C-FIND MODULE NUMBER OF DYNAMIC MODULE NUMBER IDYNMD
      MODTRN = I09813(IDYNMD)
C*FOLLOWING LINES INSERTED BY RAG ON 22/2/83
      CALL R09800(MODTRN,1)
      CALL R09806(MODTRN,LM223,JRW223,IPS223)
      IF (LM223.EQ.0) GO TO 100
      INE2 = INE * 2
      INE4 = INE + 4
      CALL R09810(MODV,INE2,INE4,LM,JROW,IPOSV)
  100 IF (IBASE(39).EQ.0)  GO TO 110
C-OBTAIN NEXT ELEMENT
      CALL R09600 (IERNU,IADREL,IIEPA,IENM)
      IF (IERNU.EQ.IERN)  GO TO 120
C-BEFORE RETURNING, IF SURFACE HEAT TRANSFER
C-MODULE EXISTS DELETE IT.
      IF (ISURF.GT.0)  CALL R09800(MODSUR,5)
      IF (LM223.GT.0)  CALL R09800(MODV,5)
  110 RETURN
  120 CONTINUE
C-Insert by I.G.Ediz--------------------
C
      IELE=IELE+1
C
C-End of insert-----------------------
      IBASE(12) = IBASE(12)+1
C-IBASE(39) IS COUNT OF ELEMENTS LEFT TO BE MERGED
      IBASE(39) = IBASE(39)-1
C*FOLLOWING LINES INSERTED BY RAG ON 22/2/83
      IF(LM223.NE.0) CALL DNULL(BASE(IPOSV),INE,INE4)
      IFLAG = 0
C*END.OF.INSERT
      IF (INIT.EQ.1)  GO TO 150
      INIT = 1
C-FOLLOWING SECTION IS FOR THIS ELEMENT TYPE,TYPE IERN
      IDE  = INE
      IS   = INE*(INE+1)
      ISN  = IBASE(25)
      IB45 = IBASE(45)
      ICES = IBASE(14)
C-INITIALISE BASE FOR THIS SERIES OF ELEMENTS
      CALL D09500 (IFE,ISE,ITE,IWE,IPE,IXE,IDE,INE)
C-RETRIEVE INTEGERS FROM IBASE
      CALL R09720 (IP,IX,IDT,ID,IDF,ILO,IE,IELE,IM)
C-Insert by I.G.Ediz------------
C
      CALL R09800(33,1)
      CALL R09806(33,LM33,JROW33,IPOS33)
      IXTN=0
      IYTN=0
C
C-End of insert----------------
C-DECODE IERN FOR ORTHOTROPIC FLAG
      IORTH = IERN/10
```

```
      IORTH = IORTH*10
      IORTH = IERN-IORTH
C-SET DCA,IDG
      CALL DUNIT(DCA,3)
      CALL INULL (IDG,6,1)
      IDG(1)=1
C-OBTAIN GAUSS VALUES
      CALL D13100 (GVALS,II)
C-COMPUTE THE A MATRIX
      CALL R39017 (CNDS,INE)
      DO 140 L1=1,INE
      XI = CNDS(L1,1)
      ETA= CNDS(L1,2)
      CALL D35090 (PV,XI,ETA,INE)
      DO 130 L2=1,INE
      A(L1,L2) = PV(L2)
  130 CONTINUE
  140 CONTINUE
      CALL DMATIN (DET,AINV,A,INE)
C-SET  NUMBER  OF  ELEMENT  SIDES  FROM  ELEMENT TYPE
C-NUMBER.
      NSIDES = 4
      IF (IERN.LT.39200)  NSIDES = 3
C-DETERMINE  WHETHER  THERE IS  SURFACE HEAT TRANSFER
C-FOR ANY ELEMENT.
      ISURF = I09891(29)
C-IF SO,  FILL  TABLES  ISIDNO  AND  ISIDCO, RETRIEVE
C-REQUIRED MODULE ADDRESSES, AND CREATE MODULE MODSUR
      IF(ISURF.GT.0) CALL R39041(ISIDNO,ISIDCO,NSIDES
     +          ,INE,IBM234,MDX232,MODSUR,LBMSUR,JROSUR)
  150 CONTINUE
C-REMAINING SECTION IS FOR THIS ELEMENT, ELEMENT
C-NUMBER IENM.
      INEGV=0
C-OBTAIN MATERIAL PROPERTIES
      IF (IORTH.EQ.5) GO TO 160
      CALL R39011 (RK,SH,TH,IADREL)
      IF(RK.GT.0.0D0.AND.SH.GT.0.0D0) GO TO 170
      IF(RK.GT.0.0D0.AND.IBASE(32).EQ.1) GO TO 170
      CALL NEWLIN( 2 )
      WRITE(6,1) IENM
      IBASE(27)=IBASE(27)+1
      GO TO 170
  160 CONTINUE
      CALL R39031(RKLAM,SH,THO,IADREL)
C-IN THE ORTHOTROPIC CASE THE THICKNESS IS INCLUDED
C-IN THE CONDUCTANCE RKLAM AND HEAT CAPACITY SH.
      TH = 1.D0
      RK = 1.D0
C-OBTAIN NODAL COORDINATES
  170 CALL R39006 (CNDS,INE)
C-FOR MAGNETIC PROBLEMS USE 1/RK
      IF( IMAG .NE. 0 ) RK = 1.0D0/RK
C*FOLLOWING LINES INSERTED BY RAG ON 22/2/83
      IF(IBASE(25).EQ.2) GO TO 126
      CALL D12100(CNDS,CDS,DCA,INE)
```

```
        CALL DUNIT(DCA,3)
  126   CONTINUE
C*END.OF.INSERT
        INE1=INE+1
        ICOL = INE1
        IF( MAGNL .EQ. 1 ) ICOL = INE*II*II
        CALL DNULL (BASE(ISE),INE,ICOL)
        CALL DNULL (QQ,INE,INE)
C-FORM THE CONSTANT COLUMNS UX,UY (POLYNOMIAL
C-COEFFICIENTS FOR X, Y COORDINATES).
        CALL DMATMU (UX,AINV,CNDS(1,1),INE,INE,1)
        CALL DMATMU (UY,AINV,CNDS(1,2),INE,INE,1)
C-IF THERE MAY BE SURFACE HEAT TRANSFER,CALL S.H.T.
C-ROUTINE  FOR THIS ELEMENT.
        IF(ISURF.GT.0) CALL R39042(ISURF,SURHES,
       +      ISIDNO,2,NSIDES,NSIDES,IADREL,IBM234,
       +      MDX232,LBMSUR,JROSUR)
C-(ISURF-1) IS NOW THE NUMBER OF SIDES WHICH HAVE
C-S.H.T. INTEGRATION LOOPS START HERE.INTEGRATION
C-ALONG SIDES UTILISES THE OUTER LOOP.
C-SET UP NODAL VALUES OF HEAT FLOW IN Q(FOR ILOAD=1)
        CALL R39049(ILOAD,BASE(ITE),BASE(IIEPA),IERN,
       +          INE)
        IF(ILOAD.NE.0) CALL NULL(BASE(IFE),IDE,ILO)
        ISS = ISE
        ICOUNT = 1
C-Insert by I.G.Ediz----------------
C
        CALL R39006 (CNDS,INE)
C-FINDS TABLE FOR THE ELEMENT AND KX,KY
        K1=RK/100
        K2=RK-K1*100
        IF(IABS(IXTN-K1).LT.0.5) GO TO 1001
        IXTN=K1
        CALL TABLES(IXTN,IPOS33,TX,TKX,ICOUNT1,LM33)
 1001   IF(IABS(IYTN-K2).LT.0.5) GO TO 1002
        IYTN=K2
        CALL TABLES(IYTN,IPOS33,TX,TKY,ICOUNT1,LM33)
 1002 DO 1003 NODE=1,INE
        XNOD = CNDS(NODE,1)
        XNOD = INT(XNOD+0.1)
        XNODE= ABS(XNOD)
        YNODE= CNDS(NODE,2)
        DO 1004 ITABLE=1,ICOUNT1
        XTABLE=TX(ITABLE)
        IF(XTABLE.GT.XNODE) GO TO 1005
 1004 CONTINUE
 1005 SLOPE=(XNODE-TX(ITABLE-1))/(XTABLE-
       +          TX(ITABLE-1))
        RKXA(NODE)=TKX(ITABLE-1)+(TKX(ITABLE)-
       +          TKX(ITABLE-1))*SLOPE
 1003 RKYA(NODE)=TKY(ITABLE-1)+(TKY(ITABLE)-
       +          TKY(ITABLE-1))*SLOPE
        CALL DMATMU (UKX,AINV,RKXA,INE,INE,1)
        CALL DMATMU (UKY,AINV,RKYA,INE,INE,1)
C
```

```
C-End of insert----------------------
      DO 230 L1 = 1,II
      XI = GVALS(L1,1)
      CA = GVALS(L1,2)
      IF (ISN.NE.2)  CA = CA*TH
C-IF CALLED FOR, COMPUTE CONTRIBUTIONS TO SURFACE
C-HEAT TRANSFER INTEGRALS.
      IF (ISURF.LE.1)  GO TO 180
      CB = CA
      IF (IORTH.EQ.5)  CB = CB * THO
      CALL R39045 (XI,CB,ISIDCO,SURHES,NSIDES,PV,
     +          PXI,PETA,UX,UY,INE,ISN,ISE,LBMSUR)
  180 CONTINUE
      DO 220 L2 = 1,II
      IF(MAGNL.EQ.1) ISS=ISE+(ICOUNT-1)*INE*INE*2
      ICOUNT = ICOUNT + 1
      ETA = GVALS(L2,1)
      CB  = GVALS(L2,2)*CA
C-JUMP IF ELEMENT IS QUADRILATERAL
      IF (IERN.GT.39130) GO TO 190
      XI = XI * (1.D0-ETA) * 0.5D0
      CB = CB * (1.D0-ETA) * 0.5D0
  190 CONTINUE
      CALL D35091 (PV,PXI,PETA,XI,ETA,INE)
C-EVALUATE THE JACOBIAN MATRIX AJ
      CALL DMATMU (AJ(1,1), PXI, UX, 1,INE,1)
      CALL DMATMU (AJ(2,1), PETA,UX, 1,INE,1)
      CALL DMATMU (AJ(1,2), PXI, UY, 1,INE,1)
      CALL DMATMU (AJ(2,2), PETA,UY, 1,INE,1)
C-PUT DP/DXI,  DP/DETA IN EE THEN DIVIDE BY
C-AJ TO GIVE DP/DX, DP/DY
      CALL D11100 (EE,PXI,1,1,1,1,1,INE,2,INE,1,INE)
      CALL D11100 (EE,PETA,2,1,1,1,1,INE,2,INE,1,INE)
      CALL DMATDI (DET,EE,AJ,2,INE)
      IF (DET.GT.0.0D0) GOTO 200
      DET  = -DET
      INEGV= INEGV+1
  200 CONTINUE
      IF (ISN.LT.2) GOTO 210
C---------------------------------------------------------
C FOR THE AXISYMMETRIC  CASE FIND THICKNESS AS RADIUS
C FROM AXIS OF SYMMETRY TIMES 2*PI
C NOTE THAT THE FACTOR 2*P IS OMITTED FOR LEVEL 1,2,3
C---------------------------------------------------------
      CALL DVECMU (YV,PV,UY,INE)
      TH = YV*6.283185307D0
      CB = CB*TH
  210 CONTINUE
C*FOLLOWING LINES INSERTED BY RAG ON 22/2/83
      IF (LM223.EQ.0) GO TO 155
      CALL R09806(MODV,LMMODV,JRMODV,IPOSV)·
      IPSVN  = IPOSV + INE*INE2
      IPSVND = IPSVN + INE2
      IPSVNW = IPSVND + INE2*2
      CALL ASYMAT  (AINV,PV,EE,BASE (IPOSV),
     +BASE(IPSVN),BASE(IPSVND),BASE(IPSVNW),
```

```
     +CB, DET, INE, IADREL, IFLAG, SH)
  155 CONTINUE
C-Insert by I.G.Ediz-------------------
C
      CALL   DMATMU (SCAL,PV,UKX,1,INE,1)
      RKXG= SCAL(1,1)
      CALL   DMATMU (SCAL,PV,UKY,1,INE,1)
      RKYG= SCAL(1,1)
      CB   = CB*DET
      CBB = CB
      CE   = CB*SH
C
C-End of insert------------------------
C-Modified by I.G.Ediz------------------
C
      IF (IORTH.NE.5) CALL R39018
     +(BASE(ISS),QQ,EE,PV,CE,CB,INE,IM,RKXG,RKYG)
C
C-End of modification-------------------
      IF (IORTH.EQ.5) CALL R39038
     +(BASE(ISS),QQ,EE,PV,CE,CB,INE,IM,RKLAM)
C-FIND LOADS DUE TO INTERNAL HEAT GENERATION (CURRENT
C-DENSITY MAGNETIC FIELD PROBLEMS)
      IF(ILOAD.NE.0) CALL R39051(BASE(IFE),BASE(ITE),
     +  CBB,PV,AINV,A,INE )
C-ADD IN EXTRA TERMS FOR AXISYMMETRIC MAGNETIC PROBLEMS
      IF( ISN .EQ. 2 .AND. IMAG .NE. 0 )
     +  CALL R39052( BASE(ISS),PV,CBB,RK,YV,INE )
  220 CONTINUE
  230 CONTINUE
      IF(INEGV.EQ.0) GOTO 250
      INUM=II*II
      IF(INEGV.EQ.INUM) GOTO 240
      CALL NEWLIN( 2 )
      WRITE(6,2) IENM
      IBASE(26)=IBASE(26)+1
      GO TO 100
  240 CONTINUE
      CALL NEWLIN( 1 )
      WRITE(6,3) IENM
      IBASE(27)=IBASE(27)+1
  250 CONTINUE
C-TRANSFORM CONDUCTANCE AND MASS MATRICES TO NODAL
C-BASIS, (A IS USED FOR WORKSPACE).
      CALL R39005 (BASE(ISE),QQ,A,AINV,INE,IM)
      NFACES = ISURF - 1
C-IF THERE IS SURFACE HEAT TRANSFER FOR THIS ELEMENT,
C-TRANSFORM  SURFACE  CONDUCTANCE MATRIX(S) AND LOAD
C-VECTOR(S)  TO  NODAL  BASIS  AND CONVERT TO SINGLE
C-PRECISION IF REQUIRED
      IF (NFACES.GE.1)  CALL R39047
     +(ISURF,AINV,A,INE,LBMSUR,JROSUR,IS,IB45,2)
      IF (IB45.EQ.1)  GO TO 260
C-FOR SINGLE PRECISION COPY SE,DCA INTO THEMSELVES
      IF( MAGNL .EQ. 1 ) IS = INE*INE*II*II
      CALL SDCOP (BASE(ISE), BASE(ISE), 1, IS)
```

```
      CALL SDCOP (SDCA,       DCA,        1,  9)
C-WRITE CONDUCTANCE MATRIX,TOPOLOGY,ETC,TO ES FILE.
      CALL R14000 (BASE(ISE),BASE(IIEPA),IDG,SDCA,IDE,
     +             INE,IENM)
      IF (ISURF.LT.1)  GO TO 270
C-IF THERE IS SURFACE HEAT TRANSFER IN PROBLEM, CALL
C-ROUTINE TO WRITE TO ES FILE FROM S.H.T. MODULE.(CALL
C-ROUTINE  EVEN IF NFACES IS ZERO.)
      CALL R39043 (ICES,NFACES,INE,2,1,LBMSUR,JROSUR)
      GO TO 270
  260 CALL D14000 (BASE(ISE),BASE(IIEPA),IDG,DCA,IDE,
     +             INE,IENM)
      IF (ISURF.GE.1)
     +CALL R39043 (ICES,NFACES,INE,2,2,LBMSUR,JROSUR)
  270 CONTINUE
C*FOLLOWING LINE INSERTED BY RAG ON 22/2/83
      IF (IFLAG.EQ.1) CALL ESWRIT(BASE(IPOSV),INE)
C-THIS ROUTINE WRITES MODV TO TP FILE
      GO TO 100
    1 FORMAT(8H WARNING,/,35H NEGATIVE OR ZERO  FORMAT
     + PROPERTY GIVEN TO,8H ELEMENT,I5)         FORMAT
    2 FORMAT(6H ERROR,/,8H ELEMENT,I5,20H IS    FORMAT
     +  HIGHLY DISTORTED)                       FORMAT
    3 FORMAT(14H ***WARNING***,12H ELEMENT NO., FORMAT
     + I5,11H INSIDE OUT)                       FORMAT
      END
C
      SUBROUTINE TABLES(ITN,IPOS33,TX,T,ITNUM1,LM33)
C-COMMENT-----------------------------------------------
C THIS SUBROUTINE EXTRACTS A TABLE FROM BASE-NO
C ITNUM = TABLE NUMBER
C TX    = BASIS VALUE (X-COORDINATE)
C T     = VALUE (PERMEABILITY VALUE)
C
C-COMMENT END------------------------------------------
      DIMENSION T(30)
      INTEGER   TX(30)
      COMMON/IBASE/IBASE(1500)
      COMMON BASE(33000)
      IIPOS33=IPOS33-4
 1006 IIPOS33=IIPOS33+4
      ITNUM=BASE(IIPOS33)
      IF(ITNUM.NE.ITN) GO TO 1006
      ITNUM1=1
 1007 IF(IIPOS33.GE.IPOS33+LM33) GO TO 1008
      IT=BASE(IIPOS33)
      IF(IT.NE.ITN) GO TO 1008
      TX(ITNUM1)=BASE(IIPOS33+1)
      T(ITNUM1)=BASE(IIPOS33+3)
      IIPOS33=IIPOS33+4
      ITNUM1=ITNUM1+1
      GO TO 1007
 1008 ITNUM1=ITNUM1-1
      RETURN
      END
C
```

```
      SUBROUTINE R39018 (SE,QQ,EE,PV,CE,CB,INE,IM,
     +                    RKXG,RKYG)
C-THIS   SUBROUTINE   CREATES   THE   MATRIX   FROM THE
C-MINIMISATION
      DOUBLE PRECISION SE(INE,1),EE(2,INE),PV(INE),
     +                    QQ(INE,INE),CE,CB,RKXG,RKYG
      DO 110 L1=1,INE
      DO 100 L2=1,L1
C-Insert by I.G.Ediz----------------
C
      SE(L1,L2)=SE(L1,L2)+((EE(1,L1)*EE(1,L2)*RKXG)
     +          +(EE(2,L1)*EE(2,L2)*RKYG))*CB
C
C-End of insert---------------------
C-FORM THE THERMAL MASS KERNEL
C
      IF(IM.NE.4) QQ(L1,L2) = QQ(L1,L2)+PV(L1)*
     +                        PV(L2)*CE
  100 CONTINUE
  110 CONTINUE
      RETURN
      END
C
      SUBROUTINE R39006(CNDS,INE)
C-THIS SUBROUTINE OBTAINS THE GLOBAL COORDINATES
C-FOR  EACH ELEMENT
      DOUBLE PRECISION CNDS(INE,3)
      COMMON/IBASE/IBASE(1500)
      COMMON BASE(33000)
C-DETERMINE START OF TOPOLOGY, MODULE 72
      CALL R09806(72,LM,JROW,IADR)
      IADR=IADR-1
C-OBTAIN START OF COORDINATE DATA, MODULE1
      CALL R09800(1,1)
      CALL R09806(1,LM,JROW,INODES)
      DO 110 L1=1,INE
      IADR=IADR+1
      INODE=NYNT(BASE(IADR))
      IZ=(INODE-1)*3+INODES-1
      DO 100 L2=1,3
      IPRIME=IZ+L2
      CNDS(L1,L2)=BASE(IPRIME)
  100 CONTINUE
  110 CONTINUE
      RETURN
      END
```

APPENDIX 4 DATA USED IN GAS FLOW ANALYSIS

```
RPAFEC(RUNNAME=GAS_FLOW)
----
CONTROL
FULL.CONTROL
PHASE=1
CALC.STEADY.TEMPS
CALC.TRANS.TEMPS
TOLERANCE=10E-1
PHASE=2
PHASE=4
PHASE=6
USE.GOK.ELEMENT
PHASE=7
ADD.PROG:
     CALL R09808(282,1,1,LM282,JR282,IP282)
     CALL R09800(282,4)
END.OF.ADD.PROG:
USE.GOK.SOLUTION
PHASE=8
PHASE=9
USE.GOK.FLOW
PHASE=10
SAVE.TEMPS
STOP
CONTROL.END
NODES
```

NODE.NUMBER	X	Y
1	0	0
3	0	-5
5	0	-15
7	0	-28
9	0	-32
11	0	-35
13	0	-40
15	0	5
17	0	15
19	0	28
21	0	32
23	0	35
25	0	40
2	120	0
4	120	-5
6	120	-15
8	120	-28
10	120	-32
12	120	-35
14	120	-40
16	120	5
18	120	15
20	120	28
22	120	32

24	120	35
26	120	40

PAFBLOCKS

BLOCK	TYPE	ELEMENT	PROPERTY	N1	N2	TOPOLOGY
1	1	39210	1	1	2	1 2 3 4
2	1	39210	2	1	2	3 4 5 6
3	1	39210	3	1	2	5 6 7 8
4	1	39210	4	1	2	7 8 9 10
5	1	39210	5	1	2	9 10 11 12
6	1	39210	6	1	2	11 12 13 14
7	1	39210	7	1	2	1 2 15 16
8	1	39210	8	1	2	15 16 17 18
9	1	39210	9	1	2	17 18 19 20
10	1	39210	10	1	2	19 20 21 22
11	1	39210	11	1	2	21 22 23 24
12	1	39210	12	1	2	23 24 25 26

MESH

REFERENCE	SPACING
1	12
2	1

PLATES.AND.SHELLS

PLATE.NUMBER	MATERIAL.NUMBER	THICKNES
1	1	1
2	2	1
3	3	1
4	4	1
5	5	1
6	6	1
7	7	1
8	8	1
9	9	1
10	10	1
11	11	1
12	12	1

MATERIAL

MATERIAL.NUMB	K	RO	SH
1	0102	0.20	1.087
2	0304	0.20	1.087
3	0505	0.20	1.087
4	0606	0.20	1.087
5	0606	0.20	1.087
6	1616	0.20	1.087
7	0708	0.20	1.087
8	0910	0.20	1.087
9	1111	0.20	1.087
10	1212	0.20	1.087
11	1212	0.20	1.087
12	2222	0.20	1.087

TABLES

TABLE	BASIS	VALUE
C FLOOR STRATA		
01	0	15.00
01	10	20.00
01	20	25.00
01	30	23.00
01	40	21.00

01	50	20.00
01	60	18.00
01	70	16.80
01	80	14.00
01	90	13.00
01	100	12.00
01	110	11.00
01	120	10.00
01	130	9.00
02	0	16.00
02	10	21.00
02	20	26.00
02	30	23.00
02	40	22.00
02	50	20.00
02	60	17.50
02	70	15.00
02	80	14.00
02	90	13.80
02	100	12.00
02	110	11.00
02	120	10.00
02	130	9.00
03	0	10.00
03	10	12.00
03	20	14.00
03	30	13.00
03	40	11.00
03	50	10.00
03	60	9.00
03	70	8.60
03	80	8.00
03	90	7.50
03	100	7.00
03	110	6.70
03	120	6.20
03	130	5.50
04	0	12.00
04	10	14.00
04	20	17.00
04	30	15.00
04	40	13.00
04	50	11.00
04	60	9.50
04	70	8.80
04	80	8.00
04	90	7.50
04	100	7.00
04	110	6.50
04	120	6.00
04	130	5.20
05	0	3.00
05	10	4.00
05	20	6.00
05	30	4.00
05	40	3.50

05	50	3.20
05	60	3.00
05	70	3.00
05	80	3.00
05	90	3.00
05	100	3.00
05	110	3.00
05	120	3.00
05	130	3.00
06	0	3.00
06	10	3.50
06	20	4.00
06	30	2.50
06	40	2.00
06	50	2.00
06	60	2.00
06	70	2.00
06	80	2.00
06	90	2.00
06	100	2.00
06	110	2.00
06	120	2.00
06	130	2.00
16	0	1.00
16	10	1.00
16	20	1.00
16	30	1.00
16	40	1.00
16	50	1.00
16	60	1.00
16	70	1.00
16	80	1.00
16	90	1.00
16	100	1.00
16	110	1.00
16	120	1.00
16	130	1.00

C ROOF STRATA

07	0	30.00
07	10	48.00
07	20	60.00
07	30	51.00
07	40	46.00
07	50	42.00
07	60	40.00
07	70	38.00
07	80	35.00
07	90	33.00
07	100	30.00
07	110	28.00
07	120	26.00
07	130	24.00
08	0	35.00
08	10	50.00
08	20	68.00
08	30	59.00

08	40	51.00
08	50	46.00
08	60	43.00
08	70	40.00
08	80	38.00
08	90	35.00
08	100	33.00
08	110	30.00
08	120	28.00
08	130	26.00
09	0	15.00
09	10	22.00
09	20	35.00
09	30	29.00
09	40	27.00
09	50	26.00
09	60	25.00
09	70	24.00
09	80	23.00
09	90	22.00
09	100	21.00
09	110	19.00
09	120	17.00
09	130	15.00
10	0	20.00
10	10	27.00
10	20	36.00
10	30	32.00
10	40	30.00
10	50	28.00
10	60	27.00
10	70	26.00
10	80	25.00
10	90	24.00
10	100	22.00
10	110	20.00
10	120	18.00
10	130	17.00
11	0	5.00
11	10	8.00
11	20	12.00
11	30	9.00
11	40	8.50
11	50	8.00
11	60	7.50
11	70	7.00
11	80	6.50
11	90	6.20
11	100	6.10
11	110	5.20
11	120	5.00
11	130	4.50
12	0	3.00
12	10	3.00
12	20	4.00
12	30	3.50

```
12              40          3.30
12              50          3.00
12              60          3.00
12              70          3.00
12              80          3.00
12              90          3.00
12             100          3.00
12             110          3.00
12             120          3.00
12             130          3.00
22               0          1.50
22              10          1.50
22              20          1.50
22              30          1.50
22              40          1.50
22              50          1.50
22              60          1.50
22              70          1.50
22              80          1.50
22              90          1.50
22             100          1.50
22             110          1.50
22             120          1.50
22             130          1.50
TEMP
TEMP,START,FINI,STEP,LIST
1,27,49,1,1,2
100,243,246,1,13,14
100,254,265,1
50,250,0,1
100,459,462,1,25,26
100,470,481,1
50,466,0,1
0.81,248,0,1,233,212
0.81,252,0,1,235,216
0.81,464,0,1,449,428
0.81,468,0,1,451,432
UNSTEADY.THERMAL.TIMES
TIME.STEP,MAX.TIME,NUMBER
50,1000
THERMAL.SHOCK
27,1,0,1,1000
28,1,0,1,1000
29,1,0,1,1000
30,1,0,1,1000
31,1,0,1,1000
32,1,0,1,1000
33,1,0,1,1000
34,1,0,1,1000
35,1,0,1,1000
36,1,0,1,1000
37,1,0,1,1000
38,1,0,1,1000
39,1,0,1,1000
40,1,0,1,1000
41,1,0,1,1000
```

```
42,1,0,1,1000
43,1,0,1,1000
44,1,0,1,1000
45,1,0,1,1000
46,1,0,1,1000
47,1,0,1,1000
48,1,0,1,1000
49,1,0,1,1000
1,1,0,1,1000
2,1,0,1,1000
243,100,0,100,1000
244,100,0,100,1000
245,100,0,100,1000
246,100,0,100,1000
247,100,0,100,1000
C 248,100,0,100,1000
249,100,0,100,1000
250,100,0,100,1000
251,100,0,100,1000
C 252,100,0,100,1000
253,100,0,100,1000
254,100,0,100,1000
255,100,0,100,1000
256,100,0,100,1000
257,100,0,100,1000
258,100,0,100,1000
259,100,0,100,1000
260,100,0,100,1000
261,100,0,100,1000
262,100,0,100,1000
263,100,0,100,1000
264,100,0,100,1000
265,100,0,100,1000
13,100,0,100,1000
14,100,0,100,1000
459,100,0,100,1000
460,100,0,100,1000
461,100,0,100,1000
462,100,0,100,1000
463,100,0,100,1000
C 464,100,0,100,1000
465,100,0,100,1000
466,100,0,100,1000
467,100,0,100,1000
C 468,100,0,100,1000
469,100,0,100,1000
470,100,0,100,1000
471,100,0,100,1000
472,100,0,100,1000
473,100,0,100,1000
474,100,0,100,1000
475,100,0,100,1000
476,100,0,100,1000
477,100,0,100,1000
478,100,0,100,1000
479,100,0,100,1000
```

```
480,100,0,100,1000
481,100,0,100,1000
25,100,0,100,1000
26,100,0,100,1000
230,100,0,100,1000
11,100,0,100,1000
194,100,0,100,1000
9,100,0,100,1000
158,100,0,100,1000
7,100,0,100,1000
122,100,0,100,1000
5,100,0,100,1000
86,100,0,100,1000
3,100,0,100,1000
50,100,0,100,1000
266,100,0,100,1000
15,100,0,100,1000
302,100,0,100,1000
17,100,0,100,1000
338,100,0,100,1000
19,100,0,100,1000
374,100,0,100,1000
21,100,0,100,1000
410,100,0,100,1000
23,100,0,100,1000
446,100,0,100,1000
C ROOF BOREHOLE-1
464,0.81,0,0.81,1000
449,0.81,0,0.81,1000
428,0.81,0,0.81,1000
C ROOF BOREHOLE-2
468,0.81,0,0.81,1000
451,0.81,0,0.81,1000
432,0.81,0,0.81,1000
C FLOOR BOREHOLE-1
248,0.81,0,0.81,1000
233,0.81,0,0.81,1000
212,0.81,0,0.81,1000
C FLOOR BOREHOLE-2
252,0.81,0,0.81,1000
235,0.81,0,0.81,1000
216,0.81,0,0.81,1000
IN.DRAW
DRAWING.NO,TYPE.NO,INFO
1,3,123
OUT.DRAW
PLOT,SIZE,ORIE,CASE
37,4,0,25
END.OF.DATA
++++
```

```
      SUBROUTINE B62200(TEMP,COORD,MODSW)
      COMMON/IBASE/IBASE(1500)
      DIMENSION TEMP(1),COORD(1)
C-COMMENT--------------------------------------
C PRINTS THE COORDINATES AND TEMPERATURES  IN  A
C STEADY STATE THERMAL SOLUTION.THE TEMPERATURES
C ARE HELD LOADCASE BY LOADCASE IN TEMP, AND THE
C COORDINATES ARE HELD IN COORD. ONLY STRUCTUREL
C NODES ARE PRINTED. A SWITCH SET TO 1 IN MODULE
C MODSW INDICATES A PRESCRIBED TEMPERATURE AT  A
C PARTICULAR FREEDOM.
C-COMMENT-END----------------------------------
      IP = IBASE(3)
C-FOR A THERMAL SOLUTION ONLY 1 LOADCASE...
      ILO = IBASE(8)
C-...AND 1 DIRECTION
      IDIR = 1
      DO 120 L1 = 1,ILO
C-WRITE TITLE AND TABLE HEADER
      CALL R14901(1)
      IPOS = -2
      DO 110 L2 = 1,IP
      IPOS = IPOS + 3
C-CHECK IF NODE NON STRUCTURAL
      IF(I09896(137,L2).EQ.0) GO TO 110
C-FIND TEMPERATURE AT NODE L2
      IFREE = IAB(NDFREE(L2,IDIR))
      IF(IFREE.EQ.0) GO TO 110
      IADR  = (L1 - 1)*ILO + IFREE
      CALL NEWLIN(1)
      ISW = 0
      IF(MPTSUB(53).EQ.1) ISW=I09896(MODSW,IFREE)
      IF (I09891(89).EQ.1) GO TO 100
C-PRINT SPECIFIED TEMPERATURE
C-Insert by I.G.Ediz----------------
C
      IF(ISW.EQ.1) THEN
      PRESSURE=ABS(TEMP(IADR))**0.5
      WRITE(6,2) L2,COORD(IPOS),COORD(IPOS+1),
     +          COORD(IPOS+2),PRESSURE
      END IF
C
C-End of insert--------------------
C-PRINT UNSPECIFIED TEMPERATURE
C-Insert by I.G.Ediz--------------
C
      IF(ISW.EQ.0) THEN
      PRESSURE=ABS(TEMP(IADR))**0.5
      WRITE(6,2)  L2,COORD(IPOS),COORD(IPOS+1),
     +          COORD(IPOS+2),PRESSURE
      END IF
```

```
C-End of insert--------------------
      GO TO 110
 100  CONTINUE
C-PRINT SPECIFIED POTENTIAL FOR MAGNETIC
      IF(ISW.EQ.1) WRITE(6,3)
     +L2,COORD(IPOS),COORD(IPOS+1),COORD(IPOS+2),
     +TEMP(IADR)
C-PRINT UNSPECIFIED POTENTIAL FOR MAGNETIC
      IF(ISW.EQ.0) WRITE(6,4)
     +L2,COORD(IPOS),COORD(IPOS+1),COORD(IPOS+2),
     +TEMP(IADR)
 110  CONTINUE
C-PRINT TABLE TRAILER
      CALL R14901(2)
 120  CONTINUE
      RETURN
 1    FORMAT(I6,F15.3,F10.3,F10.3,F20.3,   FORMAT
     +       6(1H ),10H SPECIFIED)         FORMAT
 2    FORMAT(I6,F15.3,F10.3,F10.3,F20.3,   FORMAT
     +       6(1H ),6H    *     )          FORMAT
 3    FORMAT(I6,F15.3,F10.3,F10.3,E20.3,   FORMAT
     +       6(1H ),10H SPECIFIED)         FORMAT
 4    FORMAT(I6,F15.3,F10.3,F10.3,E20.3,   FORMAT
     +       6(1H ),6H    *     )          FORMAT
      END
C
      SUBROUTINE C15030(STIFF,FORCE,DOF,IDE)
      COMMON/BFTRML/MT,MTDOT,MODSUM,MODAVE,MODSAV,
     +              MTEMP,ISOLVE,FACTOR,TYMESS
      COMMON/IBASE/IBASE(1500)
      DIMENSION FORCE(1),DOF(1)
      DOUBLE PRECISION STIFF(1),DFACT
      COMMON BASE(33000)
C-COMMENT----------------------------------------
C TRANSIENT THERMAL BLOCK FRONT MERGE ROUTINES.FOR
C ISOLVE=2 3 SUITABLY AMENDS STIFF AND FORCE ( THE
C LHS AND RHS OF THE EQUATION RESPECTIVELY). STIFF
C IS  IDE  BY IDE+1, CONTAINING  THE  CONDUCTIVITY
C MATRIX AS THE LOWER TRIANGLE AND THE MASS MATRIX
C AS THE UPPER  TRIANGLE.FORCE, IDT LONG, CONTAINS
C THE RHS FOR FREEDOMS NOT YET MERGED. THE FREEDOM
C NUMBERS  FOR  THE ELEMENT CURRENTLY BEING MERGED
C ARE HELD IN DOF.
C              DOUBLE PRECISION VERSION
C          MARK  TOOLE            JUNE  1984
C-COMMENT-END------------------------------------
      IF(ISOLVE.EQ.1) GO TO 110
      IF(ISOLVE.EQ.3) GO TO 100
C-SOLVING FOR THE INITIAL TEMPERATURE GRADIENTS
      CALL R09806(MT,LMT,JRT,IPT)
      CALL C15031(STIFF,FORCE,DOF,BASE(IPT),IDE)
      GO TO 110
 100  CONTINUE
C-SOLVING FOR THE TEMPERATURES
      CALL R09806(MODSUM,LMT,JRT,IPT)
      DFACT = FACTOR
```

```
          IM = 2
          IF(I09891(17).EQ.1) IM = 12
          CALL C15032 (STIFF,FORCE,DOF,BASE(IPT),DFACT,
       +               ,IDE,IM)
  110     CONTINUE
          RETURN
          END
C
          SUBROUTINE C15031(COND,Q,DOF,T,ID)
          DIMENSION Q(1),DOF(1),T(1)
          DOUBLE PRECISION COND(1)
          DOUBLE PRECISION SUM
C-COMMENT------------------------------------------
C REFORMS RHS OF REDUCTION EQUATION FROM (Q) TO
C (Q) - (K)(T) WHERE K IS THE LOWER TRIANGLE OF
C COND.THEN OVERWRITES K BY THE UPPER  TRIANGLE
C IN COND HOLDING THE MASSES. THE  ID   FREEDOMS
C INVOLVED ARE HELD IN DOF
C               DOUBLE PRECISION VERSION
C-COMMENT-END--------------------------------------
          ID1 = ID + 1
C-FIRSTLY AMEND THE RHS
          DO 130 L1 = 1,ID
          SUM = 0.0D0
          IPOSL = L1 - ID
          DO 100 L2 = 1,L1
          IPOSL = IPOSL + ID
          IADR  = NYNT(DOF(L2))
          SUM   = SUM + COND(IPOSL)*T(IADR)
  100     CONTINUE
          ISTART = L1 + 1
          IF(ISTART.GT.ID) GO TO 120
          DO 110 L2 = ISTART,ID
          IPOSL = IPOSL + 1
          IADR  = NYNT(DOF(L2))
          SUM   = SUM + COND(IPOSL)*T(IADR)
  110     CONTINUE
  120     CONTINUE
          IPT = NYNT(DOF(L1))
          Q(IPT) = Q(IPT) - SUM
  130     CONTINUE
C-FINALLY AMEND THE LHS
          DO 150 L1 = 1,ID
          IPOSL = (L1 - 1)*ID + L1
          IPOSU = IPOSL + ID
          COND(IPOSL) = COND(IPOSU)
          ISTART = L1 + 1
          IF(ISTART.GT.ID) GO TO 150
          DO 140 L2 = ISTART,ID
          IPOSL = IPOSL + 1
          IPOSU = IPOSU + ID
          COND(IPOSL) = COND(IPOSU)
  140     CONTINUE
  150     CONTINUE
          RETURN
          END
```

```
      SUBROUTINE C15032(COND,Q,DOF,T,FACT,ID,IM)
      DIMENSION Q(1),DOF(1),T(1)
      DOUBLE PRECISION COND(1),FACT
      DOUBLE PRECISION SUM
C-COMMENT----------------------------------------
C REFORMS RHS OF REDUCTION EQUATION FROM (Q) TO
C (Q) + (M)(T) WHERE M IS THE UPPER TRIANGLE OF
C COND.  IF IM IS LESS THAN 10 THEN ALSO REFORM
C LHS FROM (K) TO (K) + FACT*(M) WHERE K IS THE
C LOWER TRIAG. OF COND.THE ID FREEDOMS INVOLVED
C ARE HELD IN DOF.
C                 DOUBLE PRECISION VERSION
C-COMMENT-END------------------------------------
      ID1 = ID + 1
C-AMEND RHS
      DO 130 L1 = 1,ID
      SUM = 0.0D0
      IPOSU = L1*ID
      DO 100 L2 = 1,L1
      IPOSU = IPOSU + 1
      IADR  = NYNT(DOF(L2))
C-Modified by I.G.Ediz at 25.2.89-------
C
      SUM = SUM+COND(IPOSU)*(ABS(T(IADR))**0.5)
C
C-End of Modification-------------------
 100  CONTINUE
      ISTART = L1 + 1
      IF(ISTART.GT.ID) GO TO 120
      DO 110 L2 = ISTART,ID
      IPOSU = IPOSU + ID
      IADR  = NYNT(DOF(L2))
C-Modified by I.G.Ediz at 25.2.89-------
C
      SUM = SUM+COND(IPOSU)*(ABS(T(IADR))**0.5)
C
C-End of Modification-------------------
 110  CONTINUE
 120  CONTINUE
      IPT = NYNT(DOF(L1))
      Q(IPT) = Q(IPT) + SUM
 130  CONTINUE
      IF(IM.GT.10) GO TO 160
C-AMEND LHS
      DO 150 L1 = 1,ID
      IPOSL = (L1 - 1)*ID + L1
      IPOSU = IPOSL + ID
C-Modified by i.G.Ediz------------------
C
      COND(IPOSL)=COND(IPOSL)+((FACT*COND(IPOSU))
     +            / (4.0D0*(ABS(T(IADR))**0.5)))
C
C-End of Modification-------------------
      ISTART = L1 + 1
      IF(ISTART.GT.ID) GO TO 150
      DO 140 L2 = ISTART,ID
```

```
         IPOSL = IPOSL + 1
         IPOSU = IPOSU + ID
C-Modified by i.G.Ediz------------------
C
         COND(IPOSL)=COND(IPOSL)+((FACT*COND(IPOSU))
     +              / (4.0D0*(ABS(T(IADR))**0.5)))
C
C-End of Modification------------------
 140     CONTINUE
 150     CONTINUE
 160     CONTINUE
         RETURN
         END
C
         SUBROUTINE B61630(PLO,TYME,IP,IOP,IVAL1)
C-COMMENT----------------------------------------
C WRITES TEMPERATURE FIELD TO PHASE SEVEN OUTPUT
C FILE AND ALSO TO CHANNEL ICTS
C               +++  PARAMETERS  +++
C PLO - HOLDS TEMPERATURES AT NODES IN DOF ORDER
C TYME- TIME IN A TRANSIENT CALCULATION
C IP  - NUMBER OF NODES IN THE STRUCTURE
C IOP - OPTION NUMBER
C     -.EQ.1 TRANSIENT CALC WITH TEMPERATR FIELD
C     - WRITTEN TO CHANNEL ICTS
C     -.NE.1 ...VARIABLE.MATERIAL CALCULATION
C IVAL1-EQUAL  1  IF THIS IS A TRANSIENT RESTART
C LOCAL ARRAY BUFFER(10)IS USED TO BUFFER OUTPUT
C BEFORE WRITING IT EITHER TO ICTS OR PHASE
C SEVEN OUTPUT FILE
C-COMMENT-END-----------------------------------
         DIMENSION PLO(1),  BUFFER(10)
         COMMON/IBASE/IBASE(1500)
C-----BRING DOWN THE NON STRUCTURAL NODES MODULE
         CALL R09800(137,1)
C-----DIRECTION ALWAYS 1 FOR THERMAL
         IDIR = 1
         ICTS=IBASE(34)
         IF ( IOP.NE.1 ) GOTO 120
         IF (ICTS.EQ.0.OR.IVAL1.NE.1.OR.IBASE(157).
     +       NE.0 ) GOTO 120
C-COMMENT----------------------------------------
C FOR A TRANSIENT THERMAL RESTART HAVE TO READ
C THROUGH FILE ON CHANNEL ICTS UNTIL GET TO END
C WHERE NEW TEMPERATURE INFORMATION WILL BE
C APPENDED
C-COMMENT-END-----------------------------------
         CALL R00407(ICTS)
         READ(ICTS) TMAX, TNUM, RIPP
         READ(ICTS) TIME1
         LL1    = (IP+9) / 10
 100     CONTINUE
         LL2    = -9
         LL3    = 0
         DO 110L2=1,LL1
         LL2  =  LL2 + 10
```

```
      LL3   =   LL3 + 10
      IF( LL2.GT.IP ) GOTO 110
      IF( LL3.GT.IP ) LL3=IP
      LL4   =   LL3 - LL2 + 1
      READ(ICTS) (BUFFER(LO),LO=1,LL4)
110   CONTINUE
      IBASE(157) = IBASE(157) + 1
      IF( IBASE(157).EQ.IBASE(156) ) GOTO 120
      READ(ICTS) TIME
      GOTO 100
120   CONTINUE
      IF(ICTS.GT.0.AND.IOP.EQ.1) WRITE(ICTS)TYME
C-COMMENT----------------------------------------
C LL1 HOLDS THE PRESENT NODE NUMBER
C LL2 HOLDS THE PRESENT POSITION IN THE ARRAY BUFFER
C LL3 HOLDS THE  NODE  NUMBER  CORRESPONDING  TO THE
C           FIRST POSITION IN THE ARRAY BUFFER
C ICOLUM   USED TO PRESERVE THE PRESENT COLUMN BEING
C          WRITTEN  TO  IN  THE OUTPUT TABLE BETWEEN
C          CALLS OF THE PRINTING ROUTINE
C
C-COMMENT-END-------------------------------------
      LL1    =  0
      LL2    =  0
      LL3    =  1
      ICOLUM =  1
      CALL R14903(TYME,LL2,LL3,IOP,1,BUFFER,ICOLUM)
130   CONTINUE
      LL1    =  LL1 + 1
      LL2    =  LL2 + 1
      IDOF   = NDFREE(LL1,IDIR)
      IDOF   = IAB(IDOF)
C-Modified by I.G.Ediz---------------
C
      IF(IDOF.NE.0) BUFFER(LL2)=ABS(PLO(IDOF))**0.5
C
C-End of Modification----------------
      IF( IDOF.EQ.0 ) BUFFER(LL2) = 0.0
140   CONTINUE
      IF( LL1.EQ.IP ) GOTO 150
      IF( LL2.LT.10 ) GOTO 130
      CALL R14903(TYME,LL2,LL3,IOP,2,BUFFER,ICOLUM)
      IF(ICTS.GT.0.AND.IOP.EQ.1)
     +WRITE(ICTS)(BUFFER(LO),LO=1,10)
      LL3    = LL3 + 10
      LL2    = 0
      GO TO 130
150   CONTINUE
      CALL R14903(TYME,LL2,LL3,IOP,3,BUFFER,ICOLUM)
      IF(ICTS.GT.0.AND.IOP.EQ.1)
     +WRITE(ICTS)(BUFFER(LO),LO=1,10)
      IF(ICTS.GT.0.AND.IOP.EQ.1)
     +IBASE(156)=IBASE(156)+1
      RETURN
      END
```

```
      SUBROUTINE PERMCAL(IADREL,IELE,XX,IERN,INE,AA)
C-COMMENT----------------------------------------
C THIS SUBROUTINE IS CALLED BY SUBROUTINE R89010 AND
C EXTRACTS PERMEABILITY VALUES FOR GIVEN NODES WHICH
C ARE GOING TO BE USED IN FLOW CALCULATION
C-COMMENT END------------------------------------
      DIMENSION TKX(30),TKY(30),RKXA(8),RKYA(8),XX(3)
      DOUBLE PRECISION TH,RK,SH
      INTEGER TX(30),XTABLE
      COMMON/IBASE/IBASE(1500)
      COMMON BASE(33000)
C-Insert by I.G.Ediz----------------
C
      COMMON/K/KSS1
      COMMON/X/XNOD(8)
      COMMON/Y/YNOD(8)
      COMMON/P/PERM(300,9)
C-OBTAIN ELEMENT TOPOLOJI
      CALL R09700(IERNU,IADREL,IIEPA,KSS1)
C-BRINGS DOWN TABLES FROM BS
      CALL R09800(33,1)
      CALL R09806(33,LM33,JROW33,IPOS33)
      IXTN=0
      IYTN=0
C
C-End of insert--------------------
C-OBTAIN MATERIAL PROPERTIES
      CALL R39011(RK,SH,TH,IADREL)
C-FINDS TABLE FOR CURRENT ELEMENT
      K1=RK/100
      K2=RK-K1*100
      IF(IABS(IXTN-K1).LT.0.5) GO TO 1000
      IXTN=K1
      CALL TABLES(IXTN,IPOS33,TX,TKX,ICOUNT1,LM33)
 1000 IF(IABS(IYTN-K2).LT.0.5) GO TO 1001
      IYTN=K2
      CALL TABLES(IYTN,IPOS33,TX,TKY,ICOUNT1,LM33)
 1001 CONTINUE
      DO 10 I=1,8
      PERM(IELE,I)=0.0
   10 CONTINUE
C-Modified by I.G.Ediz----------------
C
      DO 1002 NODE=1,INE
      XNODE = ABS(XNOD(NODE))
      XNODE = INT(XNODE+0.1)
      YNODE = YNOD(NODE)
      XND   = XNOD(NODE)
      WRITE(6,15)NODE,XND
   15 FORMAT(1X,'XCOORD(',I2,')=',F8.4)
      WRITE(6,20) NODE,YNODE
```

```
   20 FORMAT(1X,'YCOORD(',I2,')=',F8.4)
C
C-End of Modification-----------------
      DO 1003 ITABLE=1,ICOUNT1
      XTABLE=TX(ITABLE)
      IF(XTABLE.GT.XNODE) GO TO 1004
 1003 CONTINUE
 1004 SLOPE=(XNODE-TX(ITABLE-1))/(XTABLE-
     +      TX(ITABLE-1))
      RKXA(NODE)=TKX(ITABLE-1)+(TKX(ITABLE)-
     +      TKX(ITABLE-1))*SLOPE
      RKYA(NODE)=TKY(ITABLE-1)+(TKY(ITABLE)-
     +      TKY(ITABLE-1))*SLOPE
C-Insert by I.G.Ediz--------------------
C
C-FIND PERMEABILITIES FOR BOREHOLES
C-IF ELEMENT IS TRIANGULAR
      IF(IERN.GT.39200) GOTO 1005
      IF(ABS(XNOD(1)-AA).GT.0.1E-03) GOTO 1006
      IF(NODE.EQ.1) PERM(IELE,1)=RKXA(1)
      IF(NODE.EQ.6) PERM(IELE,6)=RKXA(6)
      IF(NODE.EQ.3) PERM(IELE,3)=RKXA(3)
      GOTO 1006
C
C-End of insert-------------------------
C-IF ELEMENT IS RECTANGULAR
 1005 IF(ABS(XNODE-XX(1)).GT.0.1E-03) GOTO 1007
      IF(NODE.EQ.1) PERM(IELE,1)=RKXA(1)
      IF(NODE.EQ.6) PERM(IELE,6)=RKXA(6)
      IF(NODE.EQ.3) PERM(IELE,3)=RKXA(3)
 1007 CONTINUE
      IF(ABS(XNODE-XX(3)).GT.0.1E-03) GOTO 1006
      IF(NODE.EQ.2) PERM(IELE,2)=RKXA(2)
      IF(NODE.EQ.7) PERM(IELE,7)=RKXA(7)
      IF(NODE.EQ.4) PERM(IELE,4)=RKXA(4)
 1006 CONTINUE
C-FIND PERMEABILITIES FOR ROADWAYS
      IF(ABS(YNODE-0.0).GT.0.1E-03) GO TO 1002
      IF(NODE.EQ.1) PERM(IELE,9)=RKXA(1)
      IF(NODE.EQ.2) PERM(IELE,8)=RKYA(2)
      IF(NODE.EQ.5) PERM(IELE,5)=RKYA(5)
 1002 CONTINUE
      RETURN
      END
C
      SUBROUTINE TABLES(ITN,IPOS33,TX,T,ITNUM1,LM33)
C-COMMENT-----------------------------------------
C THIS SUBROUTINE EXTRACTS A TABLE FROM BASE-NO WHERE
C ITNUN = TABLE NUMBER
C TX    = BASIS VALUE (X-COORDINATES)
C T     = VALUE (PERMEABILITIES)
C-COMMENT END-------------------------------------
      DIMENSION T(30)
      INTEGER TX(30)
      COMMON/IBASE/IBASE(1500)
      COMMON BASE(33000)
```

```
      IIPOS33=IPOS33-4
 1016 IIPOS33=IIPOS33+4
      ITNUM=BASE(IIPOS33)
      IF(ITNUM.NE.ITN) GO TO 1016
      ITNUM1=1
 1017 IF(IIPOS33.GE.IPOS33+LM33) GO TO 1018
      IT=BASE(IIPOS33)
      IF(IT.NE.ITN) GO TO 1018
      TX(ITNUM1)=BASE(IIPOS33+1)
      T(ITNUM1)=BASE(IIPOS33+3)
      IIPOS33=IIPOS33+4
      ITNUM1=ITNUM1+1
      GO TO 1017
 1018 ITNUM1=ITNUM1-1
      RETURN
      END
C
      SUBROUTINE R89010 (AINV,TEMP,TEMPC,CNDS,CNODES,
     +          NODES,PV,PXI,PETA,TR,TMP,INE,IERN,ISZ)
C-COMMENT----------------------------------------
C THIS SUBROUTINE IS CALLED BY THE R89XXX SERIES OF
C ISOPARAMETRIC 2D FLUX ROUTINES AND ORGANISES  THE
C LOCATION OF TEMPERATURES, COORDINATES,  TOPOLOGY,
C CALCULATION  OF  FLUX  IN  THE  ELEMENT  USING THE
C ROUTINES   R86001,  R89002, R89003, R89004, R3600
C-COMMENT END------------------------------------
      DIMENSION   AINV(1),TEMP(1),TEMPC(1),CNDS(1),
     + PV(1),PETA(1),CNODES(1),TR(1),PXI(1),GV(20),
     + NODES(ISZ,ISZ), DCA(3,3), UE(3), P(4)
C-Insert by I.G.Ediz---------------
C
      DIMENSION RWGRAD(300,3),BHGRAD(50,3),DRAINR(50)
     +     ,DRAINF(50),DRAINRR(10,50),DRAINFF(10,50),
     +      FLOW10RWR(50),FLOW10RWF(50),FLOW10GR(50),
     +      FLOW10GF(50), YC(300,3), XC(300,3),XX(3),
     +      IXX(3), IIX(3), DXR(50), DYR(50),IC(300),
     +      DXF(50),DYF(50),COORDYF(50), COORDYR(50),
     +      IK(50),  IKK(50),  IZ(300,3), IZZ(300,3),
     +      CUMRWR(50),CUMRWF(50),CUMGF(50),CUMGR(50)
     COMMON/IBASE/IBASE(1500)
     COMMON / MAGNL / IGAUS,ICONV,MAGM1,MAGM2,MAGM3
     COMMON BASE(33000)
     COMMON/K/KSS1
     COMMON/X/XNOD(8)
     COMMON/Y/YNOD(8)
     COMMON/P/PERM(300,9)
C
C-End of insert------------------
C-RETRIEVE COMMONLY USED CONTROL INTEGERS
      CALL R09720 (IP,IX,IDT,ID,IDF,ILO,IE,IELE,IM)
      IF (IBASE(39).EQ.0) RETURN
C-SETUP INITIAL CONDITIONS FOR MAGNETIC WORK
      IMAG  = I09891( 89 )
      MAGNL = 0
      IF(IMAG.EQ.1.AND.IBASE(33).NE.0) MAGNL=1
  100 CONTINUE
```

```
      CALL R09800 (1,1)
      CALL R09800 (17,1)
      CALL R09800 (18,1)
C-Insert by I.G.Ediz---------------
C
C-COMMENT---------------------------------------------
C MINING METHOD IS DEFINED BY IFACETYPE WHICH WAS SET
C TO 1 REPRESENTING ADVANCE MINING METHOD.IN THE CASE
C OF RETREAT MINING THE PROGRAM WILL PICK -1 VALUE BY
C ITSELF IN RETREAT MINING, IF THERE IS  ANY DRAINAGE
C APPLIED IN GOAF THEN THE METHANE EMISSION FROM GOAF
C SHOULD BE DECREASED. FOR THIS,  CHANGE THE VALUE OF
C EMISRATE WHICH WAS SET TO 1.0  (100%)  FOR THE CASE
C WITH NO DRAINAGE.
C ALFA=SLOPE OF THE ROOF BOREHOLE DRILLED FROM ROADWY
C BETA=SLOPE OF THE FLOOR BOREHOL DRILLED FROM ROADWY
C CUMRWR=CUMMULATIVE METHANE EMISSN INTO ROADWAY FROM
C               ROOF  STRATA
C CUMRWF=CUMMULATIVE METHANE EMISSN INTO ROADWAY FROM
C               FLOOR  STRATA
C TOTRW=TOT METHANE EMIS INTO ROADWY FROM BOTH STRATA
C CUMGR=CUM METHANE EMISSN INTO GOAF FROM ROOF STRATA
C CUMGF=CUM METHANE EMISN INTO GOAF FROM FLOOR STRATA
C TOTGOAF=TOT METHANE EMIS INTO GOAF FROM BOTH STRATA
C TOTEMIS=TOTAL METHANE EMISSION IN THE RETURN END OF
C               A ROADWAY
C BHTOT     = TOTAL BOREHOLE DRAINAGE,
C INVL/INTV = COMMON INTERVALS,
C IKJ/IJK   = SUM OF INTERVALS INVL,INTV RESPECTIVELY
C ISTRNO/ISTFNO = NUMBER OF STRATA THROUGH WHICH A BH
C      IS CROSSING,IN THE ROOF AND FLOOR RESPECTIVELY
C-COMMENT END----------------------------------------
      IFACETYPE=1
      EMISRATE=1.0
      ALFA=0.0
      BETA=0.0
      IJK=0
      IKJ=0
      TOTRWR=0.0
      TOTRWF=0.0
      TOTGR=0.0
      TOTGF=0.0
      TOTRW=0.0
      TOTGOAF=0.0
      TOTEMIS=0.0
      BHTOT=0.0
      IBH=0
      INVL=0
      ISPOT=1
      INTV=0
      II=1
      IY=0
      AY=0.0
      IYY=0
      ISTRNO=0
      ISTFNO=0
```

```
          RK=0.0
          FK=0.0
C-COMMENT------------------------------------
C DRAINR = DRAINAGE OF ROOF BOREHOLE
C DRAINF = DRAINAGE OF FLOOR BOREHOLE
C YC/ XC = COORDS OF NODES REPRESENTING BOREHOLE
C-COMMENT END--------------------------------
          DO 118 L=1,10
          DO 113 K=1,50
          DRAINRR(L,K)=0.0
          DRAINFF(L,K)=0.0
    113 CONTINUE
    118 CONTINUE
          DO 111 L=1,50
          DRAINR(L)=0.0
          DRAINF(L)=0.0
          FLOW10RWR(L)=0.0
          FLOW10RWF(L)=0.0
          FLOW10GR(L)=0.0
          FLOW10GF(L)=0.0
          CUMRWR(L)=0.0
          CUMRWF(L)=0.0
          CUMGR(L)=0.0
          CUMGF(L)=0.0
          IK(L)=0
          IKK(L)=0
    111 CONTINUE
          DO 222 JI=1,3
          DO 222 KI=1,100
          YC(KI,JI)=0.0
          XC(KI,JI)=0.0
    222 CONTINUE
C
C-End of Insert----------
C-OBTAIN TEMPERATURE VALUES FROM MODULE 67
          CALL R09800 (67,1)
          CALL R09806(67,LM67,JROW67,IPOS67)
C-MODULE 67 CONTAINS A LIST OF THE STEADY STATE
C-TEMPERATURES
          ISET = 0
C-ITRI=3 WHEN ELEMENT IS TRIANGULAR
          ITRI=3*ISZ-INE
          IJ=1
          IF (IERN.LT.39240) GO TO 110
          IJ=2
          ITRI=0
          IF (IERN.EQ.39250) IJ=3
    110 ISZ2=ISZ
          C=2.0/(ISZ-1.0)
C-COMMENT----------------------------------
C CREATE SOME WORKSPACE AREAS
C NODES (ISZ BY ISZ) CONTAINS NODE NUMBERS OF
C THE POINTS ON A REGULAR (ISZ,ISZ) GRID ON A
C GENERAL ELEMENT
C-COMMENT END------------------------------
          CALL R36000(TEMP,AINV,NODES,ISZ,INE)
```

```
          ITIPE   =0
          ISTRSS  =0
          IST     =0
  120   CALL R08800(IST,IFIN,ISTEP,IGRP,ISTRSS,ITIPE)
          IF (IST.EQ.0) RETURN
C-THE LOOP ON THE ELEMENTS STARTS HERE
          DO 160 L1 = IST,IFIN,ISTEP
          IBASE(12)=L1-1
C-COMMENT----------------------------------
C CREATE ELEMENT TOPOLOGY AND PROPERTY IIEPA
C IS THE  START ADDRESS OF  THE TOPOLOGY  IN
C IN THE BASE
C-COMMENT END------------------------------
C-Modified by I.G.Ediz------
C
          KSS1 = L1
          CALL R09700 (IERNU,IADREL,IIEPA,KSS1)
C
C-End of Modification-------
          IF (IERNU.NE.IERN) GO TO 160
C-COMMENT-------------------------------------
C OBTAIN ELEMENT PROPERTIES
C R86001 OBTAINS DCA AND COORDINATES IN ELEMENT
C AXES
C R89002  FINDS TEMPERATURES ON CURRENT ELEMENT
C-COMMENT END--------------------------------
          IF (IGRP.EQ.0) GO TO 130
          IGROUP=BASE(IADREL+1)+0.1
          IF (IGROUP.NE.IGRP) GO TO 160
  130   CONTINUE
          IF( ISET .NE. 0 ) GO TO 116
          ISET = 1
          IF( IMAG .NE. 0 ) GO TO 112
C-OUTPUT EDIT
          CALL NEWLIN( 6 )
          WRITE(6,1)
          GO TO 116
    112 CONTINUE
          IF( MAGNL .EQ. 1 ) GO TO 114
          CALL NEWLIN( 6 )
          WRITE(6,2)
          GO TO 116
    114 CONTINUE
          IF( ICONV .EQ. 0 ) GO TO 116
          CALL NEWLIN( 6 )
          WRITE(6,2)
    116 CONTINUE
          ISN = IBASE(25)
          CALL R86001 (DCA, AINV,CNDS,CNODES,P,INE,
        +             IM,IIEPA)
          CALL R89002 (BASE(IPOS67),DCA,AINV,TEMPC,
        +             TEMP,INE,IDT,IIEPA)
C-COMMENT-----------------------------------
C LOOPS  ON THE POINTS WITHIN THE ELEMENT START
C HERE.RR35091 IS CALLED TO EVALUATE POLYNOMIAL
C AND    DERIVATIVES  FOR  ELEMENTS  WHICH   ARE
```

```
C DEGRADED  IN  ONE  DIRECTION.  R35092 IS ALSO
C USED.   PV  WILL  CONTAIN  POLYNOMIAL;   ERMS
C EVALUATED   AT THE POINT OF INTEREST AND PXI,
C PETA,  THE  DERIVATIVES  OF  THESE TERMS WITH
C RESPECT TO XI,PETA RESPECTIVELY.
C R89003 CALCULATES GRADIENTS
C R89004  FINDS THE DIRECTION OF MAX.  GRADIEND
C AND PRINTS
C-COMMENT END--------------------------------
C-Insert by I.G.Ediz------
C
C-INITIALISE THESE VALUES FOR FLOW CALCULATION
C-ROADWAY LENGTH SHOULD NOT EXCEED 200M IN ADV MIN.
      ZZ=1.0
      DISTNX=0.0
      DISTNY=0.0
      AA=205.0
      IBHL=0
      AA=205.0
      DO 333 I=1,3
      XX(I)=205.0
      IIX(I)=205
      IXX(I)=42
  333 CONTINUE
      DRAIN=0.0
      DISTN=0.0
C
C-End of insert----------
      ILP = ISZ
      ILL = IJ
      IF( MAGNL .EQ. 0 ) GO TO 132
      IF( ICONV .EQ. 1 ) GO TO 132
      ILP = IGAUS
      ILL = 1
      CALL R13100( GV,IGAUS )
  132 CONTINUE
      ICOUNT = 0
      DO 150 L2=1,ILP
      IF (ITRI.EQ.3) ISZ2=ISZ-L2+1
      IF( IMAG .EQ. 0 ) GO TO 133
      IF(MAGNL.NE.0.AND.ICONV.EQ.0) ISZ2=IGAUS
  133 CONTINUE
      DO 140 L3 = 1,ISZ2,ILL
      ICOUNT = ICOUNT + 1
      XI=C*(L2-1.0D0)-1.0D0
      ETA=C*(L3-1.0D0)-1.0D0
      IF (ITRI.EQ.3) XI=XI+C*(L3-1.0D0)*0.5D0
      IF( MAGNL .EQ. 0 ) GO TO 134
      IF( ICONV .EQ. 1 ) GO TO 134
      XI  = GV(L2)
      ETA = GV(L3)
      IF( ITRI .EQ. 3 ) XI = XI*( 1.0 -ETA )*0.5
  134 CONTINUE
      INODE=NODES(L2,L3)
      IDY=-IBASE(12)-1
      IPRIME=IIEPA+INODE-1
```

```
       IF (INODE.GT.0) IDY= BASE(IPRIME)+0.1
       CALL R35091(PV,PXI,PETA,XI,ETA,INE)
       IF (NODES(1,2).EQ.0) CALL R35092(PV,PXI,PETA,
      +    XI,ETA,INE)
       CALL R89003(T,DTDX,DTDY,DCA,TEMPC,TEMP,CNODES,
      +    PV,PXI,PETA,UE,P,RO,INE)
       IF( MAGNL .NE. 0 ) GO TO 136
       CALL R89004(T,DTDX,DTDY,DCA,UE,IDY,CNDS,INODE,
      +    INE,IMAG )
       GO TO 139
   136 CONTINUE
C-PUT VALUES IN MODULE AND PRINT IF WE HAVE CONVERGED
       IF( ICONV .NE. 0 )
      +CALL R89004(T,DTDX,DTDY,DCA,UE,IDY,CNDS,INODE,
      +    INE,IMAG )
C-PUT GAUSS POINT VALUE IN MODULE FOR NONLIN MAGNETIC
C-IF WE HAVE NOT CONVERGED
       IF( ICONV .EQ. 0 )
      +CALL R89021( L1,IADREL,ICOUNT,DTDX,DTDY,T,
      +    UE,DCA )
C-Insert by I.G.Ediz-------
C
   139 CONTINUE
C-DEFINE ELEMENT NUMBER
       JELE=IBASE(12)+1
       IELE=IBASE(12)+1
C-IERN IS THE ELEMENT TYPE, 39210=RECTANGULAR,
C-39110=TRIANGULAR
       IF(IERN.LT.39200) GOTO 501
C-FIND COORDINATES FOR RECTANGULAR TYPE OF ELEMENTS
C-L2=COLUMN,L3=ROW INTHE ELEMENT MATRIX
C-UE(1),UE(2) GIVE X AND Y COORDINATES OF EACH NODE
       IF(L2.EQ.1) THEN
       IF(L3.EQ.1) THEN
       XNOD(1)=UE(1)
       YNOD(1)=UE(2)
       ELSE IF(L3.EQ.2) THEN
       XNOD(6)=UE(1)
       YNOD(6)=UE(2)
       ZZ=YNOD(6)
       ELSE
       XNOD(3)=UE(1)
       YNOD(3)=UE(2)
       END IF
       END IF
       IF(L2.EQ.1.AND.L3.EQ.1) THEN
       IF(ABS(XNOD(1)-0.0).LT.0.1E-03) THEN
       IYY=1
       ELSE
       II=INT(UE(1)+0.1)
       AY=ABS(UE(1))
       IY=INT(AY+0.2)
       K=2*INVL
       IYY=IY/K+1
       END IF
       END IF
```

```
      IF(L2.EQ.2) THEN
      IF(L3.EQ.1) THEN
      XNOD(5)=UE(1)
      YNOD(5)=UE(2)
      ELSE IF(L3.EQ.3) THEN
      XNOD(8)=UE(1)
      YNOD(8)=UE(2)
      END IF
      END IF
      IF(L2.EQ.3) THEN
      IF(L3.EQ.1) THEN
      XNOD(2)=UE(1)
      YNOD(2)=UE(2)
      YY=UE(1)
      ELSE IF(L3.EQ.2) THEN
      XNOD(7)=UE(1)
      YNOD(7)=UE(2)
      ELSE
      XNOD(4)=UE(1)
      YNOD(4)=UE(2)
      END IF
      END IF
      IF(L2.EQ.3.AND.L3.EQ.1) THEN
      IF(INVL.EQ.0) THEN
      ANVL=ABS((XNOD(2)-XNOD(1))/2)
      INVL=INT(ANVL+0.1)
      END IF
      END IF
C-DEFINE FACE TYPE
C-RETREAT FACE=-1, ADVANCE FACE=1
      IF(IFACETYPE.EQ.1) THEN
      IF(II.LT.0) THEN
      IFACETYPE=-1
      END IF
      END IF
      GOTO 503
  501 CONTINUE
C-FINDS COORDINATES FOR TRIANGULAR TYPE OF ELEMENTS
      IF(L2.EQ.1.AND.L3.EQ.1) IC(IELE)=INT(UE(1)+0.1)
C-INITILIASE THE IC(IELE)
      IF(IC(IELE).EQ.0) IC(IELE-1)=0
C-SEPERATE THE INITIAL ELEMENT FROM SECONDARY ELEM.
      IF(IC(IELE).EQ.IC(IELE-1)) GOTO 502
C-THIS IS SECONDARY ELEMENT
      IF(L2.EQ.1) THEN
      IF(L3.EQ.1) THEN
      XNOD(3)=UE(1)
      YNOD(3)=UE(2)
      ISPOT=0
      ZZ=YNOD(3)
      ELSE IF(L3.EQ.2) THEN
      XNOD(6)=UE(1)
      YNOD(6)=UE(2)
      ELSE
      XNOD(1)=UE(1)
      YNOD(1)=UE(2)
```

```fortran
      END IF
      END IF
C-INSERT TO FIND THE SLOPE OF THE BOREHOLE
      IF(L2.NE.2) GOTO 499
      IF(ZZ.LT.0.0) GOTO 498
      IF(ABS(ALFA-0.0).LT.0.1E-03)   THEN
      ALFA=ATAN((YNOD(3)-YNOD(1))/(XNOD(3)-XNOD(1)))
      END IF
      GOTO 499
  498 IF(ABS(BETA-0.0).LT.0.1E-03)   THEN
      BETA=ATAN((ABS(YNOD(3)-YNOD(1)))/(XNOD(3)-
     +     XNOD(1)))
      END IF
  499 CONTINUE
C-END OF INSERT
      IF(L2.EQ.2) THEN
      IF(L3.EQ.1) THEN
      XNOD(5)=UE(1)
      YNOD(5)=UE(2)
      ELSE IF(L3.EQ.2) THEN
      XNOD(4)=UE(1)
      YNOD(4)=UE(2)
      END IF
      END IF
      IF(L2.EQ.3) THEN
      IF(L3.EQ.1) THEN
      XNOD(2)=UE(1)
      YNOD(2)=UE(2)
      END IF
      END IF
C-DEFINE THE POSITION OF NODES,REPRESENTING BH.
      IF(ABS(T).GT.0.99) GOTO 400
      IF(L3.EQ.2) IBHL=1
      IF(L2.EQ.1.AND.L3.EQ.1) THEN
      XX(1)=UE(1)
      IIX(1)=INT(UE(1)+0.1)
      IXX(1)=IIX(1)/INVL+1
      END IF
      GOTO 515
  502 CONTINUE
C-THIS IS INITIAL ELEMENT
      IF(L2.EQ.1) THEN
      IF(L3.EQ.1) THEN
      ISPOT=1
      XNOD(2)=UE(1)
      YNOD(2)=UE(2)
      ZZ=YNOD(2)
      ELSE IF(L3.EQ.2) THEN
      XNOD(4)=UE(1)
      YNOD(4)=UE(2)
      ELSE
      XNOD(1)=UE(1)
      YNOD(1)=UE(2)
      END IF
      END IF
      IF(L2.EQ.2) THEN
```

```
      IF(L3.EQ.1) THEN
      XNOD(5)=UE(1)
      YNOD(5)=UE(2)
      ELSE IF(L3.EQ.2) THEN
      XNOD(6)=UE(1)
      YNOD(6)=UE(2)
      END IF
      END IF
      IF(L2.EQ.3.AND.L3.EQ.1) THEN
      XNOD(3)=UE(1)
      YNOD(3)=UE(2)
      IF(INVL.EQ.0) THEN
      ANVL=ABS((XNOD(3)-XNOD(1))/2)
      INVL=INT(ANVL+0.1)
      END IF
      END IF
C-INSERT TO FIND OUT STRATA NUMBER
      IF(L2.EQ.1.AND.L3.EQ.3) THEN
      IF(ABS(UE(1)-0.0).LT.0.1E-03) THEN
      IF(ZZ.GT.0.0) THEN
      ISTRNO=ISTRNO+1
      ELSE
      ISTFNO=ISTFNO+1
      END IF
      END IF
      END IF
C-END OF INSERT
C-DEFINE THE POSITION OF NODES REPRESENTING BH
      IF(ABS(T).GT.0.99) GOTO 400
      IF(L3.EQ.2) IBHL=1
      IF(L2.EQ.1.AND.L3.EQ.3) THEN
      XX(1)=UE(1)
      IF(ABS(XX(1)-0.0).LT.0.1E-03) THEN
      IIX(1)=0
      IXX(1)=1
      ELSE
      IIX(1)=INT(UE(1)+0.1)
      IXX(1)=IIX(1)/INVL+1
      END IF
      END IF
C-DEFINE THE POSITION OF BH FOR TRIANGULAR ELEMENT
  515 CONTINUE
      XC(JELE,L3)=UE(1)
      YC(JELE,L3)=UE(2)
      IF(L2.EQ.1.AND.L3.EQ.3) THEN
      AA=UE(1)
      IF(ISPOT.EQ.1) THEN
      IF(ZZ.LT.0.0) THEN
      IKK(IXX(1))=INT(UE(1)+0.1)+1
      ELSE
      IK(IXX(1))=INT(UE(1)+0.1)+1
      END IF
      END IF
      END IF
      WRITE(6,390) JELE,L3, YC(JELE,L3)
  390 FORMAT(1H0,3H Y(,I3,1H,,I2,4H) = ,F6.2)
```

```
          WRITE(6,391) JELE,L3, XC(JELE,L3)
      391 FORMAT(1H0,3H X(,I3,1H,,I2,4H) = ,F6.2)
          WRITE(6,392) XX(1), IIX(1),IXX(1),L3
      392 FORMAT(1H0,6H XX = ,F12.4,7H IIX = ,I5,7H
         + IXX = ,I5,8H L3 =    ,I5)
C-FINDS PRESSURE GRADIENTS OF BH FOR TRIANGULAR TYPE
          IF(L3.EQ.1) BHGRAD(IXX(1),3)=ABS(DTDX)
          IF(L3.EQ.2) BHGRAD(IXX(1),2)=ABS(DTDX)
          IF(L3.EQ.3) BHGRAD(IXX(1),1)=ABS(DTDX)
          GOTO 400
C-DEFINE THE POSITION OF BH FOR RECTANGULAR ELEMENT
      503 CONTINUE
          IF(ABS(T).GT.0.99) GOTO 400
          IF(L3.EQ.2) IBHL=1
          IF(ABS(XNOD(1)-0.0).LT.0.1E-03) GOTO 400
          YC(JELE,L3)=UE(2)
          WRITE(6,393) JELE,L3, YC(JELE,L3)
      393 FORMAT(1H0,3H Y(,I3,1H,,I2,4H) = ,F6.2)
          XX(L2)=UE(1)
          IIX(L2)=INT(UE(1)+0.2)
          IXX(L2)=IIX(L2)/INVL+1
C-INSERT TO FIND OUT STRATA NUMBER
          IF(L2.EQ.3.AND.L3.EQ.1) THEN
          IF(ZZ.LT.0.0) GOTO 1330
          IF(ABS(UE(2)-RK).LT.0.1E-03) GOTO 1331
          RK=ABS(UE(2))
          ISTRNO=ISTRNO+1
          GOTO 1331
     1330 IF(ABS(UE(2)-FK).LT.0.1E-03) GOTO 1331
          FK=UE(2)
          ISTFNO=ISTFNO+1
     1331 CONTINUE
          END IF
C-INSERT TO DEFINE COMMON BOUNDARIES FOR ADJACENT
C-ELEMENTS
          IF(ZZ.LT.0.0) THEN
          IF(L2.EQ.1) IZZ(IELE,1)=IXX(1)
          IF(L2.EQ.3) IZZ(IELE,3)=IXX(3)
          ELSE
          IF(L2.EQ.1) IZ(IELE,1)=IXX(1)
          IF(L2.EQ.3) IZ(IELE,3)=IXX(3)
          END IF
C-END OF INSERT FOR COMMON BOUNDARIES
          WRITE(6,394) XX(L2), IIX(L2),IXX(L2),L3
      394 FORMAT(1H0,6H XX = ,F12.4,7H IIX = ,I5,7H
         + IXX = ,I5,8H L3 =    ,I5)
C-FINDS PRESSURE GRADIENTS OF BH FOR RECTANGULAR TYPE
          IF(L3.EQ.1) BHGRAD(IXX(L2),1)=ABS(DTDX)
          IF(L3.EQ.2) BHGRAD(IXX(L2),2)=ABS(DTDX)
          IF(L3.EQ.3) BHGRAD(IXX(L2),3)=ABS(DTDX)
      400 CONTINUE
C-FINDS PRESSURE GRADIENTS FOR ROADWAY
          IF(L3.EQ.1.AND.L2.EQ.1)
         +    RWGRAD(JELE,1)=ABS(DTDY)
          IF(L3.EQ.1.AND.L2.EQ.2)
         +    RWGRAD(JELE,2)=ABS(DTDY)
```

```
            IF(L3.EQ.1.AND.L2.EQ.3)
      +     RWGRAD(JELE,3)=ABS(DTDY)
C-GOTO THE NEXT NODE
  140   CONTINUE
  150   CONTINUE
C-OUT OF THE INNER ELEMENT LOOP
        IF(IERN.GT.39200) GOTO 504
        IF(ABS(YC(JELE,2)-0.0).LT.0.1E-03) GOTO 504
C-DEFINE THE POSITION OF INCLINED BH ACCORDING
C-TO THE INITIAL ELEMENT
        IF(ISPOT.EQ.0) GOTO 504
C-THESE WILL PRINT OUT THE POSITION OF INCLINED
C-BH ACCORDING TO THE INITIAL ELEMENT
        IF(ZZ.LT.0.0.AND.ISTFNO.EQ.1) THEN
C-FOR  FLOOR  BOREHOLES
        DXF(IXX(1))=ABS(XC(JELE,3)-XC(JELE,1))
        DYF(IXX(1))=ABS(YC(JELE,3)-YC(JELE,1))
        COORDYF(IXX(1))=ABS(YC(JELE,3))
        WRITE(6,51)IXX(1),DXF(IXX(1))
   51   FORMAT(1X,'DXF(',I2,')=',F6.2)
        WRITE(6,52)IXX(1),DYF(IXX(1))
   52   FORMAT(1X,'DYF(',I2,')=',F6.2)
        WRITE(6,53)IXX(1),COORDYF(IXX(1))
   53   FORMAT(1X,'COORDYF(',I2,')=',F6.2)
        END IF
        IF(ZZ.GT.0.0.AND.ISTRNO.EQ.1) THEN
C-FOR  ROOF  BOREHOLES
        DXR(IXX(1))=ABS(XC(JELE,3)-XC(JELE,1))
        DYR(IXX(1))=ABS(YC(JELE,3)-YC(JELE,1))
        COORDYR(IXX(1))=ABS(YC(JELE,3))
        WRITE(6,54)IXX(1),DXR(IXX(1))
   54   FORMAT(1X,'DXR(',I2,')=',F6.2)
        WRITE(6,55)IXX(1),DYR(IXX(1))
   55   FORMAT(1X,'DYR(',I2,')=',F6.2)
        WRITE(6,56)IXX(1),COORDYR(IXX(1))
   56   FORMAT(1X,'COORDYR(',I2,')=',F6.2)
        END IF
  504   CONTINUE
C-OBTAIN THE PERMEABILITY VALUES FOR THE ELEMENT
        CALL PERMCAL(IADREL,IELE,XX,IERN,INE,AA)
C-IF THERE IS NO BH GOTO 507
        IF(IBHL.EQ.0) GOTO 507
C-GAS FLOW RATE FOR THE FIRST BH IN THE ELEMENT
C-DETERMINE THE TYPE OF  BH AND  CALCULATE  THE
C-FLOW IN DIFFERENT  WAY
        IF(IERN.GT.39200) THEN
        DISTNY=ABS(YC(JELE,1)-YC(JELE,3))
        ELSE
        DISTNY=((ABS(YC(JELE,1)-YC(JELE,3)))**2+
      +     (ABS(XC(JELE,1)-XC(JELE,3)))**2)**0.5
        END IF
        DRAIN=((BHGRAD(IXX(1),1)*PERM(IELE,1))+
      +       (2*(BHGRAD(IXX(1),2)*
      +       PERM(IELE,6)))+(BHGRAD(IXX(1),3)*
      +       PERM(IELE,3)))*
      +       ((DISTNY/4)*4.75E-05)
```

```
C-TO OBTAIN VOLUME FLOW RATE, DIVIDE THE FLUX
C-BY DENSITY
      DRAIN=DRAIN/0.7168
      IF(ABS(BHGRAD(IXX(1),2)-0.0).LT.0.1E-03)
     +   GOTO 505
      IF(IERN.GT.39200) GOTO 506
C-ASSIGHN THE POSITION OF DRAIN CALCULATED
      IF(ZZ.LT.0.0) THEN
      DRAINFF(ISTFNO,IXX(1))=DRAIN
      ELSE
      DRAINRR(ISTRNO,IXX(1))=DRAIN
      END IF
C-COMMON BOUNDARIES FOR ADJACENT ELEMENTS
C-TRIANGULAR EL. ACC. TO THE SECONDARY EL
      IF(ISPOT.EQ.1) GOTO 507
      IF(ZZ.LT.0.0) THEN
      DRAINFF(ISTFNO,IXX(1)-2)=
     +DRAINFF(ISTFNO,IXX(1))+DRAINFF(ISTFNO,IXX(1)-2)
      DRAINFF(ISTFNO,IXX(1))=0.0
      ELSE
      DRAINRR(ISTRNO,IXX(1)-2)=
     +DRAINRR(ISTRNO,IXX(1))+DRAINRR(ISTRNO,IXX(1)-2)
      DRAINRR(ISTRNO,IXX(1))=0.0
      END IF
      GOTO 508
  506 CONTINUE
C-ADJACENT ELEMENTS FOR RECTANGULAR ELEMENT
      IF(ZZ.GT.0.0) GOTO 597
      IF(IZZ(IELE,1).EQ.1) GOTO 596
      IF(IZZ(IELE,1).NE.IZZ(IELE-1,3)) GOTO 596
      DRAINFF(ISTFNO,IXX(1))=DRAINFF(ISTFNO,IXX(1))
     +                         +DRAIN
      GOTO 509
  596 DRAINFF(ISTFNO,IXX(1))=DRAIN
  509 CONTINUE
      GOTO 505
  597 IF(IZ(IELE,1).EQ.1) GOTO 595
      IF(IZ(IELE,1).NE.IZ(IELE-1,3)) GOTO 595
      DRAINRR(ISTRNO,IXX(1))=
     +   DRAINRR(ISTRNO,IXX(1))+DRAIN
      GOTO 505
  595 DRAINRR(ISTRNO,IXX(1))=DRAIN
  505 CONTINUE
C-GAS FLOW RATE FOR THE SECOND BH IN THE ELEMENT
      IF(ABS(BHGRAD(IXX(3),2)-0.0).LT.0.1E-03)
     +    GOTO 507
C-IF(ISTRNO.NE.1.OR.ISTFNO.NE.1) GOTO 1525
      DRAIN=((BHGRAD(IXX(3),1)*PERM(IELE,2))+
     +      (2*(BHGRAD(IXX(3),2)*
     +      PERM(IELE,7)))+(BHGRAD(IXX(3),3)
     +      *PERM(IELE,4)))*
     +      ((DISTNY/4)*4.75E-05)
C-TO OBTAIN VOLUME FLOW RATE, DIVIDE THE FLUX
C-BY DENSITY
      DRAIN=DRAIN/0.7168
C-FOR MULTI STRATA IN RECTANGULAR ELEMENT
```

```
      IF(ZZ.LT.0.0) THEN
      DRAINFF(ISTFNO,IXX(3))=DRAIN
      ELSE
      DRAINRR(ISTRNO,IXX(3))=DRAIN
      END IF
  507 CONTINUE
      IF(ABS(PERM(IELE,5)-0.0).LT.0.1E-03)
     +     GOTO 508
C-CALCULATION OF GAS FLOW INTO ROADWAY
      DISTNX=ABS(XNOD(1)-XNOD(2))
      IF(INTV.EQ.0) THEN
      INTV=INT(DISTNX+0.1)
      END IF
C-THIS GIVES THE CALCULATION OF FLOW FOR THE
C-GIVEN BOUNDARY,DISTNX
      FLUX10=((PERM(IELE,9)*RWGRAD(JELE,1))+
     +        (2*(PERM(IELE,5)*
     +        RWGRAD(JELE,2)))+(PERM(IELE,8)
     +        *RWGRAD(JELE,3)))*
     +        ((DISTNX/4)*4.75E-05)
C-DEFINE THE FLOW RATES ACCORDING TO THE MINING TYPE
      IF(IFACETYPE.LT.0) GOTO 518
C-THIS IS ADVANCE FACE
      IF(ZZ.LT.0.0) THEN
      IKJ=IKJ+1
      FLOW10RWF(IYY)=FLUX10/0.7168
      IF(IYY.NE.1) GOTO 4115
      CUMRWF(1)=FLOW10RWF(1)
      GOTO 508
 4115 CUMRWF(IYY)=CUMRWF(IYY-1)+FLOW10RWF(IYY)
      ELSE
      FLOW10RWR(IYY)=FLUX10/0.7168
      IF(IYY.NE.1) GOTO 4116
      CUMRWR(1)=FLOW10RWR(1)
      GOTO 508
 4116 CUMRWR(IYY)=CUMRWR(IYY-1)+FLOW10RWR(IYY)
      END IF
      GOTO 508
  518 CONTINUE
C-THIS IS RETREAT FACE
      IF(ZZ.LT.0.0) THEN
      IF(YY.LT.0.0) THEN
      IKJ=IKJ+1
      FLOW10RWF(IYY)=FLUX10/0.7168
      IF(IYY.NE.1) GOTO 4117
      CUMRWF(1)=FLOW10RWF(1)
      GOTO 508
 4117 CUMRWF(IYY)=CUMRWF(IYY-1)+FLOW10RWF(IYY)
      ELSE
      IJK=IJK+1
      FLOW10GF(IYY)=FLUX10/0.7168
      IF(IYY.NE.1) GOTO 4118
      CUMGF(1)=FLOW10GF(1)
      GOTO 508
 4118 CUMGF(IYY)=CUMGF(IYY-1)+FLOW10GF(IYY)
      END IF
```

```
      END IF
      IF(ZZ.GT.0.0) THEN
      IF(YY.LT.0.0) THEN
      FLOW10RWR(IYY)=FLUX10/0.7168
      IF(IYY.NE.1) GOTO 4119
      CUMRWR(1)=FLOW10RWR(1)
      GOTO 508
 4119 CUMRWR(IYY)=CUMRWR(IYY-1)+FLOW10RWR(IYY)
      ELSE
      FLOW10GR(IYY)=FLUX10/0.7168
      IF(IYY.NE.1) GOTO 4120
      CUMGR(1)=FLOW10GR(1)
      GOTO 508
 4120 CUMGR(IYY)=CUMGR(IYY-1)+FLOW10GR(IYY)
      END IF
      END IF
  508 CONTINUE
      DO 600 I=1,3
      BHGRAD(IXX(1),I)=0.0
      BHGRAD(IXX(3),I)=0.0
  600 CONTINUE
C-OBTAIN THE NEXT ELEMENT
  160 CONTINUE
C-OUT OF ELEMENTS LOOP NOW
C-CALCULATION OF AVERAGE TOTAL METHANE EMISSION
C-FOR A GIVEN FACE TYPE
      IF(ABS(CUMRWF(IKJ)-0.0).LT.0.1E-03.OR.ABS
     +      (CUMRWR(IKJ)-0.0).LT.
     +      0.1E-03) GOTO 510
      TOTRWF=CUMRWF(IKJ)
      TOTRWR=CUMRWR(IKJ)
      IF(IFACETYPE.GT.0) THEN
      TOTEMIS=TOTRWR+TOTRWF
      ELSE
      TOTGF=CUMGF(IJK)
      TOTGR=CUMGR(IJK)
      TOTGOAF=TOTGF+TOTGR
      TOTRW=TOTRWR+TOTRWF
      TOTEMIS=TOTRW+TOTGOAF*EMISRATE
      END IF
      WRITE(6,580)
  580 FORMAT(
     +///12X,35H *** METHANE PREDICTION SUMMARY ***)
      IF(IFACETYPE.GT.0) THEN
      WRITE(6,588)
  588 FORMAT(
     +///15X,32H *** THIS IS AN ADVANCE FACE ***)
      ELSE
      WRITE(6,589)
  589 FORMAT(
     +///15X,31H *** THIS IS A RETREAT FACE ***)
      END IF
      WRITE(6,680)
  680 FORMAT(
     +///9X,34H TOTAL PREDICTED METHANE FLOW INTO
     +/6X,35H     ROADWAY FROM  " ROOF "  STRATA)
```

```fortran
      WRITE(6,681) TOTRWR,TOTRWR*1000.0
  681 FORMAT(4X,8H********,F12.4,6H M3/S ,2H (,F12.4,
     +5H L/S),8H ******)
      WRITE(6,682)
  682 FORMAT(
     +///9X,34H TOTAL PREDICTED METHANE FLOW INTO
     +/6X,36H     ROADWAY FROM  " FLOOR "  STRATA)
      WRITE(6,683) TOTRWF,TOTRWF*1000.0
  683 FORMAT(4X,8H********,F12.4,6H M3/S ,2H (,F12.4,
     +5H L/S),8H ******)
      IF(IFACETYPE.GT.0) THEN
      WRITE(6,780)
  780 FORMAT(
     +///9X,34H TOTAL PREDICTED METHANE FLOW INTO
     +/6X,35H ROADWAY FROM ROOF AND FLOOR STRATA)
      WRITE(6,800) TOTEMIS,TOTEMIS*1000.0
  800 FORMAT(4X,8H********,F12.4,6H M3/S ,2H (,F12.4,
     +5H L/S),8H ******)
      ELSE
      WRITE(6,849)
  849 FORMAT(
     +///9X,34H TOTAL PREDICTED METHANE FLOW INTO
     +/6X,35H ROADWAY FROM ROOF AND FLOOR STRATA)
      WRITE(6,850) TOTRW,TOTRW*1000.0
  850 FORMAT(4X,8H********,F12.4,6H M3/S ,2H (,F12.4,
     +5H L/S),8H ******)
      WRITE(6,851)
  851 FORMAT(
     +///9X,34H TOTAL PREDICTED METHANE FLOW INTO
     +/6X,34H     GOAF  FROM " ROOF "  STRATA)
      WRITE(6,852) TOTGR,TOTGR*1000.0
  852 FORMAT(4X,8H********,F12.4,6H M3/S ,2H (,F12.4,
     +5H L/S),8H ******)
      WRITE(6,853)
  853 FORMAT(
     +///9X,34H TOTAL PREDICTED METHANE FLOW INTO
     +/6X,34H     GOAF   FROM " FLOOR "  STRATA)
      WRITE(6,854) TOTGF,TOTGF*1000.0
  854 FORMAT(4X,8H********,F12.4,6H M3/S ,2H (,F12.4,
     +5H L/S),8H ******)
      WRITE(6,858)
  858 FORMAT(
     +///9X,34H TOTAL PREDICTED METHANE FLOW INTO
     +/6X,34H   GOAF FROM ROOF AND FLOOR STRATA)
      WRITE(6,855) TOTGOAF,TOTGOAF*1000.0
  855 FORMAT(4X,8H********,F12.4,6H M3/S ,2H (,F12.4,
     +5H L/S),8H ******)
      WRITE(6,856)
  856 FORMAT(
     +///9X,37H TOTAL PREDICTED METHANE FLOW RATE IN
     +/6X,39H RETURN END FROM RF-FLR STRATA AND GOAF)
      WRITE(6,857) TOTEMIS,TOTEMIS*1000.0
  857 FORMAT(6X,8H********,F12.4,6H M3/S ,2H (,F12.4,
     +5H L/S),10H ******)
      END IF
C-PRINTS OUT FLOW FROM ROOF STRATA INTO ROADWAYS
```

```fortran
      WRITE(6,899) INTV
  899 FORMAT(
     +//42H THE FLOW RATE OF METHANE FROM ROOF STRATA
     +/21H INTO THE ROADWAY AT ,I2,15H METRE INTERVAL
     +/43HIS CALCULATED AND THE OUTPUT IS GIVEN BELOW
     +///41H DISTANCE FROM    FLOW INTO       FLOW INTO
     +/43H    THE FACE        ROADWAY         ROADWAY
     +/41H        M          M3/S            L/S)
      JCOUNTER=0
      DO 904 L=1,IKJ
      IF(ABS(FLOW1ORWR(L)-0.0).LT.0.1E-03) GOTO 904
      JCOUNTER=JCOUNTER+1
      IDIST=JCOUNTER*INTV
      WRITE(6,902) IDIST, FLOW1ORWR(L), FLOW1ORWR(L)
     +  *1000.0
  904 CONTINUE
  902 FORMAT(2X,I6,10X,F12.4,7X,F12.4)
      WRITE(6,1889) INTV
 1889 FORMAT(
     +//40H THE CUM. FLOW RATE OF METHANE FROM ROOF
     +/29H  STRATA INTO THE ROADWAY AT ,I2,6H METRE
     +/41H INTERVAL IS CALCULATED AND THE OUTPUT IS
     +///39H DISTANCE FROM    CUM FLOW        CUM FLOW
     +/41H    THE FACE        TO ROADWAY    TO ROADWAY
     +/38H        M           M3/S            L/S)
      JCOUNTER=0
      DO 1804 L=1,IKJ
      IF(ABS(CUMRWR(L)-0.0).LT.0.1E-03) GOTO 1804
      JCOUNTER=JCOUNTER+1
      IDIST=JCOUNTER*INTV
      WRITE(6,1802)IDIST,CUMRWR(L),CUMRWR(L)*1000.0
 1804 CONTINUE
 1802 FORMAT(2X,I6,10X,F12.4,7X,F12.4)
C-PRINTS OUT FLOW FROM FLOOR STRATA INTO ROADWAYS
      WRITE(6,889) INTV
  889 FORMAT(
     +//39H     THE FLOW RATE OF METHANE FROM FLOOR
     +/28H STRATA INTO THE ROADWAY AT ,I2,6H METRE
     +/40H    INTERVAL IS CALCULATED, THE OUTPUT IS
     +///38H DISTANCE FROM    FLOW INTO  FLOW INTO
     +/38H    THE FACE        ROADWAY    ROADWAY
     +/35H        M           M3/S       L/S)
      JCOUNTER=0
      DO 804 L=1,IKJ
      IF(ABS(FLOW1ORWF(L)-0.0).LT.0.1E-03)GOTO 804
      JCOUNTER=JCOUNTER+1
      IDIST=JCOUNTER*INTV
      WRITE(6,802) IDIST, FLOW1ORWF(L), FLOW1ORWF(L)
     +  *1000.0
  804 CONTINUE
  802 FORMAT(2X,I6,10X,F12.4,7X,F12.4)
      WRITE(6,1890) INTV
 1890 FORMAT(
     +//41H THE CUM. FLOW RATE OF METHANE FROM FLOOR
     +/30H    STRATA INTO THE ROADWAY AT ,I2,6H METRE
     +/42H   INTERVAL IS CALCULATED AND THE OUTPUT IS
```

```fortran
      +///40H DISTANCE FROM      CUM FLOW      CUM FLOW
      +/42H    THE FACE          TO ROADWAY  TO ROADWAY
      +/39H       M                M3/S          L/S)
       JCOUNTER=0
       DO 1891 L=1,IKJ
       IF(ABS(CUMRWF(L)-0.0).LT.0.1E-03) GOTO 1891
       JCOUNTER=JCOUNTER+1
       IDIST=JCOUNTER*INTV
       WRITE(6,1892)IDIST,CUMRWF(L),CUMRWF(L)*1000.0
 1891 CONTINUE
 1892 FORMAT(2X,I6,10X,F12.4,7X,F12.4)
C-PRINTS OUT FLOW FROM ROOF STRATA INTO GOAF
       IF(IFACETYPE.LT.0) THEN
       WRITE(6,890) INTV
  890 FORMAT(
      +//42H THE FLOW RATE OF METHANE FROM ROOF STRATA
      +/18H INTO THE GOAF AT ,I2,18H METRE INTERVAL IS
      +/43H    CALCULATED AND THE OUTPUT IS GIVEN BELOW
      +///41H DISTANCE FROM    FLOW INTO       FLOW INTO
      +/41H    THE FACE          GOAF            GOAF
      +/40H       M              M3/S            L/S)
       JCOUNTER=0
       DO 891 L=1,IJK
       IF(ABS(FLOW1OGR(L)-0.0).LT.0.1E-03) GOTO 891
       JCOUNTER=JCOUNTER+1
       IDIST=JCOUNTER*INTV
       WRITE(6,892) IDIST, FLOW1OGR(L), FLOW1OGR(L)
      +  *1000.0
  891 CONTINUE
  892 FORMAT(2X,I6,10X,F12.4,7X,F12.4)
       WRITE(6,2893) INTV
 2893 FORMAT(
      +//40H THE CUM. FLOW RATE OF METHANE FROM ROOF
      +/29H     STRATA INTO THE GOAF AT ,I2,6H METRE
      +/41H INTERVAL IS CALCULATED AND THE OUTPUT IS
      +///39H DISTANCE FROM    CUM FLOW      CUM FLOW
      +/41H    THE FACE         INTO GOAF     INTO GOAF
      +/38H       M              M3/S          L/S)
       JCOUNTER=0
       DO 2894 L=1,IJK
       IF(ABS(CUMGR(L)-0.0).LT.0.1E-03) GOTO 2894
       JCOUNTER=JCOUNTER+1
       IDIST=JCOUNTER*INTV
       WRITE(6,2895) IDIST,CUMGR(L),CUMGR(L)*1000.0
 2894 CONTINUE
 2895 FORMAT(2X,I6,10X,F12.4,7X,F12.4)
C-PRINTS OUT FLOW FROM FLOOR STRATA INTO GOAF
       WRITE(6,893) INTV
  893 FORMAT(
      +//43H THE FLOW RATE OF METHANE FROM FLOOR STRATA
      +/19H  INTO THE GOAF AT ,I2,18H METRE INTERVAL IS
      +/44H     CALCULATED AND THE OUTPUT IS GIVEN BELOW
      +///50H DISTANCE FROM     FLOW INTO       FLOW INTO
      +/47H    THE FACE           GOAF            GOAF
      +/47H       M                M3/S            L/S)
       JCOUNTER=0
```

```
      DO 894 L=1,IJK
      IF(ABS(FLOW1OGF(L)-0.0).LT.0.1E-03) GOTO 894
      JCOUNTER=JCOUNTER+1
      IDIST=JCOUNTER*INTV
      WRITE(6,895)IDIST,FLOW1OGF(L),FLOW1OGF(L)*1000.0
  894 CONTINUE
  895 FORMAT(2X,I6,10X,F12.4,7X,F12.4)
      WRITE(6,1893) INTV
 1893 FORMAT(
     +//41H THE CUM. FLOW RATE OF METHANE FROM FLOOR
     +/21H STRATA INTO GOAF AT ,I2,15H METRE INTERVAL
     +/42H IS CALCULATED,  THE OUTPUT IS GIVEN BELOW
     +///40H DISTANCE FROM   CUM FLOW        CUM FLOW
     +/42H   THE FACE         INTO GOAF      INTO GOAF
     +/40H        M             M3/S           L/S)
      JCOUNTER=0
      DO 1894 L=1,IJK
      IF(ABS(CUMGF(L)-0.0).LT.0.1E-03) GOTO 1894
      JCOUNTER=JCOUNTER+1
      IDIST=JCOUNTER*INTV
      WRITE(6,1895)IDIST,CUMGF(L),CUMGF(L)*1000.0
 1894 CONTINUE
 1895 FORMAT(2X,I6,10X,F12.4,7X,F12.4)
      END IF
      WRITE(6,585)
  585 FORMAT(
     +///12X,36H *END OF METHANE PREDICTION SUMMARY*)
  510 CONTINUE
C-INSERT FOR MULTI-STRATA BOREBOLE DRAINAGE
      IF(ABS(ALFA-0.0).LT.0.1E-03) THEN
      DO 2001 J=1, 50
      IF(ABS(DRAINRR(1,J)-0.0).LT.0.1E-03)GOTO 2001
      DRAINR(J) = DRAINRR(1,J)
      DO 2002 I=2, ISTRNO
      IF(ABS(DRAINRR(I,J)-0.0).LT.0.1E-03)GOTO 2002
      DRAINR(J) = DRAINR(J) + DRAINRR(I,J)
 2002 CONTINUE
 2001 CONTINUE
      ELSE
      DO 2003 L=1, 50
      K1 = 0
      IF(ABS(DRAINRR(1,L)-0.0).LT.0.1E-03)GOTO 2003
      K1 = L
      DRAINR(L) = DRAINRR(1,L)
      DO 2004 I=2, ISTRNO
      K1 = K1+2
      IF(ABS(DRAINRR(I,K1)-0.0).LT.0.1E-03)GOTO 2004
      DRAINR(L) = DRAINR(L) + DRAINRR(I,K1)
 2004 CONTINUE
 2003 CONTINUE
      END IF
      IF(ABS(BETA-0.0).LT.0.1E-03) THEN
      DO 2005 J=1, 50
      IF(ABS(DRAINFF(1,J)-0.0).LT.0.1E-03)GOTO 2005
      DRAINF(J) = DRAINFF(1,J)
      DO 2006 I=2, ISTFNO
```

```
      IF(ABS(DRAINFF(I,J)-0.0).LT.0.1E-03)GOTO 2006
      DRAINF(J) = DRAINF(J) + DRAINFF(I,J)
 2006 CONTINUE
 2005 CONTINUE
      ELSE
      DO 2007 L=1, 50
      K2 = 0
      IF(ABS(DRAINFF(1,L)-0.0).LT.0.1E-03)GOTO 2007
      DRAINF(L) = DRAINFF(1,L)
      K2 = L
      DO 2008 I=2, ISTFNO
      K2 = K2+2
      IF(ABS(DRAINFF(I,K2)-0.0).LT.0.1E-02)GOTO 2008
      DRAINF(L) = DRAINF(L) + DRAINFF(I,K2)
 2008 CONTINUE
 2007 CONTINUE
      END IF
C-PRINTS OUT FLOW INTO ROOF BOREHOLES
      KOUNTER1=0
      BHTOTR=0.0
      DO 969 KJI=1,21
      DSFF1=(KJI-1)*INVL
      IF(ABS(DRAINR(KJI)-0.0).LT.0.1E-02)GOTO 969
      KOUNTER1=KOUNTER1+1
      BHTOTR=BHTOTR+DRAINR(KJI)
      IF(IK(KJI).NE.0) THEN
      DSFF1=ABS(DSFF1-(DXR(KJI)*COORDYR(KJI)/
     +      DYR(KJI)))
      END IF
      IF(IBH.NE.1) THEN
      WRITE(6,581)
  581 FORMAT(
     +///15X,33H *** METHANE DRAINAGE SUMMARY ***)
      IBH=1
      END IF
      WRITE(6,961)DSFF1,DRAINR(KJI),DRAINR(KJI)
     + *1000.0
  961 FORMAT(
     +//12H ROOF BH AT ,F5.2,19H M FROM FACE,DRAINS
     +F12.4,6H M3/S ,2H (,F12.4,7H L/S   ))
  969 CONTINUE
      IF(KOUNTER1.GT.0) THEN
      WRITE(6,963)KOUNTER1,BHTOTR,BHTOTR*1000.0
  963 FORMAT(
     +//1H0,27H THE TOTAL DRAINAGE OF THE ,I2,
     +8H ROOF BH
     +,F12.4,6H M3/S ,2H (,F12.4,7H L/S   ))
      END IF
C-PRINTS OUT FLOW INTO FLOOR BOREHOLES
      KOUNTER2=0
      BHTOTF=0.0
      DO 968 KJI=1,21
      DSFF2=(KJI-1)*INVL
      IF(ABS(DRAINF(KJI)-0.0).LT.0.1E-03) GOTO 968
      IF(IBH.NE.1) THEN
      WRITE(6,956)
```

```
  956 FORMAT(
     +///15X,33H *** METHANE DRAINAGE SUMMARY ***)
      IBH=1
      END IF
      KOUNTER2=KOUNTER2+1
      BHTOTF=BHTOTF+DRAINF(KJI)
      IF(IKK(KJI).NE.0) THEN
      DSFF2=ABS(DSFF2-(DXF(KJI)*COORDYF(KJI)/DYF(KJI)))
      END IF
      WRITE(6,951)DSFF2,DRAINF(KJI),DRAINF(KJI)*1000.0
  951 FORMAT(
     +//13H FLOOR BH AT ,F5.2,19H M FROM FACE,DRAINS
     +,F12.4,6H M3/S ,2H (,F12.4,7H L/S   ))
  968 CONTINUE
      IF(KOUNTER2.EQ.0) GOTO  955
      WRITE(6,953)KOUNTER2,BHTOTF,BHTOTF*1000.0
  953 FORMAT(
     +//1H0,23H THE TOTAL DRAINAGE OF ,I2,9H FLOOR BH
     +,F12.4,6H M3/S ,2H (,F12.4,7H L/S   ))
C-PRINTS OUT TOTAL DRAINAGE OF THE SYSTEM
  955 BHTOT=BHTOTR+BHTOTF
      ITOTBHNO=KOUNTER1+KOUNTER2
      IF(ITOTBHNO.GT.0) THEN
      WRITE(6,954)ITOTBHNO,BHTOT,BHTOT*1000.0
  954 FORMAT(
     +//1H0,27H THE TOTAL DRAINAGE OF THE ,I2,
     +25H " SYSTEM   " BOREHOLES = ,F12.4,
     +6H M3/S ,2H (,F12.4,7H L/S   ))
      WRITE(6,586)
  586 FORMAT(
     +///12X,36H **END OF METHANE DRAINAGE SUMMARY**)
      END IF
C
C-End of insert by I.G.Ediz---------
      GO TO 120
    1 FORMAT(
     +///
     +40H SUBROUTINE R89010 ISOPARAMETRIC THERMAL
     +/38H DERIVATIVE ROUTINE CALCULATES MAXIMUM
     +/38H GRADIENT IN PLANE. ALPHA IS THE ANGLE
     +/38H OF MAXIMUM GRADIEND MEASURED + TO THE
     +,38H ELEMENT Y-AXIS FROM   ELEMENT X   AXIS
     +/38H BETA IS THE ANGLE RELATIVE TO   GLOBAL
     +,38H X-AXIS AND IS SET TO  9999.0   IF   THE
     +,38H ELEMENT IS NOT IN THE GLOBAL XY PLANE
     +/38H ELE TEMP    MAXIMUM     ANGLE     ANGLE
     +,38H DERIVATIVES W.R.T. GLOBAL GLOBAL COOR
     +/38H NO. VALUE  GRADIENT     ALPHA     BETA
     +,16H X-AXIS    Y-AXIS,11X,1HX,9X,1HY,9X,1HZ)
    2 FORMAT(
     +40H SUBROUTINE R89010 ISOPARAMETRIC MAG RTN
     +/39H   CALCULATES MAXIMUM GRADIENT IN PLANE
     +/39H BETA IS THE ANGLE REL TO GLOBAL X-AXIS
     +,39H AND IS SET TO 9999.0 IF THE ELEMENT IS
     +,27H NOT IN THE GLOBAL XY PLANE
     +/39H ELE  POTENTIAL   MAXIMUM            ANGLE
```

```
      +,39H MAG FIELD   GLOBAL    GLOBAL COORDINATES
      +/39H NO.     VALUE      GRADIENT          BETA
      +,17H X-AXIS    Y-AXIS,11X,1HX,9X,1HY,9X,1HZ)
        END
C
      SUBROUTINE R89002(TEMPN,DCA,AINV,TEMPC,
      +                    TEMP,INE,IDT,IIEPA)
C-COMMENT-------------------------------------------
C THIS SUBROUTINE FINDS THE  TEMPERATURES  AT THE
C NODES OF AN ELEMENT AND PUT THEM INTO THE ARRAY
C TEMP ON EXIT THE ARRAY TEMPC HOLDS THE CONSTANTS
C IN TEMPERATURE POLYNOMIALS
C-COMMENT END---------------------------------------
      DIMENSION DCA(3,3),AINV(1),TEMPC(1),TEMP(1),
      +           TEMPN(1)
      COMMON/IBASE/IBASE(1500)
      COMMON BASE(33000)
      CALL NULL (TEMP,INE,1)
      DO 110 L1 = 1,INE
      IADR = IIEPA+L1-1
      INODE = BASE(IADR)+0.1
C-Insert by I.G.Ediz-------
C
      TEMP(L1) = (TEMPN(INODE))**2.0
C
C-End of insert-----------
  110  CONTINUE
      CALL MATMUL(TEMPC,AINV,TEMP,INE,INE,1)
      RETURN
      END
```

APPENDIX 7 AN OUTPUT OF GAS FLOW ANALYSIS

*** METHANE PREDICTION SUMMARY ***

*** THIS IS AN ADVANCE FACE ***

TOTAL PREDICTED METHANE FLOW INTO ROADWAY
FROM " ROOF " STRATA
******** 0.1376 M3/S (137.6194 L/S) ******

TOTAL PREDICTED METHANE FLOW INTO ROADWAY
FROM " FLOOR " STRATA
******** 0.0837 M3/S (83.6501 L/S) *******

TOTAL PREDICTED METHANE FLOW INTO ROADWAY
FROM " ROOF " AND " FLOOR " STRATA
******** 0.2213 M3/S (221.2695 L/S) *******

THE FLOW RATE OF METHANE FROM " ROOF " STRATA INTO
THE ROADWAY AT 10 METRE INTERVALS IS CALCULATED AND
THE OUTPUT IS GIVEN BELOW

DISTANCE FROM THE FACE M	FLOW INTO ROADWAY M3/S	FLOW INTO ROADWAY L/S
10	0.0098	9.8180
20	0.0120	12.0273
30	0.0105	10.4769
40	0.0077	7.7274
50	0.0074	7.3686
60	0.0089	8.8631
70	0.0112	11.2179
80	0.0133	13.2728
90	0.0143	14.3349
100	0.0148	14.8000
110	0.0143	14.2502
120	0.0135	13.4622

THE CUMMULATIVE FLOW RATE OF METHANE FROM " ROOF "
STRATA INTO THE ROADWAY AT 10 METRE INTERVALS IS
CALCULATED AND THE OUTPUT IS GIVEN BELOW

DISTANCE FROM THE FACE M	CUM FLOW INTO ROADWAY M3/S	CUM FLOW INTO ROADWAY L/S
10	0.0098	9.8180
20	0.0218	21.8454
30	0.0323	32.3223
40	0.0400	40.0497
50	0.0474	47.4183
60	0.0563	56.2814
70	0.0675	67.4992
80	0.0808	80.7720
90	0.0951	95.1069

100	0.1099	109.9070
110	0.1242	124.1571
120	0.1376	137.6194

THE FLOW RATE OF METHANE FROM "FLOOR" STRATA INTO
THE ROADWAY AT 10 METRE INTERVALS IS CALCULATED AND
            THE OUTPUT IS GIVEN BELOW

DISTANCE FROM THE FACE M	FLOW INTO ROADWAY M3/S	FLOW INTO ROADWAY L/S
10	0.0072	7.1909
20	0.0080	7.9684
30	0.0067	6.7071
40	0.0049	4.9077
50	0.0044	4.3923
60	0.0051	5.1028
70	0.0063	6.3257
80	0.0076	7.5813
90	0.0083	8.2742
100	0.0085	8.4634
110	0.0085	8.5094
120	0.0082	8.2270

THE CUMMULATIVE FLOW RATE OF METHANE FROM " FLOOR "
STRATA INTO THE ROADWAY AT 10 METRE INTERVALS IS
       CALCULATED AND THE OUTPUT IS GIVEN BELOW

DISTANCE FROM THE FACE M	CUM FLOW INTO ROADWAY M3/S	CUM FLOW INTO ROADWAY L/S
10	0.0072	7.1909
20	0.0152	15.1593
30	0.0219	21.8664
40	0.0268	26.7741
50	0.0312	31.1664
60	0.0363	36.2692
70	0.0426	42.5949
80	0.0502	50.1762
90	0.0585	58.4504
100	0.0669	66.9138
110	0.0754	75.4232
120	0.0837	83.6501

*** END OF METHANE PREDICTION SUMMARY ***

*** METHANE DRAINAGE SUMMARY ***

ROOF BH AT 30.00 METRE FROM FACE, DRAINS 0.2528 M3/S
            (252.86 L/S)

ROOF BH AT 50.00 METRE FROM FACE, DRAINS 0.2400 M3/S
            (240.04 L/S)

THE TOTAL DRAINAGE OF THE 2 ROOF BH =   0.4929 M3/S
                (492.90 L/S)

FLOOR BH AT 30.00 METRE FROM FACE, DRAINS 0.1663 M3/S
                (166.34 L/S)

FLOOR BH AT 50.00 METRE FROM FACE, DRAINS 0.1498 M3/S
                (149.82 L/S)

THE TOTAL DRAINAGE OF THE 2 FLOOR BH =   0.3161 M3/S
                (316.16 L/S)

THE TOTAL DRAINAGE OF THE 4 SYSTEM BH = 0.8089 M3/S
                (808.96 L/S)

            *** END OF METHANE DRAINAGE SUMMARY ***